

Probing strongly interacting atomic gases with energetic atoms

Yusuke Nishida

*Center for Theoretical Physics, Massachusetts Institute of Technology, Cambridge, Massachusetts 02139, USA and
Theoretical Division, Los Alamos National Laboratory, Los Alamos, New Mexico 87545, USA*

(Dated: October 2011)

We investigate properties of an energetic atom propagating through strongly interacting atomic gases. The operator product expansion is used to systematically compute a quasiparticle energy and its scattering rate both in a spin-1/2 Fermi gas and in a spinless Bose gas. Reasonable agreement with recent quantum Monte Carlo simulations even at a relatively small momentum $k/k_F \gtrsim 1.5$ indicates that our large-momentum expansions are valid in a wide range of momentum. We also study a differential scattering rate when a probe atom is shot into atomic gases. Because the number density and current density of the target atomic gas contribute to the forward scattering only, its contact density (measure of short-range pair correlation) gives the leading contribution to the backward scattering. Therefore, such an experiment can be used to measure the contact density and thus provides a new local probe of strongly interacting atomic gases.

PACS numbers: 03.75.Ss, 03.75.Nt, 34.50.-s, 31.15.-p

CONTENTS

I. Introduction	1	VII. Conclusions	24
II. Summary of results and discussions	3	Acknowledgments	25
A. Quasiparticle energy and scattering rate	3	A. Derivation of Wilson coefficients	25
B. Differential scattering rate	3	1. One-body and two-body sectors	25
C. Comparison with Monte Carlo simulations	4	2. Three-body sector	26
III. Spin-1/2 Fermi gas	6	B. Details of solving integral equations	28
A. Formulation	6	1. Spin-1/2 Fermi gas	28
B. Operator product expansion	7	2. Spinless Bose gas	30
C. Wilson coefficients	8	C. Derivation of optical theorem in Eq. (5.24)	31
D. Expectation values of local operators	8	References	33
E. Single-particle Green's function	9		
F. Three-body problem	10		
IV. Spinless Bose gas	12		
A. Formulation	12		
B. Operator product expansion	12		
C. Wilson coefficients	13		
D. Single-particle Green's function	13		
E. Three-body problem	14		
V. Differential scattering rate	15		
A. Spin-1/2 Fermi gas	15		
B. Three-body problem	16		
C. Differential scattering rate	17		
1. Contribution of number density	17		
2. Contribution of current density	18		
3. Contribution of contact density	18		
D. Spinless Bose gas	20		
E. Three-body problem	21		
VI. Weak-probe limit	22		
A. Spin-1/2 Fermi gas	22		
B. Dynamic structure factor	22		
C. Differential scattering rate	23		
D. Spinless Bose gas	24		

I. INTRODUCTION

Strongly interacting many-body systems appear in various subfields of physics ranging from atomic physics to condensed matter physics to nuclear and particle physics. An understanding of their properties is always important and challenging. Among others, ultracold atoms offer ideal grounds to develop our understanding of many-body physics because we can control their interaction strength, dimensionality of space, and quantum statistics at will [1–3]. Many-body properties of strongly interacting atomic gases have been probed by a number of experimental methods including hydrodynamic expansions [4–8], Bragg spectroscopies [9–12], radio-frequency spectroscopies [13–15], precise thermodynamic measurements [16–22], and collisions of two atomic clouds [23–25]. In particular, the photoemission spectroscopy employed in Refs. [26, 27] is a direct analog of that known to be powerful in condensed matter physics [28].

On the other hand, often in nuclear and particle physics, high-energy particles play important roles to reveal the nature of target systems. For example, neutron-deuteron or proton-deuteron scatterings at intermedi-

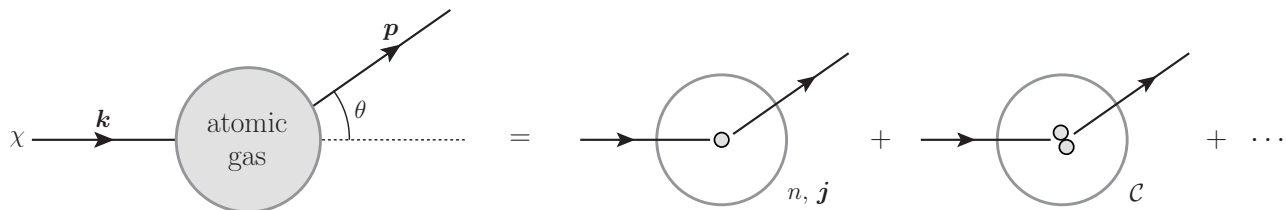


FIG. 1. Schematic of a proposed scattering experiment in which we shoot a probe atom χ into an atomic gas with a large momentum \mathbf{k} and measure its differential scattering rate. Three leading contributions come from two-body scatterings proportional to the number density n and current density \mathbf{j} of the target atomic gas and from a three-body scattering proportional to its contact density C (measure of short-range pair correlation). We will find that the number and current densities contribute to the forward scattering ($\theta < 90^\circ$) only and therefore the contact density gives the dominant contribution to the backward scattering ($\theta > 90^\circ$).

ate or higher energies are important to reveal the existence of three-nucleon forces in nuclei [29–31]. Also, two-nucleon knockout reactions by high-energy protons or electrons have been employed to reveal short-range pair correlations in nuclei [32, 33]. Furthermore, the discovery of “jet quenching” (i.e., significant energy loss of high-energy quarks and gluons) at Relativistic Heavy Ion Collider (RHIC) [34, 35] and Large Hadron Collider (LHC) [36, 37] is one of the most striking pieces of evidence that the matter created there is a strongly interacting quark-gluon plasma [38]. Such high-energy degrees of freedom to probe the nature of a quark-gluon plasma are generally referred to as “hard probes” [39]. In condensed matter physics, the use of high-energy neutrons to probe the momentum distribution of helium atoms in liquid helium was first suggested in Refs. [40, 41] and has been widely employed in experiments [42–44].

Now in ultracold-atom experiments, analogs of the hard probe naturally exist because a recombination of three atoms into a two-body bound state (dimer) produces an atom-dimer “dijet” propagating through the medium. Such three-body recombinations rarely occur in spin-1/2 Fermi gases because of the Pauli exclusion principle [45] but frequently occur in spinless Bose gases and have been used as a probe of the Efimov effect [46–50]. While atom-dimer “dijets” are normally considered to simply escape from the system, multiple collisions of the produced energetic dimer with atoms in the atomic gas were argued in Ref. [47] to account for the observed enhancement in atom loss. A well-founded understanding of collisional properties of an energetic atom or dimer in the medium is clearly desired here (see early works [51, 52] and also recent one [53]). In addition to these naturally produced energetic atoms, it is also possible to externally shoot energetic atoms into an atomic gas in a controlled way and measure the momentum distribution of scattered atoms. Indeed, closely related experiments to collide two atomic clouds have been performed successfully for Bose gases [54–61] and strongly interacting Fermi gases [23–25], which have been analyzed theoretically [62–65].

In this paper, we investigate various properties of an

energetic atom propagating through strongly interacting atomic gases. Such properties include a quasiparticle energy and a rate at which the atom is scattered in the medium. Both the quantities reflect many-body properties of the atomic gas and, in particular, the scattering rate may be useful to better understand multiple-atom loss mechanisms due to atom-dimer “dijets” produced by three-body recombination events [47, 53]. Also we propose a scattering experiment in which we shoot a probe atom into the atomic gas with a large momentum and measure its differential scattering rate (see Fig. 1). Resulting scattering data must bring out some information about the target atomic gas. What can we learn about the strongly interacting atomic gas from these scattering data? This question will be addressed in this paper.

Seemingly, these problems are difficult to tackle because of the nature of strong interactions. Quite remarkably, however, these problems can be addressed in a systematic way. This is because the atom with a large momentum probes a short distance at which it finds only a few atoms. Therefore, apart from probabilities of finding such few atoms in the medium, our problem reduces to few-body scattering problems. At the end, we will find that such an energetic atom can be useful to locally probe many-body aspects of strongly interacting atomic gases.

Atomic gases created in laboratories at ultralow temperatures and quark-gluon plasmas created at RHIC and LHC at ultrahigh temperatures are both strongly interacting many-body systems. In spite of the fact that they are at two extremes, various analogies have been discussed in the literature such as hydrodynamic behaviors and small shear viscosity to entropy density ratios [66]. This work intends to build a new bridge between them from the perspective of “hard probes.”

Since this paper turns out to be long, we first summarize our main results in Sec. II, discuss their consequences, and compare them with recent quantum Monte Carlo simulations. Our main results consist of the quasiparticle energy and scattering rate of an energetic atom in a spin-1/2 Fermi gas (Sec. III), those in a spinless Bose gas (Sec. IV), and the differential scattering rate of a different spin state of atoms shot into a spin-1/2

Fermi gas or a spinless Bose gas (Sec. V). Furthermore, a connection of our hard-probe formula derived in Sec. V with dynamic structure factors in the weak-probe limit is elucidated in Sec. VI. Finally, Sec. VII is devoted to conclusions of this paper and some details of calculations are presented in Appendices A–C.

Throughout this paper, we set $\hbar = 1$, $k_B = 1$, and use shorthand notations $(k) \equiv (k_0, \mathbf{k})$, $(x) \equiv (t, \mathbf{x})$, $kx \equiv k_0 t - \mathbf{k} \cdot \mathbf{x}$, and $\psi^\dagger \overleftrightarrow{\partial} \psi \equiv [\psi^\dagger (\partial \psi) - (\partial \psi^\dagger) \psi] / 2$. Also, note that implicit sums over repeated spin indices $\sigma = \uparrow, \downarrow$ are *not* assumed in this paper.

II. SUMMARY OF RESULTS AND DISCUSSIONS

We suppose that atoms interact with each other by a short-range potential and its potential range r_0 is much smaller than other length scales in the atomic gas such as an s -wave scattering length a , a mean interparticle distance $n^{-1/3}$, and a thermal de Broglie wavelength $\lambda_T \sim 1/\sqrt{mT}$. Furthermore, we suppose that a wavelength of the energetic atom $|\mathbf{k}|^{-1}$ is much smaller than the latter length scales but still much larger than the potential range. Therefore, the following hierarchy is assumed in the length scales:

$$r_0 \ll |\mathbf{k}|^{-1} \ll |a|, n^{-1/3}, \lambda_T. \quad (2.1)$$

Since the potential range is much smaller than all other length scales, we can take the zero-range limit $r_0 \rightarrow 0$. Then physical observables of our interest are expanded in terms of small quantities $1/(a|\mathbf{k}|)$, $n^{1/3}/|\mathbf{k}|$, $1/(\lambda_T|\mathbf{k}|) \ll 1$, which are collectively denoted by $O(\mathbf{k}^{-1})$, and various contributions are organized systematically according to their inverse powers of $|\mathbf{k}|$.

A. Quasiparticle energy and scattering rate

In the case of a spin-1/2 Fermi gas with equal masses $m = m_\uparrow = m_\downarrow$, the quasiparticle energy and scattering rate of spin-up fermions have the following systematic expansions in the large-momentum limit (see Sec. III for details):¹

$$E_\uparrow(\mathbf{k}) = \left[1 + 32\pi \frac{n_\downarrow}{a_f |\mathbf{k}|^4} - 7.54 \frac{\mathcal{C}_f}{|\mathbf{k}|^4} + O(\mathbf{k}^{-6}) \right] \frac{\mathbf{k}^2}{2m} \quad (2.2)$$

and

$$\Gamma_\uparrow(\mathbf{k}) = \left[32\pi \left(1 - \frac{4}{a_f^2 |\mathbf{k}|^2} \right) \frac{n_\downarrow}{|\mathbf{k}|^3} + 44.2 \frac{\mathcal{C}_f}{a_f |\mathbf{k}|^5} + O(\mathbf{k}^{-6}) \right] \frac{\mathbf{k}^2}{2m}. \quad (2.3)$$

¹ The energy is often measured with respect to a chemical potential. In this case, the quasiparticle energies in Eq. (2.2) and (2.4) should be replaced with $E_\uparrow(\mathbf{k}) - \mu_\uparrow$ and $E_b(\mathbf{k}) - \mu_b$, respectively.

Here, a_f is an s -wave scattering length between spin-up and -down fermions, n_\downarrow is a number density of spin-down fermions, and \mathcal{C}_f is a contact density which measures the probability of finding spin-up and -down fermions close to each other [67–69]. The results for spin-down fermions are obtained simply by exchanging spin indices $\uparrow \leftrightarrow \downarrow$.

On the other hand, in the case of a spinless Bose gas, the quasiparticle energy and scattering rate of bosons have the following systematic expansions in the large-momentum limit (see Sec. IV for details):¹

$$E_b(\mathbf{k}) = \left[1 + 64\pi \frac{n_b}{a_b |\mathbf{k}|^4} - 2 \operatorname{Re} f \left(\frac{|\mathbf{k}|}{\kappa_*} \right) \frac{\mathcal{C}_b}{|\mathbf{k}|^4} + O(\mathbf{k}^{-5}) \right] \frac{\mathbf{k}^2}{2m} \quad (2.4)$$

and

$$\Gamma_b(\mathbf{k}) = \left[64\pi \frac{n_b}{|\mathbf{k}|^3} + 4 \operatorname{Im} f \left(\frac{|\mathbf{k}|}{\kappa_*} \right) \frac{\mathcal{C}_b}{|\mathbf{k}|^4} + O(\mathbf{k}^{-5}) \right] \frac{\mathbf{k}^2}{2m}. \quad (2.5)$$

Here, a_b is an s -wave scattering length between two identical bosons, n_b is a number density of bosons, and \mathcal{C}_b is a contact density which measures the probability of finding two bosons close to each other [70]. $f(|\mathbf{k}|/\kappa_*)$ with κ_* being the Efimov parameter is a universal log-periodic function determined in Sec. IV [see Fig. 7 and Eq. (4.31)]. Note that the coefficient of the contact density in the scattering rate is always negative because $\operatorname{Im} f$ ranges from -13.3 to -11.2 . This rather counterintuitively means that the energetic boson can escape from the medium easier than we naively estimate from a binary collision.

Each term has a simple physical meaning. Besides the free particle kinetic energy in Eq. (2.2) or (2.4), the leading term represents a contribution from a two-body scattering in which the energetic atom collides with one atom coming from the atomic gas. The probability of finding such an atom in the atomic gas is quantified by the number density $n_{\sigma,b}$. Similarly, the subleading term represents a contribution from a three-body scattering in which the energetic atom collides with a small pair of two atoms coming from the atomic gas. The probability of finding such a small pair in the atomic gas is quantified by the contact density $\mathcal{C}_{f,b}$.

These results are valid for an arbitrary many-body state with translational and rotational symmetries (i.e., for any scattering length, density, and temperature) as long as Eq. (2.1) is satisfied. All nontrivial information about the many-body state is encoded into the various densities $n_{\sigma,b}$ and $\mathcal{C}_{f,b}$.

B. Differential scattering rate

We then consider the proposed scattering experiment in which we shoot a probe atom into the atomic gas and measure its differential scattering rate (see Fig. 1). We assume that the probe atom denoted by χ is distinguishable from the rest of the atoms constituting the target atomic gas but has the same mass m , which is possible

by using a different atomic spin state. When the χ atom is shot into a spin-1/2 Fermi gas, its differential scatter-

ing rate has the following systematic expansion in the large-momentum limit (see Sec. V for details):

$$\begin{aligned} \frac{d\Gamma_\chi(\mathbf{k})}{d\Omega} = & \left[32 \cos\theta \Theta(\cos\theta) \frac{n_\uparrow(\mathbf{x}) + n_\downarrow(\mathbf{x})}{|\mathbf{k}|^3} + 32 \left\{ 2 \cos\theta \Theta(\cos\theta) \hat{\mathbf{k}} - \delta(\cos\theta) \hat{\mathbf{k}} + \Theta(\cos\theta) \hat{\mathbf{p}} \right\} \cdot \frac{\mathbf{j}_\uparrow(\mathbf{x}) + \mathbf{j}_\downarrow(\mathbf{x})}{|\mathbf{k}|^4} \right. \\ & \left. + 2g\left(\cos\theta, \frac{|\mathbf{k}|}{\kappa'_*}\right) \frac{\mathcal{C}_f(\mathbf{x})}{|\mathbf{k}|^4} + O(\mathbf{k}^{-5}) \right] \frac{\mathbf{k}^2}{2m}. \end{aligned} \quad (2.6)$$

Here, $\Theta(\cdot)$ is the Heaviside step function and θ is a polar angle of the measured momentum \mathbf{p} with respect to the incident momentum chosen to be $\mathbf{k} = |\mathbf{k}|\hat{\mathbf{z}}$. Accordingly, when a bunch of independent χ atoms with a total number N_χ is shot into the atomic gas, the number of scattered χ atoms measured at an angle (θ, φ) is predicted to be

$$N_{\text{sc}}(\theta, \varphi) = N_\chi \frac{m}{|\mathbf{k}|} \int dl \frac{d\Gamma_\chi(\mathbf{k})}{d\Omega}, \quad (2.7)$$

where the line integral is taken along a classical trajectory of the χ atom.

The differential scattering rate of the χ atom shot into a spinless Bose gas is obtained from Eq. (2.6) by replacing the number density $n_\uparrow + n_\downarrow$, the current density $\mathbf{j}_\uparrow + \mathbf{j}_\downarrow$, and the contact density \mathcal{C}_f of a spin-1/2 Fermi gas with those of a spinless Bose gas, n_b , \mathbf{j}_b , and $\mathcal{C}_b/2$, respectively [see Eq. (5.45)]. These parameters are the same as those in Eqs. (2.2)–(2.5), while translational or rotational symmetries are not assumed here and thus the current density $\mathbf{j}_{\sigma,b}$ can be nonzero. On the other hand, κ'_* in Eq. (2.6) is the Efimov parameter associated with a three-body system of the χ atom with spin-up and -down fermions (the χ atom with two identical bosons) and thus different from κ_* in Eqs. (2.4) and (2.5) associated with three identical bosons. We note that the dependence on scattering lengths between the χ atom and an atom constituting the target atomic gas appears only from $O(\mathbf{k}^{-5})$ in the brackets. The corresponding formula in the weak-probe limit can be found in Eq. (6.17).

The first two terms in Eq. (2.6) come from two-body scatterings and are proportional to the number density and current density of the target atomic gas. An important observation is that, because of kinematic constraints in the two-body scattering, they contribute to the forward scattering ($\cos\theta > 0$) only. On the other hand, the last term comes from a three-body scattering and is proportional to the contact density. Its angle distribution is determined by a universal function $g(\cos\theta, |\mathbf{k}|/\kappa'_*)$, which is mostly negative on the forward-scattering side (see Fig. 9 in Sec. V). This is no cause for alarm, of course, because it is the subleading correction suppressed by a power of $1/|\mathbf{k}|$ to the leading positive contribution of the number density.

In contrast, $g(\cos\theta, |\mathbf{k}|/\kappa'_*)$ is positive everywhere on the backward-scattering side ($\cos\theta < 0$) because it is now kinematically allowed in the three-body scattering. Therefore, the backward scattering is dominated by the contact density of the target atomic gas and its measurement can be used to extract the contact density integrated along a classical trajectory of the probe atom [see Eq. (2.7)]. Since the contact density is an important quantity to characterize strongly interacting atomic gases, a number of ultracold-atom experiments have been performed so far to measure its value but integrated over the whole volume [10, 11, 18, 71, 72]. Our proposed experiment provides a new way to *locally* probe the many-body aspect of strongly interacting atomic gases.

Also we find from Eq. (2.6) that the differential scattering rate can depend on the azimuthal angle φ only by the current density of the target atomic gas. Therefore, the azimuthal anisotropy in the differential scattering rate may be useful to reveal many-body phases accompanied by currents.

C. Comparison with Monte Carlo simulations

All the above results are valid for an arbitrary many-body state at a sufficiently large momentum $|\mathbf{k}|$ satisfying Eq. (2.1). But how large should it be? One can gain insight into this question by comparing our results with other reliable results; for example, from Monte Carlo simulations. Currently the only available Monte Carlo result comparable with ours is about the quasiparticle energy in a spin-1/2 Fermi gas [73, 74]. Quite surprisingly, we will find reasonable agreement of our result (2.2) with the recent quantum Monte Carlo simulation even at a relatively small momentum $|\mathbf{k}|/k_F \gtrsim 1.5$. This indicates that our large-momentum expansions in Eqs. (2.2)–(2.6) are valid in a momentum range wider than we naively expect.

In Ref. [74], P. Magierski *et al.* extracted the quasiparticle energy $E(\mathbf{k})$ from quantum Monte Carlo data in a balanced Fermi gas $n_\uparrow = n_\downarrow$ at finite temperature. Their results are shown by points in Fig. 2 for $(ak_F)^{-1} = 0$ at $T/\epsilon_F = 0.15$ (left panel) and for $(ak_F)^{-1} = 0.2$ at $T/\epsilon_F = 0.19$ (right panel) in units of the Fermi energy $\epsilon_F = k_F^2/(2m)$ as functions of $(|\mathbf{k}|/k_F)^2$.

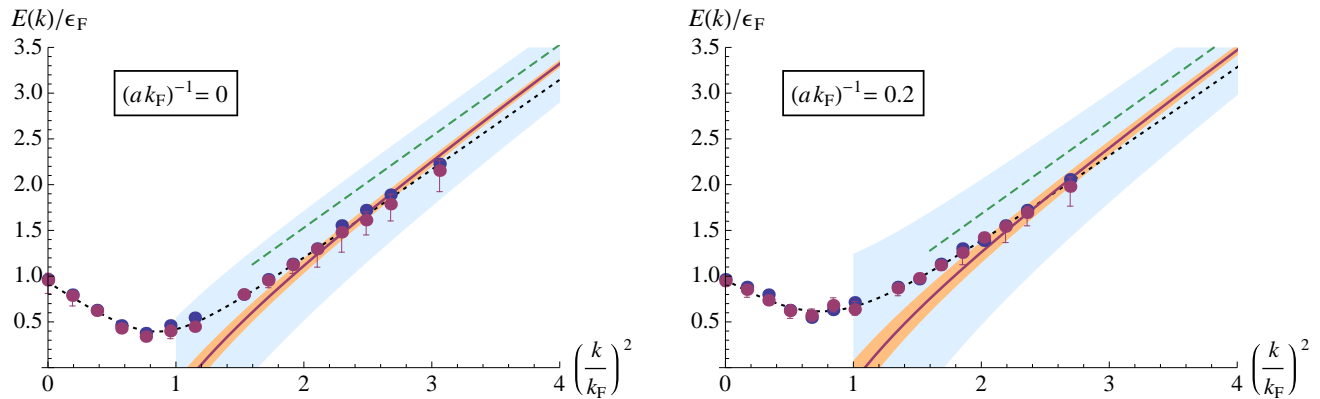


FIG. 2. (Color online) Quasiparticle energies $E(\mathbf{k})/\epsilon_F$ as functions of $(|\mathbf{k}|/k_F)^2$ for $(ak_F)^{-1} = 0$ at $T/\epsilon_F = 0.15$ (left panel) and for $(ak_F)^{-1} = 0.2$ at $T/\epsilon_F = 0.19$ (right panel). Points are results extracted from the quantum Monte Carlo simulation [74] and dotted curves behind them are fits by a BCS-type formula (2.13). Solid curves are our results from the large-momentum expansion (2.8) with the use of the contact densities obtained in Refs. [75, 76]. Narrow shaded regions behind them correspond to the contact densities varied by $\pm 20\%$ and broad ones indicate quasiparticle widths $\Gamma(\mathbf{k})/\epsilon_F$ from the large-momentum expansion (2.12) with the same inputs. For comparison, free particle dispersion relations, $E_{\text{free}}(\mathbf{k}) = \mathbf{k}^2/(2m) - \mu$, are shown by dashed lines.

Our large-momentum expansion of the quasiparticle energy (2.2) in the same units becomes

$$\frac{E(\mathbf{k})}{\epsilon_F} = \left(\frac{|\mathbf{k}|}{k_F}\right)^2 - \frac{\mu}{\epsilon_F} + \left(\frac{16}{3\pi} \frac{1}{ak_F} - 7.54 \frac{\mathcal{C}}{k_F^4}\right) \left(\frac{k_F}{|\mathbf{k}|}\right)^2 + O(k^{-4}). \quad (2.8)$$

Here we used the definition of the Fermi momentum $n_\sigma = k_F^3/(6\pi^2)$ and introduced the chemical potential μ because the quasiparticle energies in Ref. [74] are measured with respect to μ . The values of chemical potential obtained in Ref. [74] are

$$\frac{\mu}{\epsilon_F} \approx 0.471 \quad \text{and} \quad 0.319 \quad (2.9)$$

for $(ak_F)^{-1} = 0$ at $T/\epsilon_F = 0.15$ and for $(ak_F)^{-1} = 0.2$ at $T/\epsilon_F = 0.19$, respectively, with estimated errors of about 10%. Note that the self-energy correction at $O[(k_F/|\mathbf{k}|)^2]$ receives two contributions: One is from the two-body scattering which can be attractive or repulsive depending on the sign of $(ak_F)^{-1}$. The other is from the three-body scattering which is proportional to $\mathcal{C}/k_F^4 > 0$ and thus always attractive.

In order to make a comparison between our result and the Monte Carlo simulation, an input into the dimensionless contact density \mathcal{C}/k_F^4 is needed ideally at the same scattering length and temperature as in Ref. [74]. The contact density at infinite scattering length $(ak_F)^{-1} = 0$ has been measured by a number of Monte Carlo simulations [75–79] and ultracold-atom experiments [10, 11, 18, 71, 72], which are summarized in Table I. At zero temperature, they fall within the range of $\mathcal{C}/k_F^4 = 0.10 \sim 0.12$. The temperature dependence of the contact density was reported in Refs. [11, 79], although the situation is somewhat controversial: The simulation observed that the contact density increases with

T/ϵ_F up to $T/\epsilon_F \approx 0.4$ [79], while the experiment observed that the contact density monotonically decreases over the temperature range $T/\epsilon_F = 0.1 \sim 1$ [11]. Since the precise value of the contact density at $T/\epsilon_F = 0.15$ is not yet available, we choose to use the value of Ref. [75] at $T/\epsilon_F = 0.173(6)$; $\mathcal{C}/k_F^4 = 0.1102(11)$. This input fixes the self-energy correction to be

$$\left(\frac{16}{3\pi} \frac{1}{ak_F} - 7.54 \frac{\mathcal{C}}{k_F^4}\right) \left(\frac{k_F}{|\mathbf{k}|}\right)^2 = -0.831 \left(\frac{k_F}{|\mathbf{k}|}\right)^2, \quad (2.10)$$

and our result from the large-momentum expansion (2.8) is shown by the solid curve in Fig. 2 (left panel). In order to incorporate uncertainties of the contact density, its value is varied by $\pm 20\%$ which is represented by the narrow shaded region in the same plot. This variation of $\pm 20\%$ is a very conservative estimate of the uncertainties because the contact density increases only by 15% even from $T/\epsilon_F \approx 0$ to 0.4 according to Ref. [79].

On the other hand, the contact density away from the infinite scattering length is less understood, in particular, at finite temperature. Therefore, in order to facilitate

TABLE I. Dimensionless contact density \mathcal{C}/k_F^4 at infinite scattering length $(ak_F)^{-1} = 0$ from Monte Carlo simulations and ultracold-atom experiments at low and finite temperatures.

Simulations			Experiments		
Ref.	\mathcal{C}/k_F^4	T/ϵ_F	Ref.	\mathcal{C}/k_F^4	T/ϵ_F
[77, 78]	0.115	0	[18]	0.118(6)	0.03(3)
[76]	0.1147(3)	0	[10]	0.101(4)	0.10(2)
[79]	0.0996(34)	0	[11]	0.105(8)	0.09(3)
[75]	0.1102(11)	0.173(6)			
[79]	0.1040(17)	0.178			

a comparison between our result and the Monte Carlo result for $(ak_F)^{-1} = 0.2$ at $T/\epsilon_F = 0.19$, we choose to use the contact density of Ref. [76] for the same scattering length but at zero temperature; $C/k_F^4 = 0.156(2)$. This input fixes the self-energy correction to be

$$\left(\frac{16}{3\pi} \frac{1}{ak_F} - 7.54 \frac{C}{k_F^4}\right) \left(\frac{k_F}{|\mathbf{k}|}\right)^2 = -0.839 \left(\frac{k_F}{|\mathbf{k}|}\right)^2, \quad (2.11)$$

and our result from the large-momentum expansion (2.8) is shown by the solid curve in Fig. 2 (right panel). Note that the self-energy correction at $(ak_F)^{-1} = 0.2$ is close to that at $(ak_F)^{-1} = 0$ because opposite changes in the contributions from two-body and three-body scatterings happen to cancel each other. Again uncertainties of the contact density are incorporated by varying its value by $\pm 20\%$ which is represented by the narrow shaded region in the same plot.

In both cases of $(ak_F)^{-1} = 0$ and 0.2 , one can see from Fig. 2 that our results are not very sensitive to the variations of the contact densities and, furthermore, they are in reasonable agreement with the quantum Monte Carlo simulation even at a relatively small momentum; $(|\mathbf{k}|/k_F)^2 \gtrsim 2$. This indicates that our large-momentum expansions in Eqs. (2.2)–(2.6) are valid in a wide range of momentum.

Having our large-momentum expansions tested on the quasiparticle energy, we now present the quasiparticle width in the balanced spin-1/2 Fermi gas. Its large-momentum expansion (2.3) in units of the Fermi energy becomes

$$\frac{\Gamma(\mathbf{k})}{\epsilon_F} = \frac{16}{3\pi} \frac{k_F}{|\mathbf{k}|} - \frac{1}{ak_F} \left(\frac{64}{3\pi} \frac{1}{ak_F} - 44.2 \frac{C}{k_F^4}\right) \left(\frac{k_F}{|\mathbf{k}|}\right)^3 + O(\mathbf{k}^{-4}), \quad (2.12)$$

which is shown by the broad shaded region in Fig. 2 by using the same input into the contact density. Note that the correction at $O[(k_F/|\mathbf{k}|)^3]$ vanishes for $(ak_F)^{-1} = 0$ (left panel), while it is given by $+1.11(k_F/|\mathbf{k}|)^3$ for $(ak_F)^{-1} = 0.2$ (right panel). In both cases, the quasiparticle widths gradually increase with decreasing momentum and eventually become comparable to the quasiparticle energies. This takes place at $(|\mathbf{k}|/k_F)^2 \approx 2.1$ and 2.2 , respectively, which roughly correspond to the point where our large-momentum expansions break down.

P. Magierski *et al.* also extracted the pairing gap or pseudogap Δ , self-energy U , and effective mass m^* parameters by fitting a BCS-type formula

$$E_{\text{BCS}}(\mathbf{k}) = \sqrt{\left(\frac{\mathbf{k}^2}{2m^*} - \mu + U\right)^2 + \Delta^2} \quad (2.13)$$

to their quasiparticle energies [74]. However, the fitted results (dotted curves in Fig. 2) do not capture the correct asymptotic behaviors at $(|\mathbf{k}|/k_F)^2 \gtrsim 3$. This is because $E_{\text{BCS}}(\mathbf{k})$ has the asymptotic expansion

$$\frac{E_{\text{BCS}}(\mathbf{k})}{\epsilon_F} = \frac{m}{m^*} \left(\frac{|\mathbf{k}|}{k_F}\right)^2 - \frac{\mu}{\epsilon_F} + \frac{U}{\epsilon_F} + O(\mathbf{k}^{-4}), \quad (2.14)$$

in which the self-energy $U < 0$ is taken to be a constant, while according to Eq. (2.8), U should be momentum dependent and decay as

$$\frac{U}{\epsilon_F} \rightarrow \left(\frac{16}{3\pi} \frac{1}{ak_F} - 7.54 \frac{C}{k_F^4}\right) \left(\frac{k_F}{|\mathbf{k}|}\right)^2 \quad (2.15)$$

at $|\mathbf{k}|/k_F \gg 1$. Further analysis of their quantum Monte Carlo data incorporating our exact large-momentum expansions may allow us better access to the intriguing pseudogap physics.

III. SPIN-1/2 FERMION GAS

Here we study properties of an energetic atom in a spin-1/2 Fermi gas and derive its quasiparticle energy and scattering rate presented in Eqs. (2.2) and (2.3).

A. Formulation

The Lagrangian density describing spin-1/2 fermions with a zero-range interaction is

$$\mathcal{L}_F = \sum_{\sigma=\uparrow,\downarrow} \psi_{\sigma}^{\dagger} \left(i\partial_t + \frac{\nabla^2}{2m_{\sigma}} \right) \psi_{\sigma} + c \psi_{\uparrow}^{\dagger} \psi_{\downarrow}^{\dagger} \psi_{\downarrow} \psi_{\uparrow}. \quad (3.1)$$

It is more convenient to introduce an auxiliary dimer field $\phi = c \psi_{\downarrow} \psi_{\uparrow}$ to decouple the interaction term:

$$\mathcal{L}_F = \sum_{\sigma=\uparrow,\downarrow} \psi_{\sigma}^{\dagger} \left(i\partial_t + \frac{\nabla^2}{2m_{\sigma}} \right) \psi_{\sigma} - \frac{1}{c} \phi^{\dagger} \phi + \phi^{\dagger} \psi_{\downarrow} \psi_{\uparrow} + \psi_{\uparrow}^{\dagger} \psi_{\downarrow}^{\dagger} \phi. \quad (3.2)$$

For simplicity, we shall mainly consider the case of equal masses $m = m_{\uparrow} = m_{\downarrow}$. Some results in the case of unequal masses are presented in Appendices A and B. The propagator of fermion field ψ_{σ} in the vacuum is given by

$$G(k) = \frac{1}{k_0 - \epsilon_{\mathbf{k}} + i0^+} \quad \left(\epsilon_{\mathbf{k}} \equiv \frac{\mathbf{k}^2}{2m} \right). \quad (3.3)$$

Also by using the standard regularization procedure to relate the bare coupling c to the scattering length a ,

$$\frac{1}{c} = \int_{|\mathbf{k}| < \Lambda} \frac{d\mathbf{k}}{(2\pi)^3} \frac{m}{\mathbf{k}^2} - \frac{m}{4\pi a}, \quad (3.4)$$

the propagator of dimer field ϕ in the vacuum is found to be

$$D(k) = -\frac{4\pi}{m} \frac{1}{\sqrt{\frac{\mathbf{k}^2}{4} - mk_0 - i0^+ - \frac{1}{a}}}. \quad (3.5)$$

$D(k)$ coincides with the two-body scattering amplitude $A(k)$ between spin-up and -down fermions up to a minus sign; $A(k) = -D(k)$ (see Fig. 3).

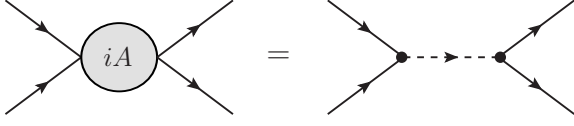


FIG. 3. Two-body scattering amplitude $iA(k)$ between spin-up and -down fermions. Solid (dashed) lines represent the fermion (dimer) propagator $iG(k)$ [$iD(k)$]. Each fermion-dimer vertex (dot) carries i , and thus, $iA(k) = -iD(k)$.

Our task here is to understand the behavior of the single-particle Green's function of spin- σ fermions

$$\int dy e^{iky} \langle T[\psi_\sigma(x + \frac{y}{2})\psi_\sigma^\dagger(x - \frac{y}{2})] \rangle \quad (3.6)$$

in the large-energy-momentum limit $k \rightarrow \infty$ for an arbitrary few-body or many-body state. Without losing generality, we can consider that of spin-up ($\sigma = \uparrow$) fermions. The result for spin-down ($\sigma = \downarrow$) fermions is obtained simply by exchanging spin indices $\uparrow \leftrightarrow \downarrow$.

B. Operator product expansion

According to the operator product expansion [68–70, 80–86], the product of operators in Eq. (3.6) can be expressed in terms of a series of local operators \mathcal{O} :

$$\int dy e^{iky} T[\psi_\uparrow(x + \frac{y}{2})\psi_\uparrow^\dagger(x - \frac{y}{2})] = \sum_i W_{\mathcal{O}_i}(k)\mathcal{O}_i(x). \quad (3.7)$$

Wilson coefficients $W_{\mathcal{O}}$ depend on $k = (k_0, \mathbf{k})$ and the scattering length a . When the scaling dimension of a local operator is $\Delta_{\mathcal{O}}$, dimensional analysis implies that its Wilson coefficient should have a form

$$W_{\mathcal{O}}(k) = \frac{1}{|\mathbf{k}|^{\Delta_{\mathcal{O}}+2}} w_{\mathcal{O}} \left(\frac{\sqrt{2mk_0}}{|\mathbf{k}|}, \frac{1}{a|\mathbf{k}|} \right). \quad (3.8)$$

Therefore, the large-energy-momentum limit of the single-particle Green's function is determined by Wilson coefficients of local operators with low scaling dimensions and their expectation values with respect to the given state.

The local operators appearing in the right-hand side of Eq. (3.7) must have a particle number $N_{\mathcal{O}} = 0$. By recalling $\Delta_{\psi_\sigma} = 3/2$ and $\Delta_\phi = 2$ [87], we can find twelve types of local operators with $N_{\mathcal{O}} = 0$ up to scaling dimensions $\Delta_{\mathcal{O}} = 5$:

$$\mathbb{1} \quad (\text{identity}) \quad (3.9)$$

for $\Delta_{\mathcal{O}} = 0$,

$$\psi_\sigma^\dagger \psi_\sigma \quad (3.10)$$

for $\Delta_{\mathcal{O}} = 3$,

$$-i\psi_\sigma^\dagger \overleftrightarrow{\partial}_i \psi_\sigma, \quad -i\partial_i(\psi_\sigma^\dagger \psi_\sigma), \quad \phi^\dagger \phi \quad (3.11)$$

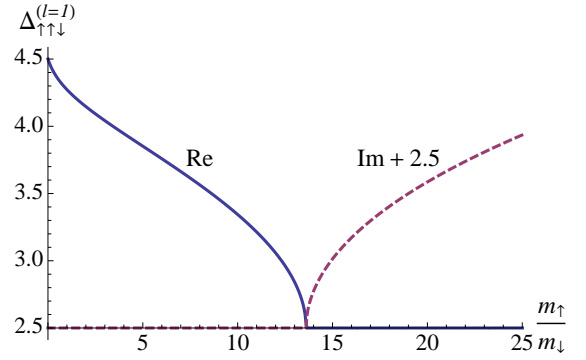


FIG. 4. (Color online) Scaling dimension of the lowest three-body operator $\mathcal{O}_3 = (m_\uparrow + m_\downarrow)\phi(\partial_i\psi_\uparrow) - m_\uparrow(\partial_i\phi)\psi_\uparrow$ as a function of the mass ratio m_\uparrow/m_\downarrow taken from Ref. [88]. The solid curve is its real part and the dashed curve is its imaginary part shifted by +2.5. The scaling dimension of $\mathcal{O}_3^\dagger\mathcal{O}_3$ is given by $2\text{Re}[\Delta_{\mathcal{O}_3}]$.

for $\Delta_{\mathcal{O}} = 4$,

$$-\psi_\sigma^\dagger \overleftrightarrow{\partial}_i \overleftrightarrow{\partial}_j \psi_\sigma, \quad -\partial_i(\psi_\sigma^\dagger \overleftrightarrow{\partial}_j \psi_\sigma), \quad -\partial_i\partial_j(\psi_\sigma^\dagger \psi_\sigma), \quad (3.12a)$$

$$i\psi_\sigma^\dagger \overleftrightarrow{\partial}_i \psi_\sigma, \quad i\partial_t(\psi_\sigma^\dagger \psi_\sigma), \quad -i\phi^\dagger \overleftrightarrow{\partial}_i \phi, \quad -i\partial_i(\phi^\dagger \phi) \quad (3.12b)$$

for $\Delta_{\mathcal{O}} = 5$. Time-space arguments of operators ($x = (t, \mathbf{x})$) are suppressed here and below. Operators accompanied by more spatial or temporal derivatives have higher scaling dimensions.

Here we comment on scaling dimensions of operators involving more ψ or $\phi \sim \psi_\downarrow\psi_\uparrow$ fields. Scaling dimensions of operators with three ψ fields can be computed exactly by solving three-body problems [87, 88]. For example, the lowest two operators are $\mathcal{O} = 2\phi(\partial_i\psi_\sigma) - (\partial_i\phi)\psi_\sigma$ and $\phi\psi_\sigma$ and the products $\mathcal{O}^\dagger\mathcal{O}$ have scaling dimensions $\Delta = 8.54545$ and 9.33244 , respectively. If more ψ fields are involved, it is in general difficult to compute their scaling dimensions. However, with the help of the operator-state correspondence [87, 89, 90], they can be inferred from numerical calculations of energies of particles in a harmonic potential at infinite scattering length [91–100]. For example, the ground-state energy of four fermions, $E = 5.01 \hbar\omega$ [96], implies that the operator $(\phi\phi)^\dagger(\phi\phi)$, which involves the lowest four-body operator $\phi\phi$, has the scaling dimension $\Delta = 10.02$. Because adding more derivatives or fields generally increases scaling dimensions, we conclude that the operators in Eqs. (3.9)–(3.12) are the complete set of local operators with $N_{\mathcal{O}} = 0$ and $\Delta_{\mathcal{O}} \leq 5$ in the case of equal masses.

In the case of unequal masses, however, this is not always the case due to the Efimov effect [101, 102]. The scaling dimension of the lowest three-body operator $\mathcal{O}_3 = (m_\uparrow + m_\downarrow)\phi(\partial_i\psi_\uparrow) - m_\uparrow(\partial_i\phi)\psi_\uparrow$ decreases with increasing mass ratio m_\uparrow/m_\downarrow and eventually reaches $\Delta_{\mathcal{O}_3} = 5/2$ at $m_\uparrow/m_\downarrow = 13.607$ so that $\Delta_{\mathcal{O}_3^\dagger\mathcal{O}_3} = 5$ (see Fig. 4). Furthermore, $\Delta_{\mathcal{O}_3}$ develops an imaginary

part for $m_\uparrow/m_\downarrow > 13.607$, which indicates the Efimov effect [88]. In general, the Efimov effect for N particles implies that the corresponding N -body operator \mathcal{O}_N has the scaling dimension $\Delta_{\mathcal{O}_N} = 5/2 + i s_\ell$ and thus $\Delta_{\mathcal{O}_N^\dagger \mathcal{O}_N} = 5$ with s_ℓ being a real number. The recent finding of the four-body Efimov effect for $m_\uparrow/m_\downarrow > 13.384$ [102] indicates the existence of a four-body operator \mathcal{O}_4 whose scaling dimension becomes $\Delta_{\mathcal{O}_4^\dagger \mathcal{O}_4} = 5$ for $m_\uparrow/m_\downarrow > 13.384$. Therefore, only when the mass ratio is below the lowest critical value for the Efimov effect, the operators in Eqs. (3.9)–(3.12) are supposed to be the complete set of local operators with $N_{\mathcal{O}} = 0$ and $\Delta_{\mathcal{O}} \leq 5$.

C. Wilson coefficients

The Wilson coefficients of local operators can be obtained by matching the matrix elements of both sides of Eq. (3.7) with respect to appropriate few-body states [68–70, 80–86]. Details of such calculations are presented in Appendix A. In short, we use states $\langle \psi_\sigma(p') |$ and $|\psi_\sigma(p)\rangle$ to determine the Wilson coefficients of operators of type $\psi_\sigma^\dagger \psi_\sigma$. The results are

$$W_{\mathbb{1}}(k) = iG(k), \quad (3.13)$$

$$W_{\psi_\downarrow^\dagger \psi_\downarrow}(k) = -iG(k)^2 A(k), \quad (3.14)$$

$$W_{-i\psi_\downarrow^\dagger \vec{\partial}_i \psi_\downarrow}(k) = -iG(k)^2 \frac{\partial}{\partial k_i} A(k), \quad (3.15)$$

$$W_{-\psi_\downarrow^\dagger \vec{\partial}_i \vec{\partial}_j \psi_\downarrow}(k) = -iG(k)^2 \frac{1}{2} \frac{\partial^2}{\partial k_i \partial k_j} A(k), \quad (3.16)$$

$$W_{i\psi_\downarrow^\dagger \vec{\partial}_i \psi_\downarrow}(k) = -iG(k)^2 \frac{\partial}{\partial k_0} A(k), \quad (3.17)$$

$$W_{-\partial_i \partial_j (\psi_\downarrow^\dagger \psi_\downarrow)}(k) = -iA(k) \frac{G(k)^3}{4m} \left[\delta_{ij} + k_i k_j \frac{G(k)}{m} \right], \quad (3.18)$$

$$W_{-i\partial_i (\psi_\downarrow^\dagger \psi_\downarrow)}(k) = W_{-\partial_i (\psi_\downarrow^\dagger \vec{\partial}_j \psi_\downarrow)}(k) = W_{i\partial_i (\psi_\downarrow^\dagger \psi_\downarrow)}(k) = 0, \quad (3.19)$$

and all $W_{\mathcal{O}}(k) = 0$ for $\sigma = \uparrow$, where $A(k)$ is the two-body scattering amplitude between spin-up and -down fermions [see Eq. (3.5)].

On the other hand, states $\langle \phi(p') |$ and $|\phi(p)\rangle$ are used to determine the Wilson coefficients of operators of type $\phi^\dagger \phi$. The results are

$$\begin{aligned} W_{\phi^\dagger \phi}(k) &= -iG(k)^2 T_\uparrow(k, 0; k, 0) \\ &- W_{\psi_\downarrow^\dagger \psi_\downarrow}(k) \int \frac{d\mathbf{q}}{(2\pi)^3} \left(\frac{m}{\mathbf{q}^2} \right)^2 \\ &- W_{-\psi_\downarrow^\dagger \vec{\partial}_i \vec{\partial}_j \psi_\downarrow}(k) \frac{\delta_{ij}}{3} \int \frac{d\mathbf{q}}{(2\pi)^3} \left(\frac{m}{\mathbf{q}} \right)^2 \\ &- W_{i\psi_\downarrow^\dagger \vec{\partial}_i \psi_\downarrow}(k) \frac{-1}{2m} \int \frac{d\mathbf{q}}{(2\pi)^3} \left(\frac{m}{\mathbf{q}} \right)^2, \end{aligned} \quad (3.20)$$

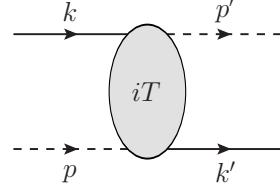


FIG. 5. Three-body scattering amplitude $iT_\uparrow(k, p; k', p')$ between a spin-up fermion (solid line) and a dimer (dashed line).

$$\begin{aligned} W_{-i\phi^\dagger \vec{\partial}_i \phi}(k) &= -iG(k)^2 \frac{\partial}{\partial p_i} T_\uparrow(k, p; k, p) \Big|_{p \rightarrow 0} \\ &- W_{-i\psi_\downarrow^\dagger \vec{\partial}_i \psi_\downarrow}(k) \frac{1}{2} \int \frac{d\mathbf{q}}{(2\pi)^3} \left(\frac{m}{\mathbf{q}^2} \right)^2, \end{aligned} \quad (3.21)$$

$$W_{-i\partial_i (\phi^\dagger \phi)}(k) = -iG(k)^2 \frac{\partial}{\partial p_i} T_\uparrow(k - \frac{p}{2}, \frac{p}{2}; k + \frac{p}{2}, -\frac{p}{2}) \Big|_{p \rightarrow 0}. \quad (3.22)$$

Here, $T_\uparrow(k, p; k', p')$ is the three-body scattering amplitude between a spin-up fermion and a dimer with (k, p) $[(k', p')]$ being their initial (final) energy-momentum (see Fig. 5). As we will show in Sec. III F, $T_\uparrow(k, 0; k, 0)$ and $\partial T_\uparrow(k, p; k, p)/\partial p_i \Big|_{p \rightarrow 0}$ contain infrared divergences that are canceled exactly by the second terms in Eqs. (3.20) and (3.21), respectively. Therefore, it is convenient to combine them and define finite quantities by

$$T_\uparrow^{\text{reg}}(k, 0; k, 0) \equiv T_\uparrow(k, 0; k, 0) - A(k) \int \frac{d\mathbf{q}}{(2\pi)^3} \left(\frac{m}{\mathbf{q}^2} \right)^2 \quad (3.23)$$

and

$$\begin{aligned} &\frac{\partial}{\partial p_i} T_\uparrow^{\text{reg}}(k, p; k, p) \Big|_{p \rightarrow 0} \\ &\equiv \frac{\partial}{\partial p_i} T_\uparrow(k, p; k, p) \Big|_{p \rightarrow 0} - \frac{1}{2} \frac{\partial}{\partial k_i} A(k) \int \frac{d\mathbf{q}}{(2\pi)^3} \left(\frac{m}{\mathbf{q}^2} \right)^2. \end{aligned} \quad (3.24)$$

The regularized three-body scattering amplitude $T_\uparrow^{\text{reg}}(k, 0; k, 0)$ will be computed in Sec. III F. On the other hand, the ultraviolet divergences in the last two terms of Eq. (3.20) are canceled by those from expectation values of local operators as we will see below.

D. Expectation values of local operators

Now the single-particle Green's function of spin-up fermions for an arbitrary few-body or many-body state is obtained by taking the expectation value of Eq. (3.7):

$$\int dy e^{iky} \langle T[\psi_\uparrow(x + \frac{y}{2}) \psi_\uparrow^\dagger(x - \frac{y}{2})] \rangle = \sum_i W_{\mathcal{O}_i}(k) \langle \mathcal{O}_i(x) \rangle. \quad (3.25)$$

The expectation values of local operators in Eqs. (3.9)–(3.12) have simple physical meanings. For example,

$$\langle \psi_\sigma^\dagger \psi_\sigma \rangle = n_\sigma(x) \quad (3.26)$$

and

$$\langle -i\psi_\sigma^\dagger \overleftrightarrow{\nabla} \psi_\sigma \rangle = \mathbf{j}_\sigma(x) \quad (3.27)$$

are the number density and current density of spin- σ fermions and $\langle \partial_i(\psi_\sigma^\dagger \psi_\sigma) \rangle = \partial_i n_\sigma(x)$, $\langle \partial_i \partial_j(\psi_\sigma^\dagger \psi_\sigma) \rangle = \partial_i \partial_j n_\sigma(x)$, $\langle \partial_t(\psi_\sigma^\dagger \psi_\sigma) \rangle = \partial_t n_\sigma(x)$, $\langle \partial_i(-i\psi_\sigma^\dagger \overleftrightarrow{\nabla} \psi_\sigma) \rangle = \partial_i \mathbf{j}_\sigma(x)$ are their spatial or temporal derivatives. Furthermore, it is well known [68–70, 80–86] that the expectation value of $\phi^\dagger \phi$ is related to the contact density $\mathcal{C}(x)$ by

$$\langle \phi^\dagger \phi \rangle = \frac{\mathcal{C}(x)}{m^2}, \quad (3.28)$$

and $\langle \partial_i(\phi^\dagger \phi) \rangle = \partial_i \mathcal{C}(x)/m^2$ is its spatial derivative. The contact density measures the probability of finding spin-up and -down fermions close to each other [67–69]. $\mathbf{j}_\phi(x) \equiv m^2 \langle -i\phi^\dagger \overleftrightarrow{\nabla} \phi \rangle$ is an analog of the current density for dimer field ϕ and shall be called a contact current density.

If the given state is translationally invariant, the expectation values of $-\psi_\sigma^\dagger \overleftrightarrow{\partial}_i \overleftrightarrow{\partial}_j \psi_\sigma$ and $i\psi_\sigma^\dagger \overleftrightarrow{\partial}_t \psi_\sigma$ can be expressed in terms of the momentum distribution function of spin- σ fermions:

$$\rho_\sigma(\mathbf{q}) = \int d\mathbf{y} e^{-i\mathbf{q}\cdot\mathbf{y}} \langle \psi_\sigma^\dagger(t, \mathbf{x} - \frac{\mathbf{y}}{2}) \psi_\sigma(t, \mathbf{x} + \frac{\mathbf{y}}{2}) \rangle. \quad (3.29)$$

By using this definition, the expectation value of $-\psi_\sigma^\dagger \overleftrightarrow{\partial}_i \overleftrightarrow{\partial}_j \psi_\sigma$ is found to be

$$\langle -\psi_\sigma^\dagger \overleftrightarrow{\partial}_i \overleftrightarrow{\partial}_j \psi_\sigma \rangle = \int \frac{d\mathbf{q}}{(2\pi)^3} q_i q_j \rho_\sigma(\mathbf{q}). \quad (3.30)$$

Similarly, the expectation value of $i\psi_\sigma^\dagger \overleftrightarrow{\partial}_t \psi_\sigma$ can be evaluated by using the equation of motion for fermion field ψ_σ :

$$\begin{aligned} \langle i\psi_\sigma^\dagger \overleftrightarrow{\partial}_t \psi_\sigma \rangle &= \frac{1}{2} \left\langle -\psi_\sigma^\dagger \left(\frac{\nabla^2}{2m} \psi_\sigma \right) - \psi_\sigma^\dagger \psi_\downarrow \psi_\uparrow \right\rangle \\ &+ \frac{1}{2} \left\langle -\left(\frac{\nabla^2}{2m} \psi_\sigma^\dagger \right) \psi_\sigma - \phi^\dagger \psi_\downarrow \psi_\uparrow \right\rangle \quad (3.31) \\ &= \int \frac{d\mathbf{q}}{(2\pi)^3} \frac{\mathbf{q}^2}{2m} \rho_\sigma(\mathbf{q}) - \frac{1}{c} \langle \phi^\dagger \phi \rangle. \end{aligned}$$

Both $\langle -\psi_\sigma^\dagger \overleftrightarrow{\partial}_i \overleftrightarrow{\partial}_j \psi_\sigma \rangle$ and $\langle i\psi_\sigma^\dagger \overleftrightarrow{\partial}_t \psi_\sigma \rangle$ contain ultraviolet divergences, which cancel those that already appeared in the last two terms of Eq. (3.20).

E. Single-particle Green's function

Since the derivatives of n_σ , \mathbf{j}_σ , and \mathcal{C} vanish for the translationally invariant state, the single-particle Green's

function of spin-up fermions (3.25) is now written as

$$\begin{aligned} i\mathcal{G}_\uparrow(k) &\equiv \int d\mathbf{y} e^{i\mathbf{k}\cdot\mathbf{y}} \langle T[\psi_\uparrow(x + \frac{\mathbf{y}}{2}) \psi_\uparrow^\dagger(x - \frac{\mathbf{y}}{2})] \rangle \\ &= W_\mathbb{1}(k) + W_{\psi_\downarrow^\dagger \psi_\downarrow}(k) n_\downarrow + W_{-i\psi_\downarrow^\dagger \overleftrightarrow{\nabla} \psi_\downarrow}(k) \cdot \mathbf{j}_\downarrow \\ &+ W_{-\psi_\downarrow^\dagger \overleftrightarrow{\partial}_i \overleftrightarrow{\partial}_j \psi_\downarrow}(k) \int \frac{d\mathbf{q}}{(2\pi)^3} q_i q_j \rho_\downarrow(\mathbf{q}) \\ &+ W_{i\psi_\downarrow^\dagger \overleftrightarrow{\partial}_t \psi_\downarrow}(k) \left[\int \frac{d\mathbf{q}}{(2\pi)^3} \frac{\mathbf{q}^2}{2m} \rho_\downarrow(\mathbf{q}) - \frac{1}{c} \frac{\mathcal{C}}{m^2} \right] \\ &+ W_{\phi^\dagger \phi}(k) \frac{\mathcal{C}}{m^2} + W_{-i\phi^\dagger \overleftrightarrow{\nabla} \phi}(k) \cdot \frac{\mathbf{j}_\phi}{m^2} + \dots \quad (3.32) \end{aligned}$$

By using the expressions of $W_\mathcal{O}(k)$ obtained in Eqs. (3.13)–(3.22), we find that $\mathcal{G}_\uparrow(k)$ can be brought into the usual form

$$\mathcal{G}_\uparrow(k) = \frac{1}{k_0 - \epsilon_k - \Sigma_\uparrow(k) + i0^+}, \quad (3.33)$$

where $\Sigma_\uparrow(k)$ is the self-energy of spin-up fermions given by

$$\begin{aligned} \Sigma_\uparrow(k) &= -A(k) n_\downarrow - \frac{\partial}{\partial \mathbf{k}} A(k) \cdot \mathbf{j}_\downarrow \\ &- \frac{1}{2} \frac{\partial^2}{\partial k_i \partial k_j} A(k) \int \frac{d\mathbf{q}}{(2\pi)^3} \left(q_i q_j - \frac{\delta_{ij}}{3} \mathbf{q}^2 \right) \rho_\downarrow(\mathbf{q}) \\ &- \frac{1}{2} \frac{\partial^2}{\partial k_i \partial k_j} A(k) \frac{\delta_{ij}}{3} \int \frac{d\mathbf{q}}{(2\pi)^3} \mathbf{q}^2 \left(\rho_\downarrow(\mathbf{q}) - \frac{\mathcal{C}}{\mathbf{q}^4} \right) \\ &- \frac{\partial}{\partial k_0} A(k) \left[\int \frac{d\mathbf{q}}{(2\pi)^3} \frac{\mathbf{q}^2}{2m} \left(\rho_\downarrow(\mathbf{q}) - \frac{\mathcal{C}}{\mathbf{q}^4} \right) + \frac{\mathcal{C}}{4\pi m a} \right] \\ &- T_\uparrow^{\text{reg}}(k, 0; k, 0) \frac{\mathcal{C}}{m^2} - \frac{\partial}{\partial \mathbf{p}} T_\uparrow^{\text{reg}}(k, p; k, p) \Big|_{p \rightarrow 0} \cdot \frac{\mathbf{j}_\phi}{m^2} \\ &- \dots \quad (3.34) \end{aligned}$$

Here we eliminated the bare coupling c by using its relationship with the scattering length a [see Eq. (3.4)]. By recalling the large-momentum tail of the momentum distribution function [67–69]

$$\lim_{|\mathbf{q}| \rightarrow \infty} \rho_\sigma(\mathbf{q}) = \frac{\mathcal{C}}{\mathbf{q}^4} + O(\mathbf{q}^{-6}), \quad (3.35)$$

one can see that the ultraviolet divergences in Eq. (3.20) and Eqs. (3.30) and (3.31) canceled out so that $\Sigma_\uparrow(k)$ is now manifestly finite. Corrections to the above expression of $\Sigma_\uparrow(k)$ denoted by “ \dots ” start with $\sim \langle \mathcal{O} \rangle / k^{\Delta_\mathcal{O}-2}$, where \mathcal{O} are all possible operators with the lowest scaling dimension at $\Delta_\mathcal{O} > 5$. In the case of equal masses, $\Delta_\mathcal{O} = 6$.

So far we only assumed that the given state is translationally invariant. In addition, if the given state is rotationally invariant, \mathbf{j}_σ , \mathbf{j}_ϕ , and $\int d\mathbf{q}/(2\pi)^3 (q_i q_j - \delta_{ij} \mathbf{q}^2/3) \rho_\sigma(\mathbf{q})$ vanish. Therefore, in this case, the self-

energy of spin-up fermions is simplified to

$$\begin{aligned} \Sigma_{\uparrow}(k) = & -A(k) n_{\downarrow} - \frac{\partial}{\partial k_0} A(k) \frac{\mathcal{C}}{4\pi m a} - T_{\uparrow}^{\text{reg}}(k, 0; k, 0) \frac{\mathcal{C}}{m^2} \\ & - \left[\frac{m}{3} \sum_{i=1}^3 \frac{\partial^2}{\partial k_i^2} A(k) + \frac{\partial}{\partial k_0} A(k) \right] \\ & \times \int \frac{d\mathbf{q}}{(2\pi)^3} \frac{\mathbf{q}^2}{2m} \left(\rho_{\downarrow}(\mathbf{q}) - \frac{\mathcal{C}}{\mathbf{q}^4} \right) - \dots \end{aligned} \quad (3.36)$$

Note that if the given state has the spin symmetry $\rho_{\uparrow} = \rho_{\downarrow}$, the integral of the momentum distribution function in the last line of Eq. (3.36) can be obtained from the energy density \mathcal{E} by using the energy relationship [67–69]:

$$\sum_{\sigma=\uparrow,\downarrow} \int \frac{d\mathbf{q}}{(2\pi)^3} \frac{\mathbf{q}^2}{2m} \left(\rho_{\sigma}(\mathbf{q}) - \frac{\mathcal{C}}{\mathbf{q}^4} \right) = \mathcal{E} - \frac{\mathcal{C}}{4\pi m a}. \quad (3.37)$$

The pole of the single-particle Green's function (3.33) determines the quasiparticle energy and scattering rate of spin-up fermions in a many-body system [103, 104]:

$$k_0 - \epsilon_{\mathbf{k}} - \Sigma_{\uparrow}(k_0, \mathbf{k}) = 0. \quad (3.38)$$

Because Σ_{\uparrow} is as small as $\sim 1/k$, we can set $k_0 = \epsilon_{\mathbf{k}}$ in $\Sigma_{\uparrow}(k)$ within the accuracy of $O(\mathbf{k}^{-4})$. Then the real part of the solution to Eq. (3.38) gives the quasiparticle energy

$$E_{\uparrow}(\mathbf{k}) = \epsilon_{\mathbf{k}} + \text{Re}[\Sigma_{\uparrow}(\epsilon_{\mathbf{k}}, \mathbf{k})] + O(\mathbf{k}^{-4}), \quad (3.39)$$

while its imaginary part gives the scattering rate²

$$\Gamma_{\uparrow}(\mathbf{k}) = -2 \text{Im}[\Sigma_{\uparrow}(\epsilon_{\mathbf{k}}, \mathbf{k})] + O(\mathbf{k}^{-4}). \quad (3.40)$$

Because

$$\left[\frac{m}{3} \sum_{i=1}^3 \frac{\partial^2}{\partial k_i^2} A(k) + \frac{\partial}{\partial k_0} A(k) \right]_{k_0 \rightarrow \epsilon_{\mathbf{k}}} = O(\mathbf{k}^{-4}) \quad (3.41)$$

² The quasiparticle residue $Z_{\uparrow}(\mathbf{k})$ is given by

$$\begin{aligned} Z_{\uparrow}^{-1}(\mathbf{k}) &= 1 - \frac{\partial}{\partial k_0} \text{Re}[\Sigma_{\uparrow}(k)]_{k_0 \rightarrow E_{\uparrow}(\mathbf{k})} \\ &= 1 + \frac{4\pi}{\left[\frac{1}{4} + \frac{1}{(a|\mathbf{k}|)^2}\right]^2} \frac{n_{\downarrow}}{a|\mathbf{k}|^4} + O(\mathcal{C}/\mathbf{k}^4). \end{aligned}$$

Since $Z_{\uparrow}(\mathbf{k}) = 1 + O(\mathbf{k}^{-4})$, the single-particle spectral density function of spin-up fermions becomes

$$\mathcal{A}_{\uparrow}(k) = -\frac{1}{\pi} \text{Im}[\mathcal{G}_{\uparrow}(k)] = \frac{1}{2\pi} \frac{\Gamma_{\uparrow}(\mathbf{k})}{[k_0 - E_{\uparrow}(\mathbf{k})]^2 + [\frac{1}{2}\Gamma_{\uparrow}(\mathbf{k})]^2}$$

within the accuracy we are currently working. Note that $\mathcal{A}_{\uparrow}(k)$ at a large momentum $|\mathbf{k}| \gg k_F$ but below Fermi sea $k_0 \simeq -\epsilon_{\mathbf{k}}$ (as opposed to $k_0 \simeq \epsilon_{\mathbf{k}}$ in this paper) was studied in Ref. [105]. The single-particle spectral density function was also computed in a self-consistent T -matrix approximation [106] and in a quantum cluster expansion at high temperature [107].

can be found by using the expression of $A(k)$, we arrive at the following form of the on-shell self-energy of spin-up fermions for an arbitrary many-body state with translational and rotational symmetries:³

$$\begin{aligned} \Sigma_{\uparrow}(\epsilon_{\mathbf{k}}, \mathbf{k}) &= \frac{4\pi}{\frac{i}{2} + \frac{1}{a|\mathbf{k}|}} \frac{n_{\downarrow}}{m|\mathbf{k}|} - \frac{i}{\left(\frac{i}{2} + \frac{1}{a|\mathbf{k}|}\right)^2} \frac{\mathcal{C}}{ma|\mathbf{k}|^3} \\ &\quad - t_{\uparrow}^{\text{reg}}(\mathbf{k}; \mathbf{k}) \frac{\mathcal{C}}{m^2} + O(\mathbf{k}^{-4}). \end{aligned} \quad (3.42)$$

Here we denoted the regularized on-shell three-body scattering amplitude by $t_{\uparrow}^{\text{reg}}(\mathbf{k}; \mathbf{p}) \equiv T_{\uparrow}^{\text{reg}}(k, 0; p, k-p)|_{k_0=\epsilon_{\mathbf{k}}, p_0=\epsilon_{\mathbf{p}}}$.

The first term in the on-shell self-energy (3.42) is proportional to the two-body scattering amplitude $A(\epsilon_{\mathbf{k}}, \mathbf{k})$ and the number density of spin-down fermions n_{\downarrow} . Its physical meaning is obvious: It is the contribution from the two-body scattering of the large-momentum spin-up fermion with a spin-down fermion in the medium. Similarly, the last term originates from the three-body scattering of the large-momentum spin-up fermion with a pair of spin-up and -down fermions close to each other, which is described by the dimer field ϕ . The probability of finding such a small pair in the medium is given by the contact density $\mathcal{C} = m^2 \langle \phi^\dagger \phi \rangle$ [67–69]. We note that the spin-down fermion and the small pair of spin-up and -down fermions coming from the medium are treated as being at rest because their characteristic momentum $\sim k_F, \lambda_T^{-1}$ are much smaller than $|\mathbf{k}|$ in the large-momentum expansion [see Eq. (2.1)].

Our remaining task is thus to determine the regularized on-shell three-body scattering amplitude $t_{\uparrow}^{\text{reg}}(\mathbf{k}; \mathbf{k})$ in Eq. (3.42) up to $O(\mathbf{k}^{-4})$, which requires solving a three-body problem. Since it has a form of $t_{\uparrow}^{\text{reg}}(\mathbf{k}; \mathbf{k}) = (m/\mathbf{k}^2) \tilde{t}_{\uparrow}^{\text{reg}}[(a|\mathbf{k}|)^{-1}]$, we need to determine the first two terms in its expansion in terms of $(a|\mathbf{k}|)^{-1}$.

F. Three-body problem

We now compute the three-body scattering amplitude $T_{\uparrow}(k, 0; k, 0)$. Because $T_{\uparrow}(k, 0; k, 0)$ does not solve a closed integral equation, we need to first consider $T_{\uparrow}(k, 0; p, k-p)$, which is a solution to the integral equation depicted in Fig. 6, and then take $p = k$. By denoting

³ In the case of unequal masses $m_{\uparrow} \neq m_{\downarrow}$, this result is modified to

$$\begin{aligned} \Sigma_{\uparrow}(\epsilon_{\mathbf{k}\uparrow}, \mathbf{k}) &= \frac{4\pi}{i\frac{m_{\downarrow}}{M} + \frac{1}{a|\mathbf{k}|}} \frac{n_{\downarrow}}{2\mu|\mathbf{k}|} - \frac{i}{\left(i\frac{m_{\downarrow}}{M} + \frac{1}{a|\mathbf{k}|}\right)^2} \frac{m_{\uparrow}\mathcal{C}}{(2\mu)^2 a|\mathbf{k}|^3} \\ &\quad - T_{\uparrow}^{\text{reg}}(k, 0; k, 0)|_{k_0=\epsilon_{\mathbf{k}\uparrow}} \frac{\mathcal{C}}{(2\mu)^2} + O(\mathbf{k}^{-4}), \end{aligned}$$

where $\epsilon_{\mathbf{k}\sigma} = \mathbf{k}^2/(2m_{\sigma})$, a total mass $M = m_{\uparrow} + m_{\downarrow}$, and a reduced mass $\mu = m_{\uparrow}m_{\downarrow}/(m_{\uparrow} + m_{\downarrow})$.

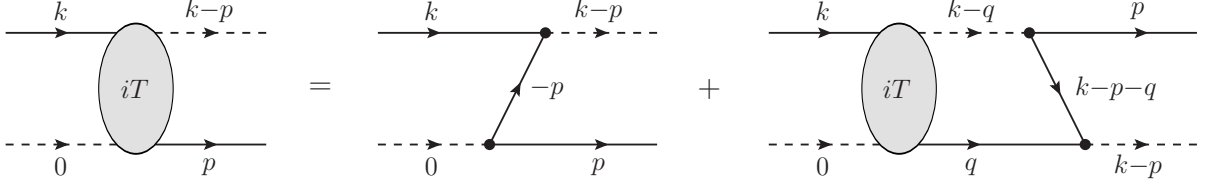


FIG. 6. Integral equation for the three-body scattering amplitude $T_{\uparrow}(k; p) \equiv T_{\uparrow}(k, 0; p, k-p)$ between a spin-up fermion and a dimer.

$T_{\uparrow}(k, 0; p, k-p)$ simply by $T_{\uparrow}(k; p)$, its integral equation is written as

$$T_{\uparrow}(k; p) = G(-p) - i \int \frac{dq_0 d\mathbf{q}}{(2\pi)^4} T_{\uparrow}(k; q) G(q) D(k-p) G(k-p-q). \quad (3.43)$$

Because $T_{\uparrow}(k; q)$ is regular in the lower half plane of q_0 , the integration over q_0 can be easily performed to lead to

$$T_{\uparrow}(k; p) = G(-p) - \int \frac{d\mathbf{q}}{(2\pi)^3} T_{\uparrow}(k; q) D(k-q) G(k-p-q) \Big|_{q_0=\epsilon_q}. \quad (3.44)$$

Then by setting $k_0 = \epsilon_{\mathbf{k}}$, $p_0 = \epsilon_{\mathbf{p}}$ and defining $t_{\uparrow}(\mathbf{k}; \mathbf{p}) \equiv T_{\uparrow}(\epsilon_{\mathbf{k}}, \mathbf{k}; \epsilon_{\mathbf{p}}, \mathbf{p})$, we obtain an integral equation solved by the on-shell three-body scattering amplitude

$$t_{\uparrow}(\mathbf{k}; \mathbf{p}) = -\frac{m}{\mathbf{p}^2} - \int \frac{d\mathbf{q}}{(2\pi)^3} \mathcal{K}_a(\mathbf{k}; \mathbf{p}, \mathbf{q}) t_{\uparrow}(\mathbf{k}; \mathbf{q}), \quad (3.45)$$

where the integral kernel $\mathcal{K}_a(\mathbf{k}; \mathbf{p}, \mathbf{q})$ is defined by

$$\mathcal{K}_a(\mathbf{k}; \mathbf{p}, \mathbf{q}) \equiv \frac{4\pi}{\frac{1}{2}\sqrt{3\mathbf{q}^2 - \mathbf{k}^2 - 2\mathbf{k} \cdot \mathbf{q} - i0^+} - \frac{1}{a}} \times \frac{1}{\mathbf{p}^2 + \mathbf{q}^2 + \mathbf{p} \cdot \mathbf{q} - \mathbf{k} \cdot \mathbf{p} - \mathbf{k} \cdot \mathbf{q} - i0^+}. \quad (3.46)$$

This integral equation has to be solved numerically to determine $t_{\uparrow}(\mathbf{k}; \mathbf{p})$. We have computed $t_{\uparrow}(\mathbf{k}; \mathbf{p})$ at $(a|\mathbf{k}|)^{-1} = 0$ and its first derivative with respect to $(a|\mathbf{k}|)^{-1}$. More details of solving the integral equation (3.45) are presented in Appendix B.

As we mentioned after Eq. (3.22), $t_{\uparrow}(\mathbf{k}; \mathbf{k}) = T_{\uparrow}(k, 0; k, 0)|_{k_0=\epsilon_{\mathbf{k}}}$ contains an infrared divergence. This can be seen by rewriting (3.45) at $\mathbf{p} = \mathbf{k}$ as

$$t_{\uparrow}(\mathbf{k}; \mathbf{k}) = -\frac{m}{\mathbf{k}^2} + \int \frac{d\mathbf{q}}{(2\pi)^3} \mathcal{K}_a(\mathbf{k}; \mathbf{k}, \mathbf{q}) \frac{m}{\mathbf{q}^2} - \int \frac{d\mathbf{q}}{(2\pi)^3} \mathcal{K}_a(\mathbf{k}; \mathbf{k}, \mathbf{q}) \left[t_{\uparrow}(\mathbf{k}; \mathbf{q}) + \frac{m}{\mathbf{q}^2} \right], \quad (3.47)$$

in which the second term is infrared divergent because

$$\mathcal{K}_a(\mathbf{k}; \mathbf{k}, \mathbf{q}) \rightarrow \frac{4\pi}{-i\frac{|\mathbf{k}|}{2} - \frac{1}{a}\mathbf{q}^2} \quad (3.48)$$

at $|\mathbf{q}| \rightarrow 0$. However, this infrared divergence is canceled exactly by the second term in Eq. (3.23). Therefore,

the regularized three-body scattering amplitude defined there is free of divergences and its on-shell version is given by

$$t_{\uparrow}^{\text{reg}}(\mathbf{k}; \mathbf{k}) = T_{\uparrow}^{\text{reg}}(k, 0; k, 0)|_{k_0=\epsilon_{\mathbf{k}}} = -\frac{m}{\mathbf{k}^2} + \int \frac{d\mathbf{q}}{(2\pi)^3} \left[\mathcal{K}_a(\mathbf{k}; \mathbf{k}, \mathbf{q}) - \frac{4\pi}{-i\frac{|\mathbf{k}|}{2} - \frac{1}{a}\mathbf{q}^2} \right] \frac{m}{\mathbf{q}^2} - \int \frac{d\mathbf{q}}{(2\pi)^3} \mathcal{K}_a(\mathbf{k}; \mathbf{k}, \mathbf{q}) \left[t_{\uparrow}(\mathbf{k}; \mathbf{q}) + \frac{m}{\mathbf{q}^2} \right]. \quad (3.49)$$

By using the numerical solutions of $t_{\uparrow}(\mathbf{k}; \mathbf{q})$ at $(a|\mathbf{k}|)^{-1} = 0$ and its first derivative, the expansion of $t_{\uparrow}^{\text{reg}}(\mathbf{k}; \mathbf{k})$ in terms of $(a|\mathbf{k}|)^{-1}$ is found to be

$$t_{\uparrow}^{\text{reg}}(\mathbf{k}; \mathbf{k}) = \left[3.771 + \frac{15.05}{a|\mathbf{k}|} i + O(\mathbf{k}^{-2}) \right] \frac{m}{\mathbf{k}^2}. \quad (3.50)$$

These numbers are universal (i.e., independent of short-range physics). We note that the Born approximation [the first term in Eq. (3.49)] gives $t_{\uparrow}^{\text{reg}}(\mathbf{k}; \mathbf{k})|_{\text{Born}} = (-1)m/\mathbf{k}^2$, which is wrong even in its sign.

The necessity of the above subtraction procedure is physically understood in the following way: The ‘‘bare’’ three-body scattering amplitude $t_{\uparrow}(\mathbf{k}; \mathbf{k})$ describes the three-body scattering of the large-momentum spin-up fermion with a pair of spin-up and -down fermions at rest. $t_{\uparrow}(\mathbf{k}; \mathbf{k})$ is obtained from the integral equation depicted in Fig. 6, which actually includes a process in which the large-momentum spin-up fermion collides only with the spin-down fermion coming from the pair and the other spin-up fermion remains a spectator staying away from the scattering event. This is seen by recalling that the momentum \mathbf{q} in the second term of Eq. (3.47) is the relative momentum between spin-up and -down fermions constituting the pair and thus small $|\mathbf{q}|$ corresponds to the large interparticle separation. This process is essentially the two-body scattering which is already included in the first term of Eq. (3.42). Therefore, to avoid the double counting, the contribution of this two-body scattering process has to be subtracted from the bare three-body scattering amplitude. This leads to the regularized three-body scattering amplitude $t_{\uparrow}^{\text{reg}}(\mathbf{k}; \mathbf{k})$ in Eq. (3.49), which appears in front of the contact density in the last term of Eq. (3.42).

Finally, by substituting the numerical solution of the three-body problem (3.50) into Eq. (3.42), we find that

the on-shell self-energy of spin-up fermions has the following systematic expansion in the large-momentum limit:

$$\begin{aligned} \Sigma_{\uparrow}(\epsilon_{\mathbf{k}}, \mathbf{k}) = & \left[16\pi \left(-i + \frac{2}{a|\mathbf{k}|} + \frac{4}{a^2|\mathbf{k}|^2}i \right) \frac{n_{\downarrow}}{|\mathbf{k}|^3} \right. \\ & \left. - \left(7.54 + \frac{22.1}{a|\mathbf{k}|}i \right) \frac{C}{|\mathbf{k}|^4} + O(\mathbf{k}^{-6}) \right] \epsilon_{\mathbf{k}}. \end{aligned} \quad (3.51)$$

This result combined with Eqs. (3.39) and (3.40) leads to the quasiparticle energy and scattering rate of spin-up fermions presented previously in Eqs. (2.2) and (2.3).

IV. SPINLESS BOSE GAS

Here we study properties of an energetic atom in a spinless Bose gas and derive its quasiparticle energy and scattering rate presented in Eqs. (2.4) and (2.5). The analysis is similar to the previous case of a spin-1/2 Fermi gas.

A. Formulation

The Lagrangian density describing spinless bosons with a zero-range interaction is

$$\begin{aligned} \mathcal{L}_B = & \psi^{\dagger} \left(i\partial_t + \frac{\nabla^2}{2m} \right) \psi + \frac{c}{2} \psi^{\dagger} \psi^{\dagger} \psi \psi \quad (4.1) \\ = & \psi^{\dagger} \left(i\partial_t + \frac{\nabla^2}{2m} \right) \psi - \frac{1}{2c} \phi^{\dagger} \phi + \frac{1}{2} \phi^{\dagger} \psi \psi + \frac{1}{2} \psi^{\dagger} \psi^{\dagger} \phi, \end{aligned}$$

where an auxiliary dimer field $\phi = c\psi\psi$ is introduced to decouple the interaction term. The propagator of boson field ψ in the vacuum is given by

$$G(k) = \frac{1}{k_0 - \epsilon_{\mathbf{k}} + i0^+} \quad \left(\epsilon_{\mathbf{k}} \equiv \frac{\mathbf{k}^2}{2m} \right). \quad (4.2)$$

Also by using the standard regularization procedure to relate the bare coupling c to the scattering length a ,

$$\frac{1}{c} = \int_{|\mathbf{k}| < \Lambda} \frac{d\mathbf{k}}{(2\pi)^3} \frac{m}{\mathbf{k}^2} - \frac{m}{4\pi a}, \quad (4.3)$$

the propagator of dimer field ϕ in the vacuum is found to be

$$D(k) = -\frac{8\pi}{m} \frac{1}{\sqrt{\frac{\mathbf{k}^2}{4} - mk_0 - i0^+} - \frac{1}{a}}. \quad (4.4)$$

$D(k)$ coincides with the two-body scattering amplitude $A(k)$ between two identical bosons up to a minus sign; $A(k) = -D(k)$ (see Fig. 3). Note that $D(k)$ and $A(k)$ in the case of bosons are twice as large as those for fermions [see Eq. (3.5)].

Our task here is to understand the behavior of the single-particle Green's function of bosons

$$\int dy e^{iky} \langle T[\psi(x + \frac{y}{2})\psi^{\dagger}(x - \frac{y}{2})] \rangle \quad (4.5)$$

in the large-energy-momentum limit $k \rightarrow \infty$ for an arbitrary few-body or many-body state.

B. Operator product expansion

According to the operator product expansion [68–70, 80–86], the product of operators in Eq. (4.5) can be expressed in terms of a series of local operators \mathcal{O} :

$$\int dy e^{iky} T[\psi(x + \frac{y}{2})\psi^{\dagger}(x - \frac{y}{2})] = \sum_i W_{\mathcal{O}_i}(k) \mathcal{O}_i(x). \quad (4.6)$$

The local operators \mathcal{O} appearing in the right-hand side must have a particle number $N_{\mathcal{O}} = 0$. By recalling $\Delta_{\psi} = 3/2$ and $\Delta_{\phi} = 2$ [87], we can find thirteen types of local operators with $N_{\mathcal{O}} = 0$ up to scaling dimensions $\Delta_{\mathcal{O}} = 5$:

$$\mathbb{1} \quad (\text{identity}) \quad (4.7)$$

for $\Delta_{\mathcal{O}} = 0$,

$$\psi^{\dagger} \psi \quad (4.8)$$

for $\Delta_{\mathcal{O}} = 3$,

$$-i\psi^{\dagger} \overleftrightarrow{\partial}_i \psi, \quad -i\partial_i(\psi^{\dagger} \psi), \quad \phi^{\dagger} \phi \quad (4.9)$$

for $\Delta_{\mathcal{O}} = 4$,

$$-\psi^{\dagger} \overleftrightarrow{\partial}_i \overleftrightarrow{\partial}_j \psi, \quad -\partial_i(\psi^{\dagger} \overleftrightarrow{\partial}_j \psi), \quad -\partial_i \partial_j(\psi^{\dagger} \psi), \quad (4.10a)$$

$$i\psi^{\dagger} \overleftrightarrow{\partial}_i \psi, \quad i\partial_i(\psi^{\dagger} \psi), \quad -i\phi^{\dagger} \overleftrightarrow{\partial}_i \phi, \quad -i\partial_i(\phi^{\dagger} \phi), \quad (4.10b)$$

$$(\phi\psi)^{\dagger}(\phi\psi) \quad (4.10c)$$

for $\Delta_{\mathcal{O}} = 5$.

The striking difference between the cases of fermions and bosons is the presence of the Efimov effect in a system of three identical bosons [108]. As we discussed at the end of Sec. III B, the Efimov effect implies that the corresponding three-body operator $\phi\psi$ has the scaling dimension $\Delta = 5/2 + is_0$ so that $(\phi\psi)^{\dagger}(\phi\psi)$ in Eq. (4.10c) has $\Delta = 5$ [70, 88]. The determination of its Wilson coefficient requires solving a four-body problem, which is beyond the scope of this paper. Therefore, in this section, we only consider the local operators with $N_{\mathcal{O}} = 0$ and $\Delta_{\mathcal{O}} \leq 4$ in Eqs. (4.7)–(4.9). As before, their expectation values have simple physical meanings such as the number density of bosons,

$$\langle \psi^{\dagger} \psi \rangle = n(x), \quad (4.11)$$

and its spatial derivative $\langle \partial_i(\psi^\dagger \psi) \rangle = \partial_i n(x)$, the current density of bosons,

$$\langle -i\psi^\dagger \overleftrightarrow{\nabla} \psi \rangle = \mathbf{j}(x), \quad (4.12)$$

and the contact density

$$\langle \phi^\dagger \phi \rangle = \frac{\mathcal{C}(x)}{m^2}, \quad (4.13)$$

which measures the probability of finding two bosons close to each other. This definition of the contact density coincides with that used in Ref. [70] and thus the large-momentum tail of the momentum distribution function of bosons is given by $\lim_{|\mathbf{q}| \rightarrow \infty} \rho(\mathbf{q}) = \mathcal{C}/\mathbf{q}^4 + O(\mathbf{q}^{-5})$.

C. Wilson coefficients

The Wilson coefficients of local operators can be obtained by matching the matrix elements of both sides of Eq. (4.6) with respect to appropriate few-body states [68–70, 80–86]. Details of such calculations are presented in Appendix A. The results are formally equivalent to those in the case of fermions as long as $A(k)$ in Eqs. (3.13)–(3.22) is understood as the two-body scattering amplitude between two identical bosons [see Eq. (4.4)]:

$$W_{\mathbb{1}}(k) = iG(k), \quad (4.14)$$

$$W_{\psi^\dagger \psi}(k) = -iG(k)^2 A(k), \quad (4.15)$$

$$W_{-i\psi^\dagger \overleftrightarrow{\partial}_i \psi}(k) = -iG(k)^2 \frac{\partial}{\partial k_i} A(k), \quad (4.16)$$

$$W_{-i\partial_i(\psi^\dagger \psi)}(k) = 0, \quad (4.17)$$

$$W_{\phi^\dagger \phi}(k) = -iG(k)^2 T(k, 0; k, 0) - W_{\psi^\dagger \psi}(k) \int \frac{d\mathbf{q}}{(2\pi)^3} \left(\frac{m}{\mathbf{q}^2} \right)^2. \quad (4.18)$$

Here, $T(k, p; k', p')$ is the three-body scattering amplitude between a boson and a dimer with (k, p) [(k', p')] being their initial (final) energy-momentum (see Fig. 5). Because $T(k, 0; k, 0)$ contains an infrared divergence that is canceled exactly by the second term in Eq. (4.18), it is convenient to combine them and define a finite quantity by

$$T^{\text{reg}}(k, 0; k, 0) \equiv T(k, 0; k, 0) - A(k) \int \frac{d\mathbf{q}}{(2\pi)^3} \left(\frac{m}{\mathbf{q}^2} \right)^2. \quad (4.19)$$

This regularized three-body scattering amplitude will be computed in Sec. IV E.

D. Single-particle Green's function

Now the single-particle Green's function of bosons for an arbitrary few-body or many-body state is obtained by taking the expectation value of Eq. (4.6). By using the expressions of $W_{\mathcal{O}}(k)$ obtained in Eqs. (4.14)–(4.18), we find that it can be brought into the usual form

$$i\mathcal{G}(k) \equiv \int dy e^{iky} \langle T[\psi(x + \frac{y}{2})\psi^\dagger(x - \frac{y}{2})] \rangle = \frac{i}{k_0 - \epsilon_{\mathbf{k}} - \Sigma(k) + i0^+}, \quad (4.20)$$

where $\Sigma(k)$ is the self-energy of bosons given by

$$\Sigma(k) = -A(k)n - \frac{\partial}{\partial \mathbf{k}} A(k) \cdot \mathbf{j} - T^{\text{reg}}(k, 0; k, 0) \frac{\mathcal{C}}{m^2} - \dots. \quad (4.21)$$

Corrections to this expression denoted by “...” start with $\sim \langle \mathcal{O} \rangle / k^{\Delta_{\mathcal{O}} - 2}$, where \mathcal{O} are all operators in Eq. (4.10) with the scaling dimension $\Delta_{\mathcal{O}} = 5$.

As in Eq. (3.38), the pole of the single-particle Green's function (4.20) determines the quasiparticle energy and scattering rate of bosons in a many-body system. Within the accuracy of $O(\mathbf{k}^{-4})$, the real part of $\Sigma(\epsilon_{\mathbf{k}}, \mathbf{k})$ gives the quasiparticle energy

$$E(\mathbf{k}) = \epsilon_{\mathbf{k}} + \text{Re}[\Sigma(\epsilon_{\mathbf{k}}, \mathbf{k})] + O(\mathbf{k}^{-4}), \quad (4.22)$$

while its imaginary part gives the scattering rate

$$\Gamma(\mathbf{k}) = -2 \text{Im}[\Sigma(\epsilon_{\mathbf{k}}, \mathbf{k})] + O(\mathbf{k}^{-4}). \quad (4.23)$$

By setting $k_0 = \epsilon_{\mathbf{k}}$ in Eq. (4.21), the on-shell self-energy of bosons for an arbitrary state is found to be

$$\Sigma(\epsilon_{\mathbf{k}}, \mathbf{k}) = \frac{8\pi}{\frac{i}{2} + \frac{1}{a|\mathbf{k}|}} \frac{n}{m|\mathbf{k}|} + \frac{4\pi i}{(\frac{i}{2} + \frac{1}{a|\mathbf{k}|})^2} \frac{\hat{\mathbf{k}} \cdot \mathbf{j}}{m|\mathbf{k}|^2} - t^{\text{reg}}(\mathbf{k}; \mathbf{k}) \frac{\mathcal{C}}{m^2} + O(\mathbf{k}^{-3}), \quad (4.24)$$

where we denoted the regularized on-shell three-body scattering amplitude by $t^{\text{reg}}(\mathbf{k}; \mathbf{p}) \equiv T^{\text{reg}}(k, 0; p, k-p)|_{k_0=\epsilon_{\mathbf{k}}, p_0=\epsilon_{\mathbf{p}}}$. The second term in Eq. (4.24), which is proportional to $\partial A(k_0, \mathbf{k})/\partial \mathbf{k}|_{k_0 \rightarrow \epsilon_{\mathbf{k}}}$ and the current density \mathbf{j} , represents the contribution from the two-body scattering in which the large-momentum boson collides with a boson moving with a small momentum. The physical meanings of the other two terms were discussed at the end of Sec. III E.

Our remaining task is thus to determine the regularized on-shell three-body scattering amplitude $t^{\text{reg}}(\mathbf{k}; \mathbf{k})$ in Eq. (4.24) up to $O(\mathbf{k}^{-3})$, which requires solving a three-body problem. Because three identical bosons suffer from the Efimov effect, $(\mathbf{k}^2/m) t^{\text{reg}}(\mathbf{k}; \mathbf{k}) = \hat{t}^{\text{reg}}[(a|\mathbf{k}|)^{-1}, |\mathbf{k}|/\kappa_*]$ depends not only on $(a|\mathbf{k}|)^{-1}$ but also on $|\mathbf{k}|/\kappa_*$, where κ_* is the Efimov parameter. As long as we are interested in $t^{\text{reg}}(\mathbf{k}; \mathbf{k}) \sim m/\mathbf{k}^2$ within the accuracy of $O(\mathbf{k}^{-3})$, we can set the scattering length infinite

$(a|\mathbf{k}|)^{-1} = 0$, because the dependence on it appears only from $O(\mathbf{k}^{-3})$. Then the resulting quantity $\tilde{t}^{\text{reg}}[0, |\mathbf{k}|/\kappa_*]$ needs to be determined, which is a log-periodic function of $|\mathbf{k}|/\kappa_*$ as we will see below.

E. Three-body problem

We now compute the three-body scattering amplitude $T(k, 0; k, 0)$. Because $T(k, 0; k, 0)$ does not solve a closed integral equation, we need to first consider $T(k, 0; p, k-p)$, which is a solution to the integral equation depicted in Fig. 6, and then take $p = k$. By denoting $T(k, 0; p, k-p)$ simply by $T(k; p)$, its integral equation is written as

$$T(k; p) = -G(-p) + i \int \frac{dq_0 d\mathbf{q}}{(2\pi)^4} T(k; q) G(q) D(k-p) G(k-p-q). \quad (4.25)$$

Then by performing the integration over q_0 and defining $t(\mathbf{k}; \mathbf{p}) \equiv T(\epsilon_{\mathbf{k}}, \mathbf{k}; \epsilon_{\mathbf{p}}, \mathbf{p})$, we obtain an integral equation solved by the on-shell three-body scattering amplitude

$$t(\mathbf{k}; \mathbf{p}) = \frac{m}{\mathbf{p}^2} + 2 \int \frac{d\mathbf{q}}{(2\pi)^3} \mathcal{K}_a(\mathbf{k}; \mathbf{p}, \mathbf{q}) t(\mathbf{k}; \mathbf{q}), \quad (4.26)$$

where the integral kernel $\mathcal{K}_a(\mathbf{k}; \mathbf{p}, \mathbf{q})$ is defined in Eq. (3.46). This integral equation has to be solved numerically to determine $t(\mathbf{k}; \mathbf{p})$ at $(a|\mathbf{k}|)^{-1} = 0$.

Compared to the case of fermions in Eq. (3.45), both signs in the right-hand side of Eq. (4.26) are opposite due to different statistics and the second term has the factor 2 originating from the fact that the two-body scattering amplitude between two identical bosons is twice larger. The former difference leads to the striking consequence: As is known [109, 110], the three-boson problem described by the integral equation (4.26) is ill defined without introducing an ultraviolet momentum cutoff Λ in the zero orbital angular momentum channel. Λ can be related to the Efimov parameter κ_* which is defined so that three identical bosons at infinite scattering length have the following infinite tower of binding energies:

$$E_n \rightarrow -e^{-2\pi n/s_0} \frac{\kappa_*^2}{m} \quad (n \rightarrow \infty), \quad (4.27)$$

with $s_0 = 1.00624$ [110, 111]. Because κ_* is defined up to multiplicative factors of $\lambda \equiv e^{\pi/s_0} = 22.6944$, the solution to the integral equation (4.26) at $(a|\mathbf{k}|)^{-1} = 0$ has to be a log-periodic function of $|\mathbf{k}|/\kappa_*$. We have computed such $t(\mathbf{k}; \mathbf{p})$ in a range $1 \leq |\mathbf{k}|/\kappa_* \leq \lambda^2$ corresponding to two periods. More details of solving the integral equation (4.26) are presented in Appendix B.

As we mentioned after Eq. (4.18), $t(\mathbf{k}; \mathbf{k}) = T(k, 0; k, 0)|_{k_0=\epsilon_k}$ contains an infrared divergence. This can be seen by rewriting (4.26) at $\mathbf{p} = \mathbf{k}$ as

$$t(\mathbf{k}; \mathbf{k}) = \frac{m}{\mathbf{k}^2} + 2 \int \frac{d\mathbf{q}}{(2\pi)^3} \mathcal{K}_a(\mathbf{k}; \mathbf{k}, \mathbf{q}) \frac{m}{\mathbf{q}^2} + 2 \int \frac{d\mathbf{q}}{(2\pi)^3} \mathcal{K}_a(\mathbf{k}; \mathbf{k}, \mathbf{q}) \left[t(\mathbf{k}; \mathbf{q}) - \frac{m}{\mathbf{q}^2} \right], \quad (4.28)$$

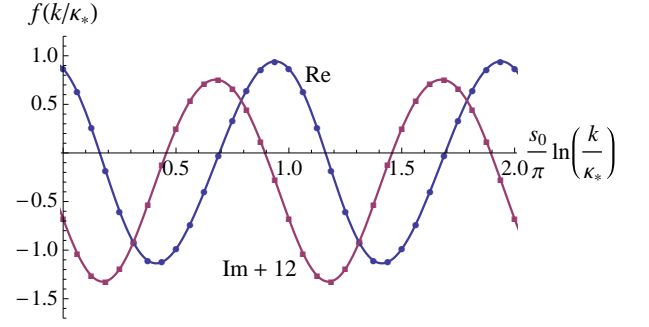


FIG. 7. (Color online) Universal log-periodic function $f(|\mathbf{k}|/\kappa_*)$ defined in Eq. (4.30) as a function of $(s_0/\pi) \ln(|\mathbf{k}|/\kappa_*)$. Circles (squares) with steps $1/16$ correspond to its real part (imaginary part shifted by $+12$) and solid curves are fits by the approximate formula (4.31). Two periods in the range $1 \leq |\mathbf{k}|/\kappa_* \leq e^{2\pi/s_0}$ are shown here.

in which the second term is infrared divergent at $|\mathbf{q}| \rightarrow 0$ [see Eq. (3.48)]. However, this infrared divergence is canceled exactly by the second term in Eq. (4.19). Therefore, the regularized three-body scattering amplitude defined there is free of divergences and its on-shell version is given by

$$\begin{aligned} t^{\text{reg}}(\mathbf{k}; \mathbf{k}) &= T^{\text{reg}}(k, 0; k, 0)|_{k_0=\epsilon_k} \\ &= \frac{m}{\mathbf{k}^2} + 2 \int \frac{d\mathbf{q}}{(2\pi)^3} \left[\mathcal{K}_a(\mathbf{k}; \mathbf{k}, \mathbf{q}) - \frac{4\pi}{-i\frac{|\mathbf{k}|}{2} - \frac{1}{a}} \frac{1}{\mathbf{q}^2} \right] \frac{m}{\mathbf{q}^2} \\ &\quad + 2 \int \frac{d\mathbf{q}}{(2\pi)^3} \mathcal{K}_a(\mathbf{k}; \mathbf{k}, \mathbf{q}) \left[t(\mathbf{k}; \mathbf{q}) - \frac{m}{\mathbf{q}^2} \right]. \end{aligned} \quad (4.29)$$

The physical meaning of this subtraction procedure was discussed at the end of Sec. III F.

By using the numerical solutions of $t(\mathbf{k}; \mathbf{q})$ at $(a|\mathbf{k}|)^{-1} = 0$, $t^{\text{reg}}(\mathbf{k}; \mathbf{k})$ is computed in the range $1 \leq |\mathbf{k}|/\kappa_* \leq \lambda^2$ and the resulting universal function

$$f\left(\frac{|\mathbf{k}|}{\kappa_*}\right) \equiv \frac{\mathbf{k}^2}{m} t^{\text{reg}}(\mathbf{k}; \mathbf{k})|_{(a|\mathbf{k}|)^{-1}=0} \quad (4.30)$$

is shown by points in Fig. 7. The logarithmic periodicity is clearly seen and we find that our numerical results are excellently reproduced by

$$f(z) \approx X + \frac{Y_1 \cos(2s_0 \ln z + \delta_1) + iY_2 \sin(2s_0 \ln z + \delta_1)}{1 + Z \sin(2s_0 \ln z + \delta_2)}, \quad (4.31)$$

with fitting parameters $X \approx -0.09656 - 12.20i$, $Y_1 \approx 1.036$, $Y_2 \approx -1.032$, $Z \approx -0.08460$, and $\delta_1 \approx \delta_2 \approx 0.4653$. The approximate formula (4.31) is plotted by solid curves in Fig. 7 and differs from the numerical points only by the amount $\lesssim 4 \times 10^{-6}$. Whether Eq. (4.31) is the true analytic expression of $f(|\mathbf{k}|/\kappa_*)$ or not needs to be investigated further.

Finally, by substituting the numerical solution of the three-body problem (4.30) into Eq. (4.24), we find that

the on-shell self-energy of bosons has the following systematic expansion in the large-momentum limit:

$$\begin{aligned} \Sigma(\epsilon_{\mathbf{k}}, \mathbf{k}) = & \left[32\pi \left(-i + \frac{2}{a|\mathbf{k}|} \right) \frac{n}{|\mathbf{k}|^3} - 32\pi i \frac{\hat{\mathbf{k}} \cdot \mathbf{j}}{|\mathbf{k}|^4} \right. \\ & \left. - 2f \left(\frac{|\mathbf{k}|}{\kappa_*} \right) \frac{\mathcal{C}}{|\mathbf{k}|^4} + O(\mathbf{k}^{-5}) \right] \epsilon_{\mathbf{k}}. \end{aligned} \quad (4.32)$$

This result combined with Eqs. (4.22) and (4.23) leads to the quasiparticle energy and scattering rate of bosons presented previously in Eqs. (2.4) and (2.5), where the contribution of the current density is dropped by assuming translational and rotational symmetries.

V. DIFFERENTIAL SCATTERING RATE

So far we have studied a quasiparticle energy and a “total” scattering rate of an energetic atom both in a spin-1/2 Fermi gas (Sec. III) and in a spinless Bose gas (Sec. IV). Often in physics, differential scattering rates or cross sections also reveal many important phenomena. For example, differential cross sections in neutron-deuteron or proton-deuteron scatterings at intermediate or higher energies are important to reveal the existence of three-nucleon forces in nuclei [29–31]. Also, momentum and angular resolutions have been essential to reveal short-range pair correlations in nuclei from two-nucleon knockout reactions by high-energy protons or electrons [32, 33]. Furthermore, differential cross sections of high-energy neutrons scattered by liquid helium have been employed to extract the momentum distribution of helium atoms [40–44].

Now in ultracold-atom experiments, one can in principle imagine shooting an energetic spin-up fermion (boson) into a Fermi (Bose) gas trapped with a finite depth and measure the angle distribution of spin-up fermions (bosons) coming out of the trap. Here one needs to be cautious, however, because the incident atom cannot be distinguished from atoms constituting the atomic gas. For example, there is a process in which the energetic spin-up fermion collides with a spin-down fermion in the medium and they escape from the trap. However, such a spin-down fermion may be accompanied by another spin-up fermion nearby so that they form a small pair described by the contact density. What happens to this spin-up fermion when its partner is kicked out by the incident atom? Whether it escapes from the trap to be measured or not has to be imposed consistently on all calculations, which appears intractable in our systematic large-momentum expansion without introducing phenomenological procedures.

In order to avoid this problem and unambiguously determine the differential scattering rate, it is therefore favorable to consider an incident atom that is distinguishable from the rest of the atoms constituting the atomic gas. In this section, we imagine shooting a different spin state of atoms into a spin-1/2 Fermi gas or a spinless

Bose gas with a large momentum and measure its angle distribution. The differential scattering rate presented in Eq. (2.6) will be derived from the total scattering rate by using the optical theorem, while it coincides with the one expected on physical grounds. Here translational or rotational symmetries are not assumed and thus the densities depend on a time-space coordinate $(x) = (t, \mathbf{x})$.

A. Spin-1/2 Fermi gas

We first consider the case of a spin-1/2 Fermi gas. Here a probe atom is denoted by χ and assumed to interact with spin-up and -down fermions by scattering lengths a_\uparrow and a_\downarrow , respectively. The Lagrangian density describing such a problem is

$$\mathcal{L} = \chi^\dagger \left(i\partial_t + \frac{\nabla^2}{2m_\chi} \right) \chi + \sum_{\sigma=\uparrow,\downarrow} c_\sigma \chi^\dagger \psi_\sigma^\dagger \psi_\sigma \chi + \mathcal{L}_F, \quad (5.1)$$

where \mathcal{L}_F defined in Eq. (3.1) describes spin-1/2 fermions interacting with each other by a scattering length a . For simplicity, we shall assume that all particles have the same mass $m = m_\chi = m_\uparrow = m_\downarrow$. In analogy with Eq. (3.5), the two-body scattering amplitude between the χ atom and a spin- σ fermion is given by

$$A_\sigma(k) = \frac{4\pi}{m} \frac{1}{\sqrt{\frac{k^2}{4} - mk_0 - i0^+ - \frac{1}{a_\sigma}}}. \quad (5.2)$$

The behavior of the single-particle Green’s function of the χ atom,

$$i\mathcal{G}_\chi(x; k) \equiv \int dy e^{iky} \langle T[\chi(x + \frac{y}{2})\chi^\dagger(x - \frac{y}{2})] \rangle, \quad (5.3)$$

in the large-energy-momentum limit $k \rightarrow \infty$ can be understood by using the operator product expansion as in Secs. III and IV. Since three distinguishable particles ($\chi, \uparrow, \downarrow$) with zero-range interactions suffer from the Efimov effect [110, 111], we only consider local operators with $N_{\mathcal{O}} = 0$ up to scaling dimensions $\Delta_{\mathcal{O}} = 4$ (see discussions in Sec. IV B). Then in analogy with Eqs. (4.20) and (4.21), $\mathcal{G}_\chi(x; k)$ can be written in the usual form

$$\mathcal{G}_\chi(x; k) = \frac{1}{k_0 - \epsilon_{\mathbf{k}} - \Sigma_\chi(x; k) + i0^+}, \quad (5.4)$$

where $\Sigma_\chi(x; k)$ is the self-energy of the χ atom given by

$$\begin{aligned} \Sigma_\chi(x; k) = & - \sum_{\sigma=\uparrow,\downarrow} \left[A_\sigma(k) n_\sigma(x) + \frac{\partial}{\partial \mathbf{k}} A_\sigma(k) \cdot \mathbf{j}_\sigma(x) \right] \\ & - T_\chi^{\text{reg}}(k, 0; k, 0) \frac{\mathcal{C}(x)}{m^2} - \dots \end{aligned} \quad (5.5)$$

Here, $n_\sigma(x) = \langle \psi_\sigma^\dagger \psi_\sigma \rangle$ and $\mathbf{j}_\sigma(x) = \langle -i\psi_\sigma^\dagger \overleftrightarrow{\nabla} \psi_\sigma \rangle$ are the number density and current density of spin- σ fermions

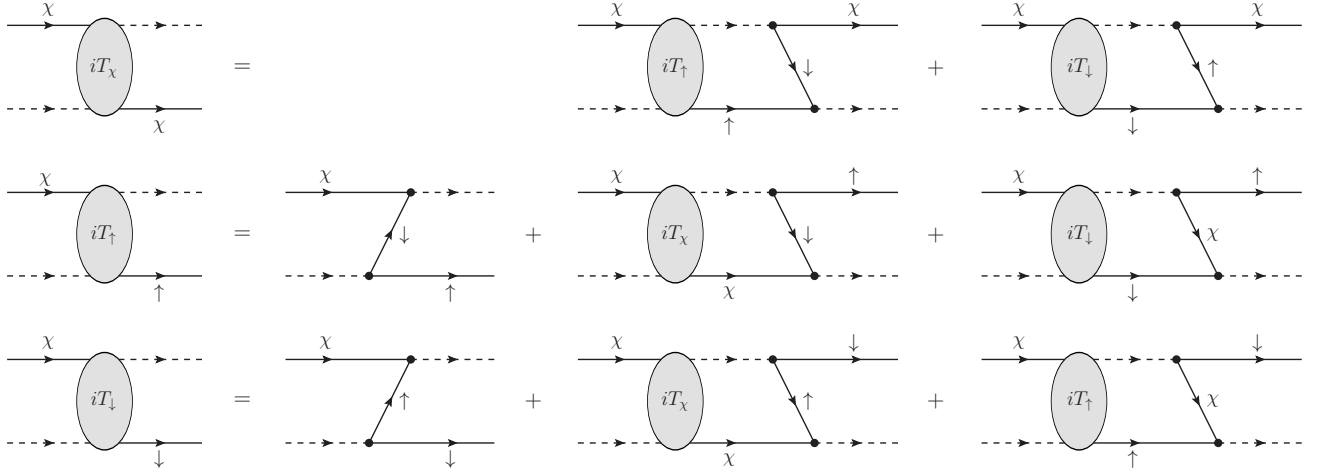


FIG. 8. Set of integral equations for three-body scattering amplitudes $T_\chi(k; p)$, $T_\uparrow(k; p)$, and $T_\downarrow(k; p)$ involving three distinguishable particles χ and spin- \uparrow and \downarrow fermions. Momentum labels are the same as those in Fig. 6.

and $\mathcal{C}(x) = m^2 \langle \phi^\dagger \phi \rangle$ is the contact density of a spin-1/2 Fermi gas. Note that these parameters only refer to many-body properties of the given spin-1/2 Fermi gas and do not involve the information related to the χ atom. On the other hand, $T_\chi^{\text{reg}}(k, 0; k, 0)$ is a finite quantity defined by

$$T_\chi^{\text{reg}}(k, 0; k, 0) \quad (5.6)$$

$$\equiv T_\chi(k, 0; k, 0) - [A_\uparrow(k) + A_\downarrow(k)] \int \frac{d\mathbf{q}}{(2\pi)^3} \left(\frac{m}{q^2} \right)^2,$$

where $T_\chi(k, p; k', p')$ is the three-body scattering amplitude between the χ atom and a dimer composed of spin-up and -down fermions with (k, p) [(k', p')] being their initial (final) energy-momentum (see Fig. 5). Corrections to the above expression of $\Sigma_\chi(x; k)$ denoted by “...” start with $\sim \langle \mathcal{O} \rangle / k^{\Delta_{\mathcal{O}} - 2}$, where \mathcal{O} are all possible operators with the scaling dimension $\Delta_{\mathcal{O}} = 5$.

Then by setting $k_0 = \epsilon_{\mathbf{k}}$ in Eq. (5.5), the on-shell self-energy of the χ atom for an arbitrary state is found to be

$$\Sigma_\chi(x; \epsilon_{\mathbf{k}}, \mathbf{k})$$

$$= \sum_{\sigma=\uparrow, \downarrow} \left[\frac{4\pi}{\frac{i}{2} + \frac{1}{a_\sigma |\mathbf{k}|}} \frac{n_\sigma(x)}{m|\mathbf{k}|} + \frac{2\pi i}{\left(\frac{i}{2} + \frac{1}{a_\sigma |\mathbf{k}|}\right)^2} \frac{\hat{\mathbf{k}} \cdot \mathbf{j}_\sigma(x)}{m|\mathbf{k}|^2} \right]$$

$$- t_\chi^{\text{reg}}(\mathbf{k}; \mathbf{k}) \frac{\mathcal{C}(x)}{m^2} + O(\mathbf{k}^{-3}). \quad (5.7)$$

The quasiparticle energy and scattering rate of the χ atom in a spin-1/2 Fermi gas are given by the real and imaginary parts of $\Sigma_\chi(x; \epsilon_{\mathbf{k}}, \mathbf{k})$ according to

$$E_\chi(x; \mathbf{k}) = \epsilon_{\mathbf{k}} + \text{Re}[\Sigma_\chi(x; \epsilon_{\mathbf{k}}, \mathbf{k})] + O(\mathbf{k}^{-4}) \quad (5.8)$$

and

$$\Gamma_\chi(x; \mathbf{k}) = -2 \text{Im}[\Sigma_\chi(x; \epsilon_{\mathbf{k}}, \mathbf{k})] + O(\mathbf{k}^{-4}), \quad (5.9)$$

respectively. Our next task is to determine the regularized on-shell three-body scattering amplitude $t_\chi^{\text{reg}}(\mathbf{k}; \mathbf{p}) \equiv T_\chi^{\text{reg}}(k, 0; p, k-p)|_{k_0=\epsilon_{\mathbf{k}}, p_0=\epsilon_{\mathbf{p}}}$ in Eq. (5.7), which requires solving a three-body problem.

B. Three-body problem

We now compute the three-body scattering amplitude $T_\chi(k, 0; k, 0)$. Unlike the previous cases in Secs. III F and IV E, $T_\chi(k; p) \equiv T_\chi(k, 0; p, k-p)$ by itself does not solve a closed integral equation. To find a closed set of integral equations, we need to introduce other three-body scattering amplitudes $T_\sigma(k; p)$ with $\sigma = \uparrow, \downarrow$, which describe processes where the χ atom and a dimer composed of spin-up and -down fermions with their energy-momentum $(k, 0)$ are scattered into a spin- σ fermion and a dimer composed of the χ atom and the other fermion with their energy-momentum $(p, k-p)$. These three scattering amplitudes are solutions to a closed set of integral equations depicted in Fig. 8. Then by following the same procedures as in Eqs. (3.43)–(3.45), the integral equations solved by the on-shell three-body scattering amplitudes $t_{\chi, \uparrow, \downarrow}(\mathbf{k}; \mathbf{p}) \equiv T_{\chi, \uparrow, \downarrow}(\epsilon_{\mathbf{k}}, \mathbf{k}; \epsilon_{\mathbf{p}}, \mathbf{p})$ can be written as

$$t_\chi(\mathbf{k}; \mathbf{p}) = \int \frac{d\mathbf{q}}{(2\pi)^3} \mathcal{K}_{a_\downarrow}(\mathbf{k}; \mathbf{p}, \mathbf{q}) t_\uparrow(\mathbf{k}; \mathbf{q})$$

$$+ \int \frac{d\mathbf{q}}{(2\pi)^3} \mathcal{K}_{a_\uparrow}(\mathbf{k}; \mathbf{p}, \mathbf{q}) t_\downarrow(\mathbf{k}; \mathbf{q}), \quad (5.10a)$$

$$t_\uparrow(\mathbf{k}; \mathbf{p}) = \frac{m}{p^2} + \int \frac{d\mathbf{q}}{(2\pi)^3} \mathcal{K}_a(\mathbf{k}; \mathbf{p}, \mathbf{q}) t_\chi(\mathbf{k}; \mathbf{q})$$

$$+ \int \frac{d\mathbf{q}}{(2\pi)^3} \mathcal{K}_{a_\uparrow}(\mathbf{k}; \mathbf{p}, \mathbf{q}) t_\downarrow(\mathbf{k}; \mathbf{q}), \quad (5.10b)$$

$$t_{\downarrow}(\mathbf{k}; \mathbf{p}) = \frac{m}{\mathbf{p}^2} + \int \frac{d\mathbf{q}}{(2\pi)^3} \mathcal{K}_a(\mathbf{k}; \mathbf{p}, \mathbf{q}) t_{\chi}(\mathbf{k}; \mathbf{q}) \\ + \int \frac{d\mathbf{q}}{(2\pi)^3} \mathcal{K}_{a_{\downarrow}}(\mathbf{k}; \mathbf{p}, \mathbf{q}) t_{\uparrow}(\mathbf{k}; \mathbf{q}), \quad (5.10c)$$

where the integral kernel $\mathcal{K}_a(\mathbf{k}; \mathbf{p}, \mathbf{q})$ is defined in Eq. (3.46).

As long as we are interested in $t_{\chi}^{\text{reg}}(\mathbf{k}; \mathbf{k}) \sim m/k^2$ up to $O(k^{-3})$ [see Eq. (5.7)], we can set all three scattering lengths infinite $(a_{\uparrow}|\mathbf{k}|)^{-1}$, $(a_{\downarrow}|\mathbf{k}|)^{-1}$, $(a|\mathbf{k}|)^{-1} = 0$, because the dependence on them appears only from $O(k^{-3})$. In this case, by defining

$$t_F(\mathbf{k}; \mathbf{p}) \equiv \frac{2t_{\chi}(\mathbf{k}; \mathbf{p}) - t_{\uparrow}(\mathbf{k}; \mathbf{p}) - t_{\downarrow}(\mathbf{k}; \mathbf{p})}{2} \quad (5.11)$$

and

$$t_B(\mathbf{k}; \mathbf{p}) \equiv \frac{t_{\chi}(\mathbf{k}; \mathbf{p}) + t_{\uparrow}(\mathbf{k}; \mathbf{p}) + t_{\downarrow}(\mathbf{k}; \mathbf{p})}{2}, \quad (5.12)$$

the three coupled integral equations (5.10) can be brought into two independent integral equations:

$$t_F(\mathbf{k}; \mathbf{p}) = -\frac{m}{\mathbf{p}^2} - \int \frac{d\mathbf{q}}{(2\pi)^3} \mathcal{K}_{\infty}(\mathbf{k}; \mathbf{p}, \mathbf{q}) t_F(\mathbf{k}; \mathbf{q}) \quad (5.13a)$$

and

$$t_B(\mathbf{k}; \mathbf{p}) = \frac{m}{\mathbf{p}^2} + 2 \int \frac{d\mathbf{q}}{(2\pi)^3} \mathcal{K}_{\infty}(\mathbf{k}; \mathbf{p}, \mathbf{q}) t_B(\mathbf{k}; \mathbf{q}). \quad (5.13b)$$

Because these two integral equations are equivalent to Eqs. (3.45) and (4.26) at $(a|\mathbf{k}|)^{-1} = 0$, their solutions are already obtained.

By using the numerical solutions obtained previously in Eqs. (3.50) and (4.30), $t_{\chi}^{\text{reg}}(\mathbf{k}; \mathbf{k})$ within the accuracy of $O(k^{-3})$ is found to be

$$t_{\chi}^{\text{reg}}(\mathbf{k}; \mathbf{k}) = \frac{2}{3} [t_F^{\text{reg}}(\mathbf{k}; \mathbf{k}) + t_B^{\text{reg}}(\mathbf{k}; \mathbf{k})] + O(k^{-3}) \\ = \frac{2}{3} \left[3.771 + f\left(\frac{|\mathbf{k}|}{\kappa'_*}\right) \right] \frac{m}{\mathbf{k}^2} + O(k^{-3}). \quad (5.14)$$

Here, $f(|\mathbf{k}|/\kappa'_*)$ is the universal log-periodic function plotted in Fig. 7 and approximately given by Eq. (4.31) with κ'_* being the Efimov parameter associated with a three-body system of the χ atom with spin-up and -down fermions. By substituting this numerical solution of the three-body problem into the on-shell self-energy in Eq. (5.7), the large-momentum expansions of the quasi-particle energy and scattering rate of the χ atom in a spin-1/2 Fermi gas are obtained from Eqs. (5.8) and (5.9):

$$E_{\chi}(x; \mathbf{k}) = \left[1 + 32\pi \sum_{\sigma=\uparrow, \downarrow} \frac{n_{\sigma}(x)}{a_{\sigma}|\mathbf{k}|^4} \right. \\ \left. - \frac{4}{3} \left\{ 3.771 + \text{Re}f\left(\frac{|\mathbf{k}|}{\kappa'_*}\right) \right\} \frac{\mathcal{C}(x)}{|\mathbf{k}|^4} + O(k^{-5}) \right] \epsilon_{\mathbf{k}} \quad (5.15)$$

and

$$\Gamma_{\chi}(x; \mathbf{k}) = \left[32\pi \sum_{\sigma=\uparrow, \downarrow} \left\{ \frac{n_{\sigma}(x)}{|\mathbf{k}|^3} + \frac{\hat{\mathbf{k}} \cdot \mathbf{j}_{\sigma}(x)}{|\mathbf{k}|^4} \right\} \right. \\ \left. + \frac{8}{3} \text{Im}f\left(\frac{|\mathbf{k}|}{\kappa'_*}\right) \frac{\mathcal{C}(x)}{|\mathbf{k}|^4} + O(k^{-5}) \right] \epsilon_{\mathbf{k}}, \quad (5.16)$$

respectively.

C. Differential scattering rate

Our final task is to determine the differential scattering rate $d\Gamma_{\chi}(\mathbf{k})/d\mathbf{p}$; that is, the rate at which the χ atom shot into a spin-1/2 Fermi gas with the initial momentum \mathbf{k} is measured at the final momentum \mathbf{p} (see Fig. 1). We start with the following expression for the total scattering rate obtained from Eqs. (5.7) and (5.9):

$$\Gamma_{\chi}(x; \mathbf{k}) \\ = \sum_{\sigma=\uparrow, \downarrow} \left[\frac{4\pi}{\frac{1}{4} + \frac{1}{(a_{\sigma}|\mathbf{k}|)^2}} \frac{n_{\sigma}(x)}{m|\mathbf{k}|} + \frac{\pi - \frac{4\pi}{(a_{\sigma}|\mathbf{k}|)^2}}{\left[\frac{1}{4} + \frac{1}{(a_{\sigma}|\mathbf{k}|)^2}\right]^2} \frac{\hat{\mathbf{k}} \cdot \mathbf{j}_{\sigma}(x)}{m|\mathbf{k}|^2} \right] \\ + 2 \text{Im} t_{\chi}^{\text{reg}}(\mathbf{k}; \mathbf{k}) \frac{\mathcal{C}(x)}{m^2} + O(k^{-3}) \\ \equiv \sum_{\sigma=\uparrow, \downarrow} \left[\Gamma_{\chi}^{(n_{\sigma})}(\mathbf{k}) + \Gamma_{\chi}^{(j_{\sigma})}(\mathbf{k}) \right] + \Gamma_{\chi}^{(\mathcal{C})}(\mathbf{k}) + O(k^{-3}). \quad (5.17)$$

Here the contributions of the number density n_{σ} , current density \mathbf{j}_{σ} , and contact density \mathcal{C} are denoted by $\Gamma_{\chi}^{(n_{\sigma})}$, $\Gamma_{\chi}^{(j_{\sigma})}$, and $\Gamma_{\chi}^{(\mathcal{C})}$, respectively.

1. Contribution of number density

In order to extract the differential scattering rate, it is instructive to rewrite the first term in Eq. (5.17) so that its physical meaning becomes transparent:

$$\Gamma_{\chi}^{(n_{\sigma})}(\mathbf{k}) = n_{\sigma}(x) \int \frac{d\mathbf{p} d\mathbf{q}}{(2\pi)^6} |A_{\sigma}(\epsilon_{\mathbf{k}}, \mathbf{k})|^2 \\ \times (2\pi)^4 \delta(\mathbf{p} + \mathbf{q} - \mathbf{k}) \delta(\epsilon_{\mathbf{p}} + \epsilon_{\mathbf{q}} - \epsilon_{\mathbf{k}}). \quad (5.18)$$

Here, $A_{\sigma}(k)$ introduced in Eq. (5.2) is the two-body scattering amplitude between the χ atom and a spin- σ fermion. It is now obvious that $\Gamma_{\chi}^{(n_{\sigma})}(\mathbf{k})$ represents the contribution from the two-body scattering in which the χ atom with the initial momentum \mathbf{k} and a spin- σ fermion at rest are scattered into those with their final momenta \mathbf{p} and \mathbf{q} , respectively. Therefore, the contribution of the number density of spin- σ fermions to the differential scattering rate of the χ atom can be read off as

$$\frac{d\Gamma_{\chi}^{(n_{\sigma})}(\mathbf{k})}{d\mathbf{p}} = n_{\sigma}(x) \int \frac{d\mathbf{q}}{(2\pi)^6} |A_{\sigma}(\epsilon_{\mathbf{k}}, \mathbf{k})|^2 \\ \times (2\pi)^4 \delta(\mathbf{p} + \mathbf{q} - \mathbf{k}) \delta(\epsilon_{\mathbf{p}} + \epsilon_{\mathbf{q}} - \epsilon_{\mathbf{k}}). \quad (5.19)$$

Then by performing the integration over the magnitude of momentum $|\mathbf{p}|^2 d|\mathbf{p}|$, the angle distribution of the scattered χ atom is found to be

$$\frac{d\Gamma_{\chi}^{(n_{\sigma})}(\mathbf{k})}{d\Omega} = \frac{4 \cos \theta \Theta(\cos \theta) n_{\sigma}(x)}{\frac{1}{4} + \frac{1}{(a_{\sigma}|\mathbf{k}|)^2}} \frac{1}{m|\mathbf{k}|}, \quad (5.20)$$

where $\Theta(\cdot)$ is the Heaviside step function and θ is a polar angle of the final momentum \mathbf{p} with respect to the initial momentum chosen to be $\mathbf{k} = |\mathbf{k}|\hat{z}$. Because of kinematic constraints (energy and momentum conservations) in the two-body scattering, the number density contributes to the forward scattering ($\cos \theta > 0$) only.⁴

2. Contribution of current density

Similarly, the second term in Eq. (5.17) can be rewritten as

$$\begin{aligned} \Gamma_{\chi}^{(j_{\sigma})}(\mathbf{k}) &= \mathbf{j}_{\sigma}(x) \cdot \frac{\partial}{\partial \mathbf{k}} \int \frac{d\mathbf{p} d\mathbf{q}}{(2\pi)^6} |A_{\sigma}(k_0, \mathbf{k})|^2 \\ &\times (2\pi)^4 \delta(\mathbf{p} + \mathbf{q} - \mathbf{k}) \delta(\epsilon_{\mathbf{p}} + \epsilon_{\mathbf{q}} - k_0) \Big|_{k_0 \rightarrow \epsilon_{\mathbf{k}}}, \end{aligned} \quad (5.21)$$

which represents the contribution from the two-body scattering in which the χ atom is scattered by a spin- σ fermion moving with a small momentum. Accordingly, the contribution of the current density of spin- σ fermions to the differential scattering rate of the χ atom can be read off as

$$\begin{aligned} \frac{d\Gamma_{\chi}^{(j_{\sigma})}(\mathbf{k})}{d\mathbf{p}} &= \mathbf{j}_{\sigma}(x) \cdot \frac{\partial}{\partial \mathbf{k}} \int \frac{d\mathbf{q}}{(2\pi)^6} |A_{\sigma}(k_0, \mathbf{k})|^2 \\ &\times (2\pi)^4 \delta(\mathbf{p} + \mathbf{q} - \mathbf{k}) \delta(\epsilon_{\mathbf{p}} + \epsilon_{\mathbf{q}} - k_0) \Big|_{k_0 \rightarrow \epsilon_{\mathbf{k}}}. \end{aligned} \quad (5.22)$$

Then by performing the integration over the magnitude of momentum $|\mathbf{p}|^2 d|\mathbf{p}|$, the angle distribution of the scattered χ atom is found to be

$$\begin{aligned} \frac{d\Gamma_{\chi}^{(j_{\sigma})}(\mathbf{k})}{d\Omega} &= \frac{2 \cos \theta \Theta(\cos \theta) \hat{\mathbf{k}} \cdot \mathbf{j}_{\sigma}(x)}{\left[\frac{1}{4} + \frac{1}{(a_{\sigma}|\mathbf{k}|)^2}\right]^2} \frac{1}{m|\mathbf{k}|^2} \\ &- \frac{\delta(\cos \theta) \hat{\mathbf{k}} - \Theta(\cos \theta) \hat{\mathbf{p}}}{\frac{1}{4} + \frac{1}{(a_{\sigma}|\mathbf{k}|)^2}} \cdot \frac{4 \mathbf{j}_{\sigma}(x)}{m|\mathbf{k}|^2}. \end{aligned} \quad (5.23)$$

Note that this differential scattering rate can be nonzero only on the forward-scattering side again and depends

⁴ The situation is different if the χ atom has a mass different from that of spin- σ fermions; $m_{\chi} \neq m_{\sigma}$. By considering the two-body scattering in which the χ atom with the initial momentum \mathbf{k} collides with a spin- σ fermion at rest, the energy and momentum conservations constrain the final momentum \mathbf{p} to be on a sphere defined by $|\mathbf{p} - \frac{m_{\chi}}{m_{\chi} + m_{\sigma}} \mathbf{k}| = |\frac{m_{\sigma}}{m_{\chi} + m_{\sigma}} \mathbf{k}|$. Therefore, when $m_{\chi} > m_{\sigma}$, the χ atom can be scattered into an angle range $\cos \theta \geq \sqrt{1 - (m_{\sigma}/m_{\chi})^2}$ only, while when $m_{\chi} < m_{\sigma}$, it can be scattered into any angles.

on the azimuthal angle φ because of the $\hat{\mathbf{p}} \cdot \mathbf{j}_{\sigma}$ term. It is easy to check that the integration of the differential scattering rate in Eq. (5.20) or (5.23) over the solid angle $d\Omega = d\cos \theta d\varphi$ reproduces the total scattering rate in Eq. (5.17).

3. Contribution of contact density

The contribution of the contact density of a spin-1/2 Fermi gas to the differential scattering rate of the χ atom can be extracted in a similar way. As we discussed at the end of Sec. III E, the last term in Eq. (5.17) represents the contribution from the three-body scattering of the χ atom with the initial momentum \mathbf{k} with a small pair of spin-up and -down fermions at rest. By using the optical theorem, the imaginary part of the forward three-body scattering amplitude $t_{\chi}(\mathbf{k}; \mathbf{k})$ can be written as a form of the total scattering rate:

$$\begin{aligned} 2 \operatorname{Im} t_{\chi}(\mathbf{k}; \mathbf{k}) & \\ &= \int \frac{d\mathbf{p} d\mathbf{q}_{\uparrow} d\mathbf{q}_{\downarrow}}{(2\pi)^9} |t_{\chi}(\mathbf{k}; \mathbf{p}) A(\epsilon_{\mathbf{k}} - \epsilon_{\mathbf{p}}, \mathbf{k} - \mathbf{p}) \\ &\quad + t_{\uparrow}(\mathbf{k}; \mathbf{q}_{\uparrow}) A_{\downarrow}(\epsilon_{\mathbf{k}} - \epsilon_{\mathbf{q}_{\uparrow}}, \mathbf{k} - \mathbf{q}_{\uparrow}) \\ &\quad + t_{\downarrow}(\mathbf{k}; \mathbf{q}_{\downarrow}) A_{\uparrow}(\epsilon_{\mathbf{k}} - \epsilon_{\mathbf{q}_{\downarrow}}, \mathbf{k} - \mathbf{q}_{\downarrow})|^2 \\ &\times (2\pi)^4 \delta(\mathbf{p} + \mathbf{q}_{\uparrow} + \mathbf{q}_{\downarrow} - \mathbf{k}) \delta(\epsilon_{\mathbf{p}} + \epsilon_{\mathbf{q}_{\uparrow}} + \epsilon_{\mathbf{q}_{\downarrow}} - \epsilon_{\mathbf{k}}). \end{aligned} \quad (5.24)$$

Here, \mathbf{p} and \mathbf{q}_{σ} are momenta of the χ atom and the spin- σ fermion in the final state, respectively. This equality can be checked by a direct calculation starting with the set of integral equations (5.10) (see Appendix C).

The right-hand side of Eq. (5.24) is infrared divergent at $|\mathbf{q}_{\sigma}| \rightarrow 0$ because of $t_{\sigma}(\mathbf{k}; \mathbf{q}_{\sigma}) \rightarrow m/\mathbf{q}_{\sigma}^2$ for both $\sigma = \uparrow, \downarrow$ [see Eq. (5.10)]. These infrared divergences are canceled exactly by the second term in Eq. (5.6) because its imaginary part also contains the same form of infrared divergences which can be seen from

$$\begin{aligned} 2 \operatorname{Im} A_{\uparrow}(\epsilon_{\mathbf{k}}, \mathbf{k}) &\int \frac{d\mathbf{q}}{(2\pi)^3} \left(\frac{m}{\mathbf{q}^2}\right)^2 \\ &= \int \frac{d\mathbf{p} d\mathbf{q}_{\uparrow} d\mathbf{q}_{\downarrow}}{(2\pi)^9} \left(\frac{m}{\mathbf{q}_{\downarrow}^2}\right)^2 |A_{\uparrow}(\epsilon_{\mathbf{k}}, \mathbf{k})|^2 \\ &\times (2\pi)^4 \delta(\mathbf{p} + \mathbf{q}_{\uparrow} - \mathbf{k}) \delta(\epsilon_{\mathbf{p}} + \epsilon_{\mathbf{q}_{\uparrow}} - \epsilon_{\mathbf{k}}), \end{aligned} \quad (5.25)$$

and the same for $\uparrow \leftrightarrow \downarrow$. Therefore, the imaginary part of the regularized on-shell three-body scattering amplitude

$$\begin{aligned} 2 \operatorname{Im} t_{\chi}^{\text{reg}}(\mathbf{k}; \mathbf{k}) &= 2 \operatorname{Im} t_{\chi}(\mathbf{k}; \mathbf{k}) \\ &- 2 \operatorname{Im}[A_{\uparrow}(\epsilon_{\mathbf{k}}, \mathbf{k}) + A_{\downarrow}(\epsilon_{\mathbf{k}}, \mathbf{k})] \int \frac{d\mathbf{q}}{(2\pi)^3} \left(\frac{m}{\mathbf{q}^2}\right)^2 \end{aligned} \quad (5.26)$$

appearing in $\Gamma_{\chi}^{(C)}(\mathbf{k})$ is free of divergences. By recalling that \mathbf{p} in Eqs. (5.24) and (5.25) corresponds to the momentum of the χ atom in the final state, the contribution of the contact density to the differential scattering rate of the χ atom can be identified as

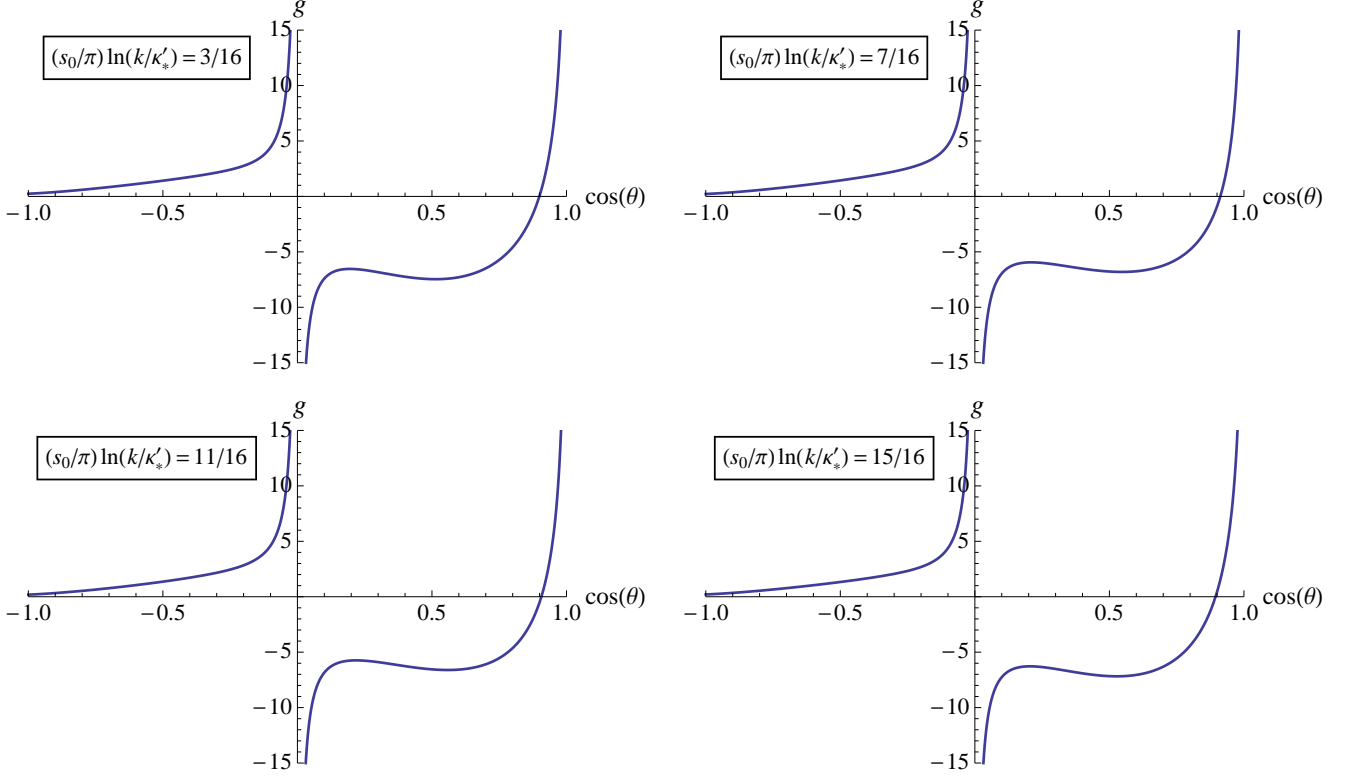


FIG. 9. (Color online) Universal function $g(\cos \theta, |\mathbf{k}|/\kappa'_*)$ to determine the contribution of the contact density to the differential scattering rate (5.28). $g(\cos \theta, |\mathbf{k}|/\kappa'_*)$ is periodic in terms of $0 \leq (s_0/\pi) \ln(|\mathbf{k}|/\kappa'_*) \leq 1$ and here its dependence on $\cos \theta$ is shown at four values of $(s_0/\pi) \ln(|\mathbf{k}|/\kappa'_*) = 3/16, 7/16, 11/16, 15/16$. These four values roughly correspond to the minimum, inflection point, maximum, and inflection point of the total scattering rate, respectively [see Eq. (5.29) and Fig. 7].

$$\begin{aligned}
\frac{d\Gamma_{\chi}^{(C)}(\mathbf{k})}{d\mathbf{p}} &= \int \frac{d\mathbf{q}_{\uparrow} d\mathbf{q}_{\downarrow}}{(2\pi)^9} \left[|t_{\chi}(\mathbf{k}; \mathbf{p}) A(\epsilon_{\mathbf{k}} - \epsilon_{\mathbf{p}}, \mathbf{k} - \mathbf{p}) + t_{\uparrow}(\mathbf{k}; \mathbf{q}_{\uparrow}) A_{\downarrow}(\epsilon_{\mathbf{k}} - \epsilon_{\mathbf{q}_{\uparrow}}, \mathbf{k} - \mathbf{q}_{\uparrow}) \right. \\
&\quad \left. + t_{\downarrow}(\mathbf{k}; \mathbf{q}_{\downarrow}) A_{\uparrow}(\epsilon_{\mathbf{k}} - \epsilon_{\mathbf{q}_{\downarrow}}, \mathbf{k} - \mathbf{q}_{\downarrow}) \right]^2 (2\pi)^4 \delta(\mathbf{p} + \mathbf{q}_{\uparrow} + \mathbf{q}_{\downarrow} - \mathbf{k}) \delta(\epsilon_{\mathbf{p}} + \epsilon_{\mathbf{q}_{\uparrow}} + \epsilon_{\mathbf{q}_{\downarrow}} - \epsilon_{\mathbf{k}}) \\
&\quad - \left(\frac{m}{q_{\uparrow}^2} \right)^2 |A_{\downarrow}(\epsilon_{\mathbf{k}}, \mathbf{k})|^2 (2\pi)^4 \delta(\mathbf{p} + \mathbf{q}_{\downarrow} - \mathbf{k}) \delta(\epsilon_{\mathbf{p}} + \epsilon_{\mathbf{q}_{\downarrow}} - \epsilon_{\mathbf{k}}) \\
&\quad \left. - \left(\frac{m}{q_{\downarrow}^2} \right)^2 |A_{\uparrow}(\epsilon_{\mathbf{k}}, \mathbf{k})|^2 (2\pi)^4 \delta(\mathbf{p} + \mathbf{q}_{\uparrow} - \mathbf{k}) \delta(\epsilon_{\mathbf{p}} + \epsilon_{\mathbf{q}_{\uparrow}} - \epsilon_{\mathbf{k}}) \right] \frac{\mathcal{C}(x)}{m^2}.
\end{aligned} \tag{5.27}$$

This differential scattering rate can be evaluated by using the on-shell three-body scattering amplitudes $t_{\chi, \uparrow, \downarrow}(\mathbf{k}; \mathbf{p})$ at infinite scattering lengths $(a_{\uparrow} |\mathbf{k}|)^{-1}$, $(a_{\downarrow} |\mathbf{k}|)^{-1}$, $(a |\mathbf{k}|)^{-1} = 0$ obtained from the numerical solutions of $t_{F, B}(\mathbf{k}; \mathbf{p})$ in Eqs. (5.11)–(5.13) [note that $t_{\uparrow}(\mathbf{k}; \mathbf{p}) = t_{\downarrow}(\mathbf{k}; \mathbf{p})$ when $a_{\uparrow} = a_{\downarrow}$]. The physical meaning of the subtracted terms was discussed at the end of Sec. III F.

Finally, by performing the integration over the magnitude of \mathbf{p} , the angle distribution of the scattered χ atom

is given by

$$\begin{aligned}
\frac{d\Gamma_{\chi}^{(C)}(\mathbf{k})}{d\Omega} &= \int_0^{\infty} d|\mathbf{p}| |\mathbf{p}|^2 \frac{d\Gamma_{\chi}^{(C)}(\mathbf{k})}{d\mathbf{p}} \\
&\equiv g\left(\cos \theta, \frac{|\mathbf{k}|}{\kappa'_*}\right) \frac{\mathcal{C}(x)}{m \mathbf{k}^2}.
\end{aligned} \tag{5.28}$$

The resulting universal function $g(\cos \theta, |\mathbf{k}|/\kappa'_*)$ depends on the polar angle θ and the momentum to Efimov parameter ratio $|\mathbf{k}|/\kappa'_*$ in a log-periodic way. $g(\cos \theta, |\mathbf{k}|/\kappa'_*)$ as a function of $\cos \theta$ is shown in Fig. 9 at four values of $(s_0/\pi) \ln(|\mathbf{k}|/\kappa'_*) = 3/16, 7/16, 11/16, 15/16$. Note that $g(\cos \theta, |\mathbf{k}|/\kappa'_*)$ is mostly negative on the forward-scattering side ($\cos \theta > 0$), while it is positive

everywhere on the backward-scattering side ($\cos\theta < 0$). The divergences of $g(\cos\theta, |\mathbf{k}|/\kappa'_*)$ at $\cos\theta = 0$ and 1 signal poor convergences of the large-momentum expansion around these angles. Higher order corrections would be important as well and ideally need to be resummed. However, away from these two singularities, we expect our large-momentum expansion to be valid in a wide range of momentum based on the observation in Sec. II C.

The integration of the differential scattering rate (5.28) over the solid angle $d\Omega = d\cos\theta d\varphi$ reproduces the total scattering rate in Eq. (5.16):⁵

$$\begin{aligned}\Gamma_\chi^{(C)}(\mathbf{k}) &= 2\pi \int_{-1}^1 d\cos\theta g\left(\cos\theta, \frac{|\mathbf{k}|}{\kappa'_*}\right) \frac{\mathcal{C}(x)}{m\mathbf{k}^2} \\ &= \frac{4}{3} \text{Im}f\left(\frac{|\mathbf{k}|}{\kappa'_*}\right) \frac{\mathcal{C}(x)}{m\mathbf{k}^2},\end{aligned}\quad (5.29)$$

which relates the integral of $g(\cos\theta, |\mathbf{k}|/\kappa'_*)$ to the imaginary part of $f(|\mathbf{k}|/\kappa'_*)$. Note that the above four values of $(s_0/\pi) \ln(|\mathbf{k}|/\kappa'_*) = 3/16, 7/16, 11/16, 15/16$ are chosen so that they roughly correspond to the minimum, inflection point, maximum, and inflection point of $\text{Im}f(|\mathbf{k}|/\kappa'_*)$, respectively (see Fig. 7). Therefore, although differences are difficult to see in the differential scattering rate from Fig. 9, the contribution of the contact density to the total scattering rate varies by up to 17% for a different momentum to Efimov parameter ratio $|\mathbf{k}|/\kappa'_*$. By combining the results in Eqs. (5.20), (5.23), and (5.28), we obtain the differential scattering rate of the χ atom shot into a spin-1/2 Fermi gas up to $O(\mathbf{k}^{-3})$:

$$\begin{aligned}\frac{d\Gamma_\chi(\mathbf{k})}{d\Omega} &= \sum_{\sigma=\uparrow,\downarrow} \left[\frac{d\Gamma_\chi^{(n_\sigma)}(\mathbf{k})}{d\Omega} + \frac{d\Gamma_\chi^{(j_\sigma)}(\mathbf{k})}{d\Omega} \right] \\ &+ \frac{d\Gamma_\chi^{(C)}(\mathbf{k})}{d\Omega} + O(\mathbf{k}^{-3}).\end{aligned}\quad (5.30)$$

This result was presented previously in Eq. (2.6), where the time dependence of the densities is suppressed by assuming a stationary state.

D. Spinless Bose gas

The analysis in the case of a spinless Bose gas is similar. Again a probe atom is denoted by χ and assumed to interact with a boson by a scattering length a_χ . The Lagrangian density describing such a problem is

$$\mathcal{L} = \chi^\dagger \left(i\partial_t + \frac{\nabla^2}{2m_\chi} \right) \chi + c_\chi \chi^\dagger \psi^\dagger \psi \chi + \mathcal{L}_B, \quad (5.31)$$

where \mathcal{L}_B defined in Eq. (4.1) describes spinless bosons interacting with each other by a scattering length a . For

simplicity, we shall assume that the χ atom and bosons have the same mass $m = m_\chi$. In analogy with Eq. (3.5), the two-body scattering amplitude between the χ atom and a boson is given by

$$A_\chi(k) = \frac{4\pi}{m} \frac{1}{\sqrt{\frac{k^2}{4} - mk_0 - i0^+} - \frac{1}{a_\chi}}. \quad (5.32)$$

The behavior of the single-particle Green's function of the χ atom,

$$i\mathcal{G}_\chi(x; k) \equiv \int dy e^{iky} \langle T[\chi(x + \frac{y}{2})\chi^\dagger(x - \frac{y}{2})] \rangle, \quad (5.33)$$

in the large-energy-momentum limit $k \rightarrow \infty$ can be understood by using the operator product expansion as in Secs. III and IV. Since the χ atom and two identical bosons with zero-range interactions suffer from the Efimov effect [110, 111], we only consider local operators with $N_{\mathcal{O}} = 0$ up to scaling dimensions $\Delta_{\mathcal{O}} = 4$ (see discussions in Sec. IV B). Then in analogy with Eqs. (4.20) and (4.21), $\mathcal{G}_\chi(x; k)$ can be written in the usual form

$$\mathcal{G}_\chi(x; k) = \frac{1}{k_0 - \epsilon_{\mathbf{k}} - \Sigma_\chi(x; k) + i0^+}, \quad (5.34)$$

where $\Sigma_\chi(x; k)$ is the self-energy of the χ atom given by

$$\begin{aligned}\Sigma_\chi(x; k) &= -A_\chi(k) n(x) + \frac{\partial}{\partial \mathbf{k}} A_\chi(k) \cdot \mathbf{j}(x) \\ &- T_\chi^{\text{reg}}(k, 0; k, 0) \frac{\mathcal{C}(x)}{m^2} - \dots.\end{aligned}\quad (5.35)$$

Here, $n(x) = \langle \psi^\dagger \psi \rangle$ and $\mathbf{j}(x) = \langle -i\psi^\dagger \overleftrightarrow{\nabla} \psi \rangle$ are the number density and current density of bosons and $\mathcal{C}(x) = m^2 \langle \phi^\dagger \phi \rangle$ is the contact density of a spinless Bose gas. Note that these parameters only refer to many-body properties of the given spinless Bose gas and do not involve the information related to the χ atom. On the other hand, $T_\chi^{\text{reg}}(k, 0; k, 0)$ is a finite quantity defined by

$$T_\chi^{\text{reg}}(k, 0; k, 0) \equiv T_\chi(k, 0; k, 0) - A_\chi(k) \int \frac{d\mathbf{q}}{(2\pi)^3} \left(\frac{m}{q^2} \right)^2, \quad (5.36)$$

where $T_\chi(k, p; k', p')$ is the three-body scattering amplitude between the χ atom and a dimer composed of two identical bosons with (k, p) [(k', p')] being their initial (final) energy-momentum (see Fig. 5). Corrections to the above expression of $\Sigma_\chi(x; k)$ denoted by “...” start with $\sim \langle \mathcal{O} \rangle / k^{\Delta_{\mathcal{O}} - 2}$, where \mathcal{O} are all possible operators with the scaling dimension $\Delta_{\mathcal{O}} = 5$.

Then by setting $k_0 = \epsilon_{\mathbf{k}}$ in Eq. (5.35), the on-shell self-energy of the χ atom for an arbitrary state is found to be

$$\begin{aligned}\Sigma_\chi(x; \epsilon_{\mathbf{k}}, \mathbf{k}) &= \frac{4\pi}{\frac{i}{2} + \frac{1}{a_\chi |\mathbf{k}|}} \frac{n(x)}{m|\mathbf{k}|} + \frac{2\pi i}{\left(\frac{i}{2} + \frac{1}{a_\chi |\mathbf{k}|}\right)^2} \frac{\hat{\mathbf{k}} \cdot \mathbf{j}(x)}{m|\mathbf{k}|^2} \\ &- t_\chi^{\text{reg}}(\mathbf{k}; \mathbf{k}) \frac{\mathcal{C}(x)}{m^2} + O(\mathbf{k}^{-3}).\end{aligned}\quad (5.37)$$

⁵ Since $d\Gamma_\chi^{(C)}(\mathbf{k})/d\Omega$ has a pole at $\cos\theta = 0$ due to $g(\cos\theta, |\mathbf{k}|/\kappa'_*) \sim -4/(\pi^2 \cos\theta)$, the integral over $\cos\theta$ is understood as the Cauchy principal value.

The quasiparticle energy and scattering rate of the χ atom in a spinless Bose gas are given by the real and imaginary parts of $\Sigma_\chi(x; \epsilon_{\mathbf{k}}, \mathbf{k})$ according to Eqs. (5.8) and (5.9), respectively. Our next task is to determine the regularized on-shell three-body scattering amplitude $t_\chi^{\text{reg}}(\mathbf{k}; \mathbf{p}) \equiv T_\chi^{\text{reg}}(k, 0; p, k-p)|_{k_0=\epsilon_{\mathbf{k}}, p_0=\epsilon_{\mathbf{p}}}$ in Eq. (5.37), which requires solving a three-body problem.

E. Three-body problem

We now compute the three-body scattering amplitude $T_\chi(k, 0; k, 0)$. Unlike the previous cases in Secs. III F and IV E, $T_\chi(k; p) \equiv T_\chi(k, 0; p, k-p)$ by itself does not solve a closed integral equation. To find a closed set of integral equations, we need to introduce another three-body scattering amplitude $T_\psi(k; p)$, which describes a process where the χ atom and a dimer composed of two identical bosons with their energy-momentum $(k, 0)$ are scattered into a boson and a dimer composed of the χ atom and the other boson with their energy-momentum $(p, k-p)$. These two scattering amplitudes are solutions to a closed set of integral equations depicted in Fig. 8 with the identification of T_\uparrow, T_\downarrow with T_ψ . Then by following the same procedures as in Eqs. (3.43)–(3.45), the integral equations solved by the on-shell three-body scattering amplitudes $t_{\chi,\psi}(\mathbf{k}; \mathbf{p}) \equiv T_{\chi,\psi}(\epsilon_{\mathbf{k}}, \mathbf{k}; \epsilon_{\mathbf{p}}, \mathbf{p})$ can be written as

$$t_\chi(\mathbf{k}; \mathbf{p}) = \int \frac{d\mathbf{q}}{(2\pi)^3} \mathcal{K}_{a_\chi}(\mathbf{k}; \mathbf{p}, \mathbf{q}) t_\psi(\mathbf{k}; \mathbf{q}) \quad (5.38a)$$

and

$$t_\psi(\mathbf{k}; \mathbf{p}) = \frac{m}{\mathbf{p}^2} + 2 \int \frac{d\mathbf{q}}{(2\pi)^3} \mathcal{K}_a(\mathbf{k}; \mathbf{p}, \mathbf{q}) t_\chi(\mathbf{k}; \mathbf{q}) + \int \frac{d\mathbf{q}}{(2\pi)^3} \mathcal{K}_{a_\chi}(\mathbf{k}; \mathbf{p}, \mathbf{q}) t_\psi(\mathbf{k}; \mathbf{q}), \quad (5.38b)$$

where the integral kernel $\mathcal{K}_a(\mathbf{k}; \mathbf{p}, \mathbf{q})$ is defined in Eq. (3.46). Note that the factor 2 in front of \mathcal{K}_a originates from the fact that the two-body scattering amplitude between two identical bosons is twice as large as that between two distinguishable particles [compare Eqs. (3.5) and (4.4)].

As long as we are interested in $t_\chi^{\text{reg}}(\mathbf{k}; \mathbf{k}) \sim m/k^2$ up to $O(\mathbf{k}^{-3})$ [see Eq. (5.37)], we can set the two scattering lengths infinite $(a_\chi |\mathbf{k}|)^{-1}, (a |\mathbf{k}|)^{-1} = 0$, because the dependence on them appears only from $O(\mathbf{k}^{-3})$. In this case, by defining

$$t_F(\mathbf{k}; \mathbf{p}) \equiv 2t_\chi(\mathbf{k}; \mathbf{p}) - t_\psi(\mathbf{k}; \mathbf{p}) \quad (5.39)$$

and

$$t_B(\mathbf{k}; \mathbf{p}) \equiv t_\chi(\mathbf{k}; \mathbf{p}) + t_\psi(\mathbf{k}; \mathbf{p}), \quad (5.40)$$

the two coupled integral equations (5.38) can be brought into two independent integral equations:

$$t_F(\mathbf{k}; \mathbf{p}) = -\frac{m}{\mathbf{p}^2} - \int \frac{d\mathbf{q}}{(2\pi)^3} \mathcal{K}_\infty(\mathbf{k}; \mathbf{p}, \mathbf{q}) t_F(\mathbf{k}; \mathbf{q}) \quad (5.41a)$$

and

$$t_B(\mathbf{k}; \mathbf{p}) = \frac{m}{\mathbf{p}^2} + 2 \int \frac{d\mathbf{q}}{(2\pi)^3} \mathcal{K}_\infty(\mathbf{k}; \mathbf{p}, \mathbf{q}) t_B(\mathbf{k}; \mathbf{q}). \quad (5.41b)$$

Because these two integral equations are equivalent to Eqs. (3.45) and (4.26) at $(a|\mathbf{k}|)^{-1} = 0$, their solutions are already obtained.

By using the numerical solutions obtained previously in Eqs. (3.50) and (4.30), $t_\chi^{\text{reg}}(\mathbf{k}; \mathbf{k})$ within the accuracy of $O(\mathbf{k}^{-3})$ is found to be

$$t_\chi^{\text{reg}}(\mathbf{k}; \mathbf{k}) = \frac{1}{3} [t_F^{\text{reg}}(\mathbf{k}; \mathbf{k}) + t_B^{\text{reg}}(\mathbf{k}; \mathbf{k})] + O(\mathbf{k}^{-3}) = \frac{1}{3} \left[3.771 + f\left(\frac{|\mathbf{k}|}{\kappa'_*}\right) \right] \frac{m}{\mathbf{k}^2} + O(\mathbf{k}^{-3}). \quad (5.42)$$

Here, $f(|\mathbf{k}|/\kappa'_*)$ is the universal log-periodic function plotted in Fig. 7 and approximately given by Eq. (4.31) with κ'_* being the Efimov parameter associated with a three-body system of the χ atom with two identical bosons. By substituting this numerical solution of the three-body problem into the on-shell self-energy in Eq. (5.37), the large-momentum expansions of the quasiparticle energy and scattering rate of the χ atom in a spinless Bose gas are obtained from Eqs. (5.8) and (5.9):

$$E_\chi(x; \mathbf{k}) = \left[1 + 32\pi \frac{n(x)}{a_\chi |\mathbf{k}|^4} - \frac{2}{3} \left\{ 3.771 + \text{Re}f\left(\frac{|\mathbf{k}|}{\kappa'_*}\right) \right\} \frac{\mathcal{C}(x)}{|\mathbf{k}|^4} + O(\mathbf{k}^{-5}) \right] \epsilon_{\mathbf{k}} \quad (5.43)$$

and

$$\Gamma_\chi(x; \mathbf{k}) = \left[32\pi \left\{ \frac{n(x)}{|\mathbf{k}|^3} + \frac{\hat{\mathbf{k}} \cdot \mathbf{j}(x)}{|\mathbf{k}|^4} \right\} + \frac{4}{3} \text{Im}f\left(\frac{|\mathbf{k}|}{\kappa'_*}\right) \frac{\mathcal{C}(x)}{|\mathbf{k}|^4} + O(\mathbf{k}^{-5}) \right] \epsilon_{\mathbf{k}}, \quad (5.44)$$

respectively.

Furthermore, by comparing Eqs. (5.39)–(5.41) with Eqs. (5.11)–(5.13), we find $t_\psi(\mathbf{k}; \mathbf{p}) = t_{\uparrow,\downarrow}(\mathbf{k}; \mathbf{p})$ and $t_\chi(\mathbf{k}; \mathbf{p})$ in a spinless Bose gas is a half of that in a spin-1/2 Fermi gas. Therefore, the contribution of the contact density to the differential scattering rate of the χ atom in a spinless Bose gas is also a half of that in a spin-1/2 Fermi gas (see also Appendix C). All discussions given in Sec. V C for a spin-1/2 Fermi gas apply equally to a spinless Bose gas with minor modifications. In particular, the differential scattering rate of the χ atom shot

into a spinless Bose gas is given by

$$\begin{aligned} \frac{d\Gamma_\chi(\mathbf{k})}{d\Omega} = & \left[32 \cos\theta \Theta(\cos\theta) \frac{n(x)}{|\mathbf{k}|^3} \right. \\ & + 32 \left\{ 2 \cos\theta \Theta(\cos\theta) \hat{\mathbf{k}} - \delta(\cos\theta) \hat{\mathbf{k}} \right. \\ & \left. \left. + \Theta(\cos\theta) \hat{\mathbf{p}} \right\} \cdot \frac{\mathbf{j}(x)}{|\mathbf{k}|^4} \right. \\ & \left. + g \left(\cos\theta, \frac{|\mathbf{k}|}{\kappa'_*} \right) \frac{\mathcal{C}(x)}{|\mathbf{k}|^4} + O(k^{-5}) \right] \frac{\mathbf{k}^2}{2m}. \end{aligned} \quad (5.45)$$

Compare this result with that for a spin-1/2 Fermi gas in Eq. (2.6).

VI. WEAK-PROBE LIMIT

A. Spin-1/2 Fermi gas

In the previous section, the differential scattering rate of a different spin state of atoms shot into an atomic gas was derived in the systematic large-momentum expansion. For a spin-1/2 Fermi gas, it is given by

$$\begin{aligned} \frac{d\Gamma_\chi(\mathbf{k})}{d\mathbf{p}} = & \sum_{\sigma=\uparrow,\downarrow} \left[\frac{d\Gamma_\chi^{(n_\sigma)}(\mathbf{k})}{d\mathbf{p}} + \frac{d\Gamma_\chi^{(j_\sigma)}(\mathbf{k})}{d\mathbf{p}} \right] \\ & + \frac{d\Gamma_\chi^{(c)}(\mathbf{k})}{d\mathbf{p}} + O(k^{-6}), \end{aligned} \quad (6.1)$$

where the three leading terms were obtained in Eqs. (5.19), (5.22), and (5.27), respectively. On the other hand, there is another limit in which a different systematic expansion is possible; that is, the limit of $a_\sigma \rightarrow 0$ where the probe atom interacts weakly with atoms constituting the target atomic gas. In this “weak-probe” limit, the self-energy of the χ atom in a spin-1/2 Fermi gas can be expanded perturbatively in terms of a_σ :

$$\begin{aligned} \Sigma_\chi(k) = & - \sum_{\sigma=\uparrow,\downarrow} c_\sigma n_\sigma \\ & + \sum_{\sigma,\sigma'} c_\sigma c_{\sigma'} \int \frac{d\mathbf{p}}{(2\pi)^3} \frac{S_{\sigma\sigma'}(k-\mathbf{p})}{p_0 - \epsilon_{\mathbf{p}} + i0^+} + O(a_\sigma^3). \end{aligned} \quad (6.2)$$

Here, $c_\sigma = -4\pi a_\sigma/m + O(a_\sigma^2)$ is the coupling strength between the χ atom and a spin- σ fermion and

$$S_{\sigma\sigma'}(k) = \frac{1}{2\pi} \int dx e^{ikx} \langle \hat{n}_\sigma(x) \hat{n}_{\sigma'}(0) \rangle \quad (6.3)$$

is a dynamic structure factor of the spin-1/2 Fermi gas with translational symmetries assumed again. As before, the imaginary part of the self-energy gives the scattering rate of the χ atom as

$$\begin{aligned} \Gamma_\chi(\mathbf{k}) = & -2 \text{Im}[\Sigma_\chi(\epsilon_{\mathbf{k}}, \mathbf{k})] \\ = & \sum_{\sigma,\sigma'} c_\sigma c_{\sigma'} \int \frac{d\mathbf{p}}{(2\pi)^2} S_{\sigma\sigma'}(\epsilon_{\mathbf{k}} - \epsilon_{\mathbf{p}}, \mathbf{k} - \mathbf{p}) + O(a_\sigma^3). \end{aligned} \quad (6.4)$$

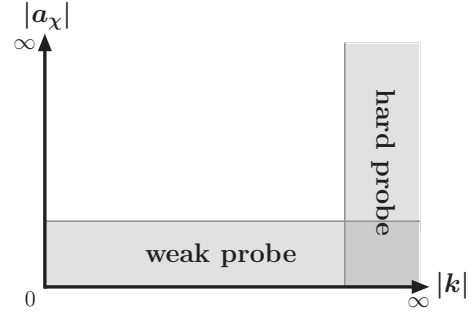


FIG. 10. Schematic of valid regions of our hard-probe formula (6.1) and the known weak-probe formula (6.5) in the plane of the incident momentum \mathbf{k} and the scattering length $a_\chi \sim a_\uparrow \sim a_\downarrow$ between the probe atom and an atom constituting the target atomic gas.

Because \mathbf{p} corresponds to the momentum of the χ atom in the final state, its differential scattering rate can be identified as

$$\frac{d\Gamma_\chi(\mathbf{k})}{d\mathbf{p}} = \sum_{\sigma,\sigma'} \frac{c_\sigma c_{\sigma'}}{(2\pi)^2} S_{\sigma\sigma'}(\epsilon_{\mathbf{k}} - \epsilon_{\mathbf{p}}, \mathbf{k} - \mathbf{p}) + O(a_\sigma^3), \quad (6.5)$$

which is well known in the context of inelastic neutron scattering in condensed matter physics [112, 113].

This formula (6.5) for the differential scattering rate is valid in the weak-probe limit $a_\sigma \rightarrow 0$ but for an arbitrary incident momentum \mathbf{k} , while our formula (6.1) derived in Sec. V is valid in the hard-probe limit $|\mathbf{k}| \rightarrow \infty$ but for an arbitrary scattering length a_σ . Therefore, they cover different regions in the plane of a_σ and $|\mathbf{k}|$, while both the results become valid in the double limit of $a_\sigma \rightarrow 0$ and $|\mathbf{k}| \rightarrow \infty$ (see Fig. 10). In this section, we show that the weak-probe limit of Eq. (6.1) is indeed equivalent to the hard-probe limit of Eq. (6.5). This serves as a nontrivial check of our results presented in the previous section as well as a new derivation of the large-energy-momentum expansion of the dynamic structure factor $S_{\sigma\sigma'}$.

B. Dynamic structure factor

For simplicity, we shall consider a spin-1/2 Fermi gas at infinite scattering length $a \rightarrow \infty$ only. In the weak-probe limit $a_\sigma \rightarrow 0$, we can make the following expansions in each term for the differential scattering rate in Eq. (6.1):

$$A_\sigma(k) = c_\sigma + O(a_\sigma^2), \quad (6.6)$$

$$t_\sigma(\mathbf{k}; \mathbf{p}) = \frac{m}{\mathbf{p}^2} + O(a_\sigma), \quad (6.7)$$

$$\begin{aligned} t_\chi(\mathbf{k}; \mathbf{p}) = & \int \frac{d\mathbf{q}}{(2\pi)^3} \frac{m}{\mathbf{q}^2} \frac{c_\uparrow + c_\downarrow}{\epsilon_{\mathbf{p}} + \epsilon_{\mathbf{q}} + \epsilon_{\mathbf{k}-\mathbf{p}-\mathbf{q}} - \epsilon_{\mathbf{k}} - i0^+} \\ & + O(a_\sigma^2). \end{aligned} \quad (6.8)$$

Accordingly, the contributions of the number density (5.19) and the current density (5.22) become

$$\frac{d\Gamma_{\chi}^{(n_{\sigma})}(\mathbf{k})}{d\mathbf{p}} = \frac{c_{\sigma}^2 n_{\sigma}}{(2\pi)^2} \delta(\omega - \epsilon_{\mathbf{K}}) + O(a_{\sigma}^3) \quad (6.9)$$

and

$$\frac{d\Gamma_{\chi}^{(j_{\sigma})}(\mathbf{k})}{d\mathbf{p}} = \frac{c_{\sigma}^2 \mathbf{j}_{\sigma}}{(2\pi)^2} \cdot \frac{\partial}{\partial \mathbf{K}} \delta(\omega - \epsilon_{\mathbf{K}}) + O(a_{\sigma}^3), \quad (6.10)$$

respectively, where we denoted the energy-momentum transfer to the medium by $(\omega, \mathbf{K}) \equiv (\epsilon_{\mathbf{k}} - \epsilon_{\mathbf{p}}, \mathbf{k} - \mathbf{p})$. Similarly, after lengthy but straightforward calculations, the contribution of the contact density (5.27) becomes

$$\begin{aligned} \frac{d\Gamma_{\chi}^{(C)}(\mathbf{k})}{d\mathbf{p}} = & \left[\frac{c_{\uparrow}^2 + c_{\downarrow}^2}{(2\pi)^2} \mathcal{S}^{(\text{SE})}(\omega, \mathbf{K}) + \frac{(c_{\uparrow} + c_{\downarrow})^2}{(2\pi)^2} \mathcal{S}^{(\text{AL})}(\omega, \mathbf{K}) \right. \\ & \left. + \frac{c_{\uparrow} c_{\downarrow} + c_{\downarrow} c_{\uparrow}}{(2\pi)^2} \mathcal{S}^{(\text{MT})}(\omega, \mathbf{K}) + O(a_{\sigma}^3) \right] m\mathcal{C}, \end{aligned} \quad (6.11)$$

where we defined⁶

$$\begin{aligned} \mathcal{S}^{(\text{SE})}(\omega, \mathbf{K}) \equiv & \frac{\Theta(\omega - \frac{\epsilon_{\mathbf{K}}}{2})}{(2\pi)^2} \left[\frac{\sqrt{m\omega - \frac{\mathbf{K}^2}{4}}}{(m\omega - \frac{\mathbf{K}^2}{2})^2} \right. \\ & \left. - \int_0^{\infty} dq \frac{2q^2}{m(q^2 - \frac{\mathbf{K}^2}{4})^2} \delta(\omega - \epsilon_{\mathbf{K}}) \right], \end{aligned} \quad (6.12)$$

$$\begin{aligned} \mathcal{S}^{(\text{AL})}(\omega, \mathbf{K}) \equiv & \frac{\Theta(\omega - \frac{\epsilon_{\mathbf{K}}}{2})}{(2\pi)^2 |\mathbf{K}|^2 \sqrt{m\omega - \frac{\mathbf{K}^2}{4}}} \left[\pi^2 \Theta(\epsilon_{\mathbf{K}} - \omega) \right. \\ & \left. - \ln^2 \left(\frac{m\omega + |\mathbf{K}| \sqrt{m\omega - \frac{\mathbf{K}^2}{4}}}{|m\omega - \frac{\mathbf{K}^2}{2}|} \right) \right], \end{aligned} \quad (6.13)$$

$$\mathcal{S}^{(\text{MT})}(\omega, \mathbf{K}) \equiv \frac{\Theta(\omega - \frac{\epsilon_{\mathbf{K}}}{2})}{(2\pi)^2 m\omega |\mathbf{K}|} \ln \left(\frac{m\omega + |\mathbf{K}| \sqrt{m\omega - \frac{\mathbf{K}^2}{4}}}{|m\omega - \frac{\mathbf{K}^2}{2}|} \right). \quad (6.14)$$

⁶ The second term in $\mathcal{S}^{(\text{SE})}(\omega, \mathbf{K})$ originates from the subtracted terms in Eq. (5.27). While it does not contribute away from the single-particle peak at $\omega = \epsilon_{\mathbf{K}}$ [82], this term is essential to compute the differential scattering rate in Eq. (6.17) below. This is because its nonintegrable singularity at $q = |\mathbf{K}|/2$ cancels that of the first term in $\mathcal{S}^{(\text{SE})}(\omega, \mathbf{K})$ which becomes apparent by rewriting Eq. (6.12) as

$$\begin{aligned} \mathcal{S}^{(\text{SE})}(\omega, \mathbf{K}) = & \frac{1}{(2\pi)^2} \int_0^{\infty} dq \frac{2q^2}{m(q^2 - \frac{\mathbf{K}^2}{4})^2} \\ & \times [\delta(\omega - \frac{\epsilon_{\mathbf{K}}}{2} - 2\epsilon_{\mathbf{q}}) - \delta(\omega - \epsilon_{\mathbf{K}})]. \end{aligned}$$

These three functions correspond to self-energy-, Aslamazov-Larkin-, and Maki-Thompson-type contributions, respectively, in a direct diagrammatic calculation [82, 114].

Then by comparing Eqs. (6.9), (6.10), and (6.11) with Eq. (6.5), we find that each spin component of the dynamic structure factor should have the following systematic expansion in the hard-probe limit $K \rightarrow \infty$:

$$\begin{aligned} S_{\sigma\sigma}(\omega, \mathbf{K}) = & n_{\sigma} \delta(\omega - \epsilon_{\mathbf{K}}) + \mathbf{j}_{\sigma} \cdot \frac{\partial}{\partial \mathbf{K}} \delta(\omega - \epsilon_{\mathbf{K}}) \\ & + [\mathcal{S}^{(\text{SE})}(\omega, \mathbf{K}) + \mathcal{S}^{(\text{AL})}(\omega, \mathbf{K})] m\mathcal{C} + O(K^{-4}) \end{aligned} \quad (6.15)$$

for both $\sigma = \uparrow, \downarrow$ and

$$\begin{aligned} S_{\uparrow\downarrow}(\omega, \mathbf{K}) = & S_{\downarrow\uparrow}(\omega, \mathbf{K}) \\ = & [\mathcal{S}^{(\text{AL})}(\omega, \mathbf{K}) + \mathcal{S}^{(\text{MT})}(\omega, \mathbf{K})] m\mathcal{C} + O(K^{-4}). \end{aligned} \quad (6.16)$$

The sum of all four components $S(\omega, \mathbf{K}) \equiv \sum_{\sigma, \sigma'} S_{\sigma\sigma'}(\omega, \mathbf{K})$ coincides with the large-energy-momentum expansion of the total dynamic structure factor found previously in Refs. [82, 83, 85, 114, 115]. This establishes the equivalence between our hard-probe formula in Eq. (6.1) and the known weak-probe formula in Eq. (6.5) in the limit $a_{\sigma} \rightarrow 0$ followed by $|\mathbf{k}| \rightarrow \infty$ where both the results become valid. However, we emphasize again that, away from this double limit, the two results are independent and cover different regions in the plane of a_{σ} and $|\mathbf{k}|$ (see Fig. 10).

C. Differential scattering rate

Finally, we present the angle distribution of the large-momentum χ atom scattered by a spin-1/2 Fermi gas at infinite scattering length $a \rightarrow \infty$ but in the weak-probe limit $a_{\sigma} \rightarrow 0$. The integration of Eq. (6.5) with the dynamic structure factor obtained in Eqs. (6.15) and (6.16) over the magnitude of momentum $|\mathbf{p}|^2 d|\mathbf{p}|$ yields

$$\begin{aligned} \frac{d\Gamma_{\chi}(\mathbf{k})}{d\Omega} = & 4 \sum_{\sigma=\uparrow, \downarrow} \left[\cos\theta \Theta(\cos\theta) |\mathbf{k}| n_{\sigma} \right. \\ & \left. - \{ \delta(\cos\theta) \hat{\mathbf{k}} - \Theta(\cos\theta) \hat{\mathbf{p}} \} \cdot \mathbf{j}_{\sigma} \right] \frac{a_{\sigma}^2}{m} \\ & + [h_{\parallel}(\cos\theta) \mathcal{C} + O(\mathbf{k}^{-1})] \frac{a_{\uparrow}^2 + a_{\downarrow}^2}{2m} \\ & + [h_{\uparrow\downarrow}(\cos\theta) \mathcal{C} + O(\mathbf{k}^{-1})] \frac{a_{\uparrow} a_{\downarrow}}{m} + O(a_{\sigma}^3). \end{aligned} \quad (6.17)$$

Here, $h_{\parallel}(\cos\theta)$ and $h_{\uparrow\downarrow}(\cos\theta)$ are universal functions plotted in Fig. 11 and defined by

$$\begin{aligned} h_{\parallel}(\cos\theta) \equiv & 8 \int_0^{\infty} d|\mathbf{p}| |\mathbf{p}|^2 [\mathcal{S}^{(\text{SE})}(\epsilon_{\mathbf{k}} - \epsilon_{\mathbf{p}}, \mathbf{k} - \mathbf{p}) \\ & + \mathcal{S}^{(\text{AL})}(\epsilon_{\mathbf{k}} - \epsilon_{\mathbf{p}}, \mathbf{k} - \mathbf{p})] \end{aligned} \quad (6.18)$$

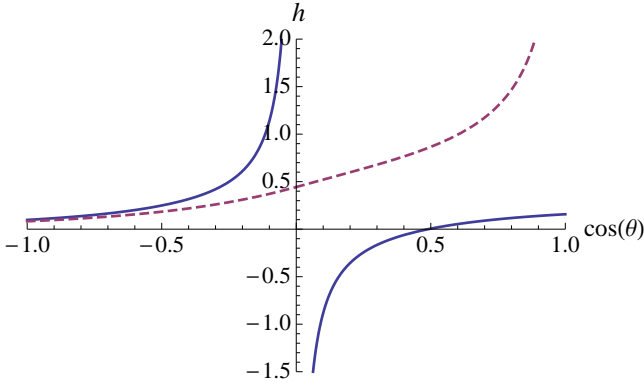


FIG. 11. (Color online) Universal functions $h_{\parallel}(\cos\theta)$ (solid curve) and $h_{\perp}(\cos\theta)$ (dashed curve) to determine the contribution of the contact density to the differential scattering rate (6.17) in the weak-probe limit $a_{\uparrow}, a_{\downarrow} \rightarrow 0$.

and

$$h_{\uparrow\downarrow}(\cos\theta) \equiv 8 \int_0^{\infty} d|\mathbf{p}||\mathbf{p}|^2 [\mathcal{S}^{(\text{AL})}(\epsilon_{\mathbf{k}} - \epsilon_{\mathbf{p}}, \mathbf{k} - \mathbf{p}) + \mathcal{S}^{(\text{MT})}(\epsilon_{\mathbf{k}} - \epsilon_{\mathbf{p}}, \mathbf{k} - \mathbf{p})]. \quad (6.19)$$

These two functions correspond to the weak-coupling limit of the function g introduced in Eq. (5.28):

$$\begin{aligned} & \lim_{a_{\uparrow}, a_{\downarrow} \rightarrow 0} g\left(\cos\theta, \frac{|\mathbf{k}|}{\kappa'_*}\right) \Big|_{a_{\sigma}|\mathbf{k}|} \\ &= h_{\parallel}(\cos\theta) \frac{a_{\uparrow}^2 + a_{\downarrow}^2}{2} \mathbf{k}^2 + h_{\perp}(\cos\theta) a_{\uparrow} a_{\downarrow} \mathbf{k}^2, \end{aligned} \quad (6.20)$$

while g was evaluated in the strong-coupling limit $a_{\uparrow}, a_{\downarrow} \rightarrow \infty$ in the previous section. Note that the Efimov effect does not appear in perturbative expansions. Again, one can see from Eq. (6.17) that the number density and current density contribute to the forward scattering only, while Fig. 11 shows $h_{\parallel}(\cos\theta) > h_{\perp}(\cos\theta) > 0$ at $\cos\theta < 0$ so that the contact density gives the leading contribution to the backward scattering.

The integration of the differential scattering rate (6.17) over the solid angle $d\Omega = d\cos\theta d\varphi$ yields the total scattering rate in the weak-probe limit $a_{\sigma} \rightarrow 0$:

$$\begin{aligned} \Gamma_{\chi}(\mathbf{k}) &= 4\pi \sum_{\sigma=\uparrow,\downarrow} \left[|\mathbf{k}| n_{\sigma} - \hat{\mathbf{k}} \cdot \mathbf{j}_{\sigma} \right] \frac{a_{\sigma}^2}{m} \\ &+ [1.60098 \mathcal{C} + O(\mathbf{k}^{-1})] \frac{a_{\uparrow}^2 + a_{\downarrow}^2}{2m} \\ &+ [9.25387 \mathcal{C} + O(\mathbf{k}^{-1})] \frac{a_{\uparrow} a_{\downarrow}}{m} + O(a_{\sigma}^3). \end{aligned} \quad (6.21)$$

Note that, since $d\Gamma_{\chi}(\mathbf{k})/d\Omega$ has a pole at $\cos\theta = 0$ due to $h_{\parallel}(\cos\theta) \sim -1/(\pi^2 \cos\theta)$, the integral over $\cos\theta$ is understood as the Cauchy principal value.

D. Spinless Bose gas

Similarly, in the case of a spinless Bose gas at infinite scattering length $a \rightarrow \infty$, the differential scattering rate of the χ atom in the weak-probe limit $a_{\chi} \rightarrow 0$ is given by

$$\frac{d\Gamma_{\chi}(\mathbf{k})}{d\mathbf{p}} = \frac{c_{\chi}^2}{(2\pi)^2} S(\epsilon_{\mathbf{k}} - \epsilon_{\mathbf{p}}, \mathbf{k} - \mathbf{p}) + O(a_{\chi}^3). \quad (6.22)$$

Here, $S(\omega, \mathbf{K})$ is a dynamic structure factor of the spinless Bose gas and has the following systematic expansion in the hard-probe limit $K \rightarrow \infty$:

$$\begin{aligned} S(\omega, \mathbf{K}) &= n \delta(\omega - \epsilon_{\mathbf{K}}) + \mathbf{j} \cdot \frac{\partial}{\partial \mathbf{K}} \delta(\omega - \epsilon_{\mathbf{K}}) \\ &+ [\mathcal{S}^{(\text{SE})}(\omega, \mathbf{K}) + 2 \mathcal{S}^{(\text{AL})}(\omega, \mathbf{K}) + \mathcal{S}^{(\text{MT})}(\omega, \mathbf{K})] m\mathcal{C} \\ &+ O(K^{-4}). \end{aligned} \quad (6.23)$$

Therefore, the contribution of the contact density to the dynamic structure factor in a spinless Bose gas is a half of that to the total dynamic structure factor in a spin-1/2 Fermi gas [83]. Accordingly, Eqs. (6.17) and (6.21) remain valid by setting $a_{\uparrow} = a_{\downarrow} \rightarrow a_{\chi}$, replacing $n_{\uparrow} + n_{\downarrow} (\mathbf{j}_{\uparrow} + \mathbf{j}_{\downarrow})$ with $n (\mathbf{j})$, and dividing the coefficients of \mathcal{C} by two.

VII. CONCLUSIONS

In this paper, we investigated various properties of an energetic atom propagating through strongly interacting atomic gases by using systematic large-momentum expansions. Our main results are summarized in Sec. II and consist of the quasiparticle energy and scattering rate of an energetic atom in a spin-1/2 Fermi gas (Sec. III), those in a spinless Bose gas (Sec. IV), and the differential scattering rate of a different spin state of atoms shot into a spin-1/2 Fermi gas or a spinless Bose gas (Sec. V). Furthermore, a connection of our hard-probe formula derived in Sec. V with dynamic structure factors in the weak-probe limit was elucidated in Sec. VI.

Our result on the quasiparticle energy in a spin-1/2 Fermi gas reasonably agrees with the recent quantum Monte Carlo simulation [74] even at a relatively small momentum $|\mathbf{k}|/k_{\text{F}} \gtrsim 1.5$. This indicates that our large-momentum expansions are valid in a wide range of momentum. Further analysis of quantum Monte Carlo data incorporating our exact large-momentum expansions may allow us better access to the intriguing pseudogap physics. Also our result on the rate at which the atom is scattered in the medium may be useful to better understand multiple-atom loss mechanisms due to atom-dimer ‘‘dijets’’ produced by three-body recombination events [47, 53]. We found that the contact density has a negative contribution to the scattering rate in a spinless Bose gas. This rather counterintuitively means that the energetic boson can escape from the medium easier than we naively estimate from a binary collision.

We also proposed a scattering experiment in which we shoot a different spin state of atoms into an atomic gas with a large momentum and measure its differential scattering rate (Fig. 1). Here a nice interplay between few-body physics and many-body physics can be seen: The angle distribution of the scattered atom is determined by few-body physics and its overall magnitude is set by many-body physics. We elucidated that, because the number density and current density of the target atomic gas contribute to the forward scattering only, its contact density gives the leading contribution to the backward scattering. Therefore, such an experiment can be used to measure the contact density (integrated along a classical trajectory of the probe atom) and thus provides a new *local* probe of strongly interacting atomic gases. Its intriguing analogy to nuclear physics experiments on short-range pair correlations in nuclei [32, 33] should be explored further. Also we found that the differential scattering rate can depend on the azimuthal angle only by the current density of the target atomic gas. Therefore, the azimuthal anisotropy in the differential scattering rate may be useful to reveal many-body phases accompanied by currents. We hope this work serves as a promising starting point for future ultracold-atom experiments and builds a new bridge between ultracold atoms and nuclear and particle physics from the perspective of “hard probes.”

ACKNOWLEDGMENTS

This work started when the author attended the MIT nuclear and particle physics colloquium in the fall of 2008 given by Krishna Rajagopal to whom he is grateful. He also thanks E. Braaten, A. Bulgac, J. Carlson, J. E. Drut, S. Gandolfi, T. Hatsuda, D. Kang, J. Levinsen, P. Pieri, D. T. Son, F. Werner, G. Wlazłowski, W. Zwerger, M. W. Zwierlein, and, in particular, Shina Tan for valuable discussions and providing numerical data in Ref. [74]. This work was supported by a MIT Pappalardo Fellowship in Physics and a LANL Oppenheimer Fellowship. Part of numerical calculations was carried out at the YITP computer facility in Kyoto University.

Appendix A: Derivation of Wilson coefficients

Here we show how the Wilson coefficients in Eqs. (3.13)–(3.22) and Eqs. (4.14)–(4.18) are derived. For generality, we consider spin-1/2 fermions with unequal masses $m_\uparrow \neq m_\downarrow$. The propagator of fermion field ψ_σ in the vacuum is given by

$$G_\sigma(k) = \frac{1}{k_0 - \epsilon_{\mathbf{k}\sigma} + i0^+} \left(\epsilon_{\mathbf{k}\sigma} \equiv \frac{\mathbf{k}^2}{2m_\sigma} \right), \quad (\text{A1})$$

and the two-body scattering amplitude between spin-up and -down fermions is

$$A(k) = \frac{2\pi}{\mu} \frac{1}{\sqrt{\frac{\mu}{M}k^2 - 2\mu k_0 - i0^+ - \frac{1}{a}}}. \quad (\text{A2})$$

Here, $M = m_\uparrow + m_\downarrow$ is a total mass and $\mu = m_\uparrow m_\downarrow / (m_\uparrow + m_\downarrow)$ is a reduced mass. Results in the case of spinless bosons are obtained by removing spin indices and replacing the two-body scattering amplitude $A(k)$ with that between two identical bosons [see Eq. (4.4)]:

$$A(k) = \frac{8\pi}{m} \frac{1}{\sqrt{\frac{k^2}{4} - mk_0 - i0^+ - \frac{1}{a}}}. \quad (\text{A3})$$

1. One-body and two-body sectors

The Wilson coefficients of local operators of type $\psi_\sigma^\dagger \psi_\sigma$ in Eqs. (3.9)–(3.12) are determined by matching the matrix elements of both sides of

$$\int dy e^{iky} T[\psi_\uparrow(x + \frac{y}{2})\psi_\uparrow^\dagger(x - \frac{y}{2})] = \sum_i W_{\mathcal{O}_i}(k)\mathcal{O}_i(x) \quad (\text{A4})$$

with respect to one-body states $\langle \psi_\sigma(p') |$ and $|\psi_\sigma(p) \rangle$. The matrix element of the left-hand side is given by

$$\begin{aligned} & \int dy e^{iky} \langle \psi_\sigma(p') | T[\psi_\uparrow(x + \frac{y}{2})\psi_\uparrow^\dagger(x - \frac{y}{2})] | \psi_\sigma(p) \rangle \\ &= iG_\uparrow(k) iG_\sigma(p) (2\pi)^4 \delta(p - p') \\ &+ (1 - \delta_{\uparrow\sigma}) iG_\uparrow(k - \frac{p-p'}{2}) iG_\sigma(p) iA(k + \frac{p+p'}{2}) \\ &\times iG_\sigma(p') iG_\uparrow(k + \frac{p-p'}{2}) e^{-i(p-p')x}. \end{aligned} \quad (\text{A5})$$

On the other hand, the matrix elements of local operators of type $\psi_\sigma^\dagger \psi_\sigma$ are

$$\langle \psi_\sigma(p') | \mathbb{1} | \psi_\sigma(p) \rangle = iG_\sigma(p) (2\pi)^4 \delta(p - p'), \quad (\text{A6})$$

$$\langle \psi_\sigma(p') | \psi_\sigma^\dagger \psi_\sigma(x) | \psi_\sigma(p) \rangle = iG_\sigma(p) iG_\sigma(p') e^{-i(p-p')x}, \quad (\text{A7})$$

$$\begin{aligned} & \langle \psi_\sigma(p') | -i\psi_\sigma^\dagger \overleftrightarrow{\partial}_i \psi_\sigma(x) | \psi_\sigma(p) \rangle \\ &= \frac{p_i + p'_i}{2} iG_\sigma(p) iG_\sigma(p') e^{-i(p-p')x}, \end{aligned} \quad (\text{A8})$$

$$\begin{aligned} & \langle \psi_\sigma(p') | -i\partial_i(\psi_\sigma^\dagger \psi_\sigma)(x) | \psi_\sigma(p) \rangle \\ &= (p_i - p'_i) iG_\sigma(p) iG_\sigma(p') e^{-i(p-p')x}, \end{aligned} \quad (\text{A9})$$

$$\begin{aligned} & \langle \psi_\sigma(p') | -\psi_\sigma^\dagger \overleftrightarrow{\partial}_i \overleftrightarrow{\partial}_j \psi_\sigma(x) | \psi_\sigma(p) \rangle \\ &= \frac{p_i + p'_i}{2} \frac{p_j + p'_j}{2} iG_\sigma(p) iG_\sigma(p') e^{-i(p-p')x}, \end{aligned} \quad (\text{A10})$$

$$\begin{aligned} & \langle \psi_\sigma(p') | -\partial_i (\psi_\sigma^\dagger \overleftrightarrow{\partial}_j \psi_\sigma)(x) | \psi_\sigma(p) \rangle \\ &= (p_i - p'_i) \frac{p_j + p'_j}{2} iG_\sigma(p) iG_\sigma(p') e^{-i(p-p')x}, \end{aligned} \quad (\text{A11})$$

$$W_{\psi_\downarrow^\dagger \psi_\downarrow}(k) = -iG_\uparrow(k)^2 A(k), \quad (\text{A16})$$

$$\begin{aligned} & \langle \psi_\sigma(p') | -\partial_i \partial_j (\psi_\sigma^\dagger \psi_\sigma)(x) | \psi_\sigma(p) \rangle \\ &= (p_i - p'_i) (p_j - p'_j) iG_\sigma(p) iG_\sigma(p') e^{-i(p-p')x}, \end{aligned} \quad (\text{A12})$$

$$W_{-i\psi_\downarrow^\dagger \overleftrightarrow{\partial}_i \psi_\downarrow}(k) = -iG_\uparrow(k)^2 \frac{\partial}{\partial k_i} A(k), \quad (\text{A17})$$

$$\begin{aligned} & \langle \psi_\sigma(p') | i\psi_\sigma^\dagger \overleftrightarrow{\partial}_i \psi_\sigma(x) | \psi_\sigma(p) \rangle \\ &= \frac{p_0 + p'_0}{2} iG_\sigma(p) iG_\sigma(p') e^{-i(p-p')x}, \end{aligned} \quad (\text{A13})$$

$$W_{-\psi_\downarrow^\dagger \overleftrightarrow{\partial}_i \overleftrightarrow{\partial}_j \psi_\downarrow}(k) = -iG(k)^2 \frac{1}{2} \frac{\partial^2}{\partial k_i \partial k_j} A(k), \quad (\text{A18})$$

$$\begin{aligned} & \langle \psi_\sigma(p') | i\partial_t (\psi_\sigma^\dagger \psi_\sigma)(x) | \psi_\sigma(p) \rangle \\ &= (p_0 - p'_0) iG_\sigma(p) iG_\sigma(p') e^{-i(p-p')x}. \end{aligned} \quad (\text{A14})$$

$$W_{i\psi_\downarrow^\dagger \overleftrightarrow{\partial}_t \psi_\downarrow}(k) = -iG_\uparrow(k)^2 \frac{\partial}{\partial k_0} A(k), \quad (\text{A19})$$

$$W_{-\partial_i \partial_j (\psi_\downarrow^\dagger \psi_\downarrow)}(k) = -iA(k) \frac{G_\uparrow(k)^3}{4m_\uparrow} \left[\delta_{ij} + k_i k_j \frac{G_\uparrow(k)}{m_\uparrow} \right], \quad (\text{A20})$$

Therefore, the expansion of Eq. (A5) up to $O(p^3)$ is reproduced by choosing their Wilson coefficients as

$$W_{-i\partial_i (\psi_\downarrow^\dagger \psi_\downarrow)}(k) = W_{-\partial_i (\psi_\downarrow^\dagger \overleftrightarrow{\partial}_j \psi_\downarrow)}(k) = W_{i\partial_t (\psi_\downarrow^\dagger \psi_\downarrow)}(k) = 0, \quad (\text{A21})$$

$$W_{\mathbb{1}}(k) = iG_\uparrow(k), \quad (\text{A15}) \quad \text{and all } W_{\mathcal{O}}(k) = 0 \text{ for } \sigma = \uparrow.$$

2. Three-body sector

The Wilson coefficients of local operators of type $\phi^\dagger \phi$ in Eqs. (3.9)–(3.12) are determined by matching the matrix elements of both sides of Eq. (A4) with respect to two-body states $\langle \phi(p') |$ and $| \phi(p) \rangle$. The matrix element of the left-hand side is given by

$$\begin{aligned} & \int dy e^{iky} \langle \phi(p') | T[\psi_\uparrow(x + \frac{y}{2}) \psi_\uparrow^\dagger(x - \frac{y}{2})] | \phi(p) \rangle \\ &= iG_\uparrow(k) iD(p) (2\pi)^4 \delta(p - p') \\ &+ iG_\uparrow(k - \frac{p-p'}{2}) iD(p) iT_\uparrow(k - \frac{p-p'}{2}, \frac{p+p'}{2} + \frac{p-p'}{2}; k + \frac{p-p'}{2}, \frac{p+p'}{2} - \frac{p-p'}{2}) iD(p') iG_\uparrow(k + \frac{p-p'}{2}) e^{-i(p-p')x}. \end{aligned} \quad (\text{A22})$$

Here, $D(k) = -A(k)$ is the dimer propagator and $T_\uparrow(k, p; k', p')$ is the three-body scattering amplitude between a spin-up fermion and a dimer with (k, p) $[(k', p')]$ being their initial (final) energy-momentum (see Fig. 5). On the other hand, the matrix elements of local operators of type $\psi_\downarrow^\dagger \psi_\downarrow$ are

$$\langle \phi(p') | \mathbb{1} | \phi(p) \rangle = iD(p) (2\pi)^4 \delta(p - p'), \quad (\text{A23})$$

$$\begin{aligned} & \langle \phi(p') | \psi_\downarrow^\dagger \psi_\downarrow(x) | \phi(p) \rangle \\ &= iD(p) iD(p') e^{-i(p-p')x} i \int \frac{dq}{(2\pi)^4} G_\uparrow(\frac{p+p'}{2} - q) G_\downarrow(q + \frac{p+p'}{2}) G_\downarrow(q - \frac{p+p'}{2}) \\ &= iD(p) iD(p') e^{-i(p-p')x} \int \frac{d\mathbf{q}}{(2\pi)^3} \left(\frac{2\mu}{\mathbf{q}^2} \right)^2 + O(p^2), \end{aligned} \quad (\text{A24})$$

$$\begin{aligned} & \langle \phi(p') | -i\psi_\downarrow^\dagger \overleftrightarrow{\partial}_i \psi_\downarrow(x) | \phi(p) \rangle \\ &= iD(p) iD(p') e^{-i(p-p')x} i \int \frac{dq}{(2\pi)^4} q_i G_\uparrow(\frac{p+p'}{2} - q) G_\downarrow(q + \frac{p+p'}{2}) G_\downarrow(q - \frac{p+p'}{2}) \\ &= iD(p) iD(p') e^{-i(p-p')x} \left(\frac{m_\downarrow}{M} \frac{p_i + p'_i}{2} \right) \int \frac{d\mathbf{q}}{(2\pi)^3} \left(\frac{2\mu}{\mathbf{q}^2} \right)^2 + O(p^2), \end{aligned} \quad (\text{A25})$$

$$\begin{aligned}
& \langle \phi(p') | -i\partial_i(\psi_\downarrow^\dagger \psi_\downarrow)(x) | \phi(p) \rangle \\
&= iD(p)iD(p')e^{-i(p-p')x} i \int \frac{dq}{(2\pi)^4} (p_i - p'_i) G_\uparrow(\frac{p+p'}{2} - q) G_\downarrow(q + \frac{p+p'}{2}) G_\downarrow(q - \frac{p+p'}{2}) \\
&= iD(p)iD(p')e^{-i(p-p')x} (p_i - p'_i) \int \frac{d\mathbf{q}}{(2\pi)^3} \left(\frac{2\mu}{\mathbf{q}^2} \right)^2 + O(p^2),
\end{aligned} \tag{A26}$$

$$\begin{aligned}
& \langle \phi(p') | -\psi_\downarrow^\dagger \overleftrightarrow{\partial}_i \overleftrightarrow{\partial}_j \psi_\downarrow(x) | \phi(p) \rangle \\
&= iD(p)iD(p')e^{-i(p-p')x} i \int \frac{dq}{(2\pi)^4} q_i q_j G_\uparrow(\frac{p+p'}{2} - q) G_\downarrow(q + \frac{p+p'}{2}) G_\downarrow(q - \frac{p+p'}{2}) \\
&= iD(p)iD(p')e^{-i(p-p')x} \frac{\delta_{ij}}{3} \int \frac{d\mathbf{q}}{(2\pi)^3} \mathbf{q}^2 \left(\frac{2\mu}{\mathbf{q}^2} \right)^2 + O(p^2),
\end{aligned} \tag{A27}$$

$$\begin{aligned}
& \langle \phi(p') | -\partial_i(\psi_\downarrow^\dagger \overleftrightarrow{\partial}_j \psi_\downarrow)(x) | \phi(p) \rangle \\
&= iD(p)iD(p')e^{-i(p-p')x} i \int \frac{dq}{(2\pi)^4} (p_i - p'_i) q_j G_\uparrow(\frac{p+p'}{2} - q) G_\downarrow(q + \frac{p+p'}{2}) G_\downarrow(q - \frac{p+p'}{2}) \\
&= O(p^2),
\end{aligned} \tag{A28}$$

$$\begin{aligned}
& \langle \phi(p') | -\partial_i \partial_j(\psi_\downarrow^\dagger \psi_\downarrow)(x) | \phi(p) \rangle \\
&= iD(p)iD(p')e^{-i(p-p')x} i \int \frac{dq}{(2\pi)^4} (p_i - p'_i)(p_j - p'_j) G_\uparrow(\frac{p+p'}{2} - q) G_\downarrow(q + \frac{p+p'}{2}) G_\downarrow(q - \frac{p+p'}{2}) \\
&= O(p^2),
\end{aligned} \tag{A29}$$

$$\begin{aligned}
& \langle \phi(p') | i\psi_\downarrow^\dagger \overleftrightarrow{\partial}_t \psi_\downarrow(x) | \phi(p) \rangle \\
&= iD(p)iD(p')e^{-i(p-p')x} i \int \frac{dq}{(2\pi)^4} q_0 G_\uparrow(\frac{p+p'}{2} - q) G_\downarrow(q + \frac{p+p'}{2}) G_\downarrow(q - \frac{p+p'}{2}) \\
&= iD(p)iD(p')e^{-i(p-p')x} \int \frac{d\mathbf{q}}{(2\pi)^3} \left(-\frac{\mathbf{q}^2}{2m_\uparrow} \right) \left(\frac{2\mu}{\mathbf{q}^2} \right)^2 + O(p^2).
\end{aligned} \tag{A30}$$

$$\begin{aligned}
& \langle \phi(p') | i\partial_t(\psi_\downarrow^\dagger \psi_\downarrow)(x) | \phi(p) \rangle \\
&= iD(p)iD(p')e^{-i(p-p')x} i \int \frac{dq}{(2\pi)^4} (p_0 - p'_0) G_\uparrow(\frac{p+p'}{2} - q) G_\downarrow(q + \frac{p+p'}{2}) G_\downarrow(q - \frac{p+p'}{2}) \\
&= O(p^2).
\end{aligned} \tag{A31}$$

Because the matrix elements of local operators of type $\phi^\dagger \phi$ are given by

$$\langle \phi(p') | \phi^\dagger \phi(x) | \phi(p) \rangle = iD(p)iD(p')e^{-i(p-p')x}, \tag{A32}$$

$$\langle \phi(p') | -i\phi^\dagger \overleftrightarrow{\partial}_i \phi(x) | \phi(p) \rangle = \frac{p_i + p'_i}{2} iD(p)iD(p')e^{-i(p-p')x}, \tag{A33}$$

$$\langle \phi(p') | -i\partial_i(\phi^\dagger \phi)(x) | \phi(p) \rangle = (p_i - p'_i) iD(p)iD(p')e^{-i(p-p')x}, \tag{A34}$$

the expansion of Eq. (A22) up to $O(p^2)$ is reproduced by choosing their Wilson coefficients as

$$\begin{aligned}
W_{\phi^\dagger \phi}(k) &= -iG(k)^2 T_\uparrow(k, 0; k, 0) - W_{\psi_\downarrow^\dagger \psi_\downarrow}(k) \int \frac{d\mathbf{q}}{(2\pi)^3} \left(\frac{2\mu}{\mathbf{q}^2} \right)^2 \\
&\quad - W_{-\psi_\downarrow^\dagger \overleftrightarrow{\partial}_i \overleftrightarrow{\partial}_j \psi_\downarrow}(k) \frac{\delta_{ij}}{3} \int \frac{d\mathbf{q}}{(2\pi)^3} \left(\frac{2\mu}{\mathbf{q}^2} \right)^2 - W_{i\psi_\downarrow^\dagger \overleftrightarrow{\partial}_t \psi_\downarrow}(k) \frac{-1}{2m_\uparrow} \int \frac{d\mathbf{q}}{(2\pi)^3} \left(\frac{2\mu}{\mathbf{q}^2} \right)^2,
\end{aligned} \tag{A35}$$

$$W_{-i\phi^\dagger \overleftrightarrow{\partial}_i \phi}(k) = -iG_\uparrow(k)^2 \frac{\partial}{\partial p_i} T_\uparrow(k, p; k, p) \Big|_{p \rightarrow 0} - W_{-i\psi_\downarrow^\dagger \overleftrightarrow{\partial}_i \psi_\downarrow}(k) \frac{m_\downarrow}{M} \int \frac{d\mathbf{q}}{(2\pi)^3} \left(\frac{2\mu}{\mathbf{q}^2} \right)^2, \quad (\text{A36})$$

$$W_{-i\partial_i(\phi^\dagger \phi)}(k) = -iG_\uparrow(k)^2 \frac{\partial}{\partial p_i} T_\uparrow(k - \frac{p}{2}, \frac{p}{2}; k + \frac{p}{2}, -\frac{p}{2}) \Big|_{p \rightarrow 0}. \quad (\text{A37})$$

These results are presented in Eqs. (3.13)–(3.22) for a spin-1/2 Fermi gas and in Eqs. (4.14)–(4.18) for a spinless Bose gas.

Appendix B: Details of solving integral equations

Here we discuss details of solving the integral equations in Eq. (3.45) for a spin-1/2 Fermi gas and in Eq. (4.26) for a spinless Bose gas.

1. Spin-1/2 Fermi gas

For generality, we consider spin-1/2 fermions with unequal masses $m_\uparrow \neq m_\downarrow$, in which the integral equation (3.45) is modified to

$$t_\uparrow(\mathbf{k}; \mathbf{p}) = -\frac{2\mu}{\mathbf{p}^2} - \int \frac{d\mathbf{q}}{(2\pi)^3} \mathcal{K}_a(\mathbf{k}; \mathbf{p}, \mathbf{q}) t_\uparrow(\mathbf{k}; \mathbf{q}), \quad (\text{B1})$$

where the integral kernel $\mathcal{K}_a(\mathbf{k}; \mathbf{p}, \mathbf{q})$ is given by

$$\mathcal{K}_a(\mathbf{k}; \mathbf{p}, \mathbf{q}) = \frac{2\pi}{\mu} \frac{1}{\sqrt{\frac{\mu}{M}(\mathbf{k} - \mathbf{q})^2 - 2\mu(\epsilon_{\mathbf{k}\uparrow} - \epsilon_{\mathbf{q}\uparrow}) - i0^+} - \frac{1}{a} \epsilon_{\mathbf{k}-\mathbf{p}-\mathbf{q}\downarrow} + \epsilon_{\mathbf{p}\uparrow} + \epsilon_{\mathbf{q}\uparrow} - \epsilon_{\mathbf{k}\uparrow} - i0^+}. \quad (\text{B2})$$

For unequal masses, the quantity we would like to compute (3.49) becomes

$$t_\uparrow^{\text{reg}}(\mathbf{k}; \mathbf{k}) = -\frac{2\mu}{\mathbf{k}^2} + \int \frac{d\mathbf{q}}{(2\pi)^3} \left[\mathcal{K}_a(\mathbf{k}; \mathbf{k}, \mathbf{q}) - \frac{4\pi}{-i\frac{m_\downarrow}{M}|\mathbf{k}| - \frac{1}{a}\mathbf{q}^2} \right] \frac{2\mu}{\mathbf{q}^2} - \int \frac{d\mathbf{q}}{(2\pi)^3} \mathcal{K}_a(\mathbf{k}; \mathbf{k}, \mathbf{q}) \left[t_\uparrow(\mathbf{k}; \mathbf{q}) + \frac{2\mu}{\mathbf{q}^2} \right]. \quad (\text{B3})$$

The second term is a simple integral and has the following analytic expression for its expansion in terms of $(a|\mathbf{k}|)^{-1}$:

$$\begin{aligned} & \int \frac{d\mathbf{q}}{(2\pi)^3} \left[\mathcal{K}_a(\mathbf{k}; \mathbf{k}, \mathbf{q}) - \frac{4\pi}{-i\frac{m_\downarrow}{M}|\mathbf{k}| - \frac{1}{a}\mathbf{q}^2} \right] \frac{2\mu}{\mathbf{q}^2} \\ &= \left[\frac{(u+1)\sqrt{2u+1} + \frac{(u+1)^3}{u} \arcsin\left(\frac{u}{u+1}\right)}{\pi} + \frac{(u+1)^3}{a|\mathbf{k}|} i + \dots \right]_{u=\frac{m_\uparrow}{m_\downarrow}} \frac{2\mu}{\mathbf{k}^2}. \end{aligned} \quad (\text{B4})$$

Therefore, the nontrivial task is the calculation of the last term in Eq. (B3) at $(a|\mathbf{k}|)^{-1} = 0$ and its first derivative with respect to $(a|\mathbf{k}|)^{-1}$, which requires solving the two-dimensional integral equation (B1) numerically.

For numerical purposes, it is more convenient to shift momentum variables as $\mathbf{p}(\mathbf{q}) \rightarrow \mathbf{p}(\mathbf{q}) + \frac{m_\uparrow}{M+m_\uparrow} \mathbf{k}$ to move to the center-of-mass frame and introduce a dimensionless function

$$s_\uparrow(\mathbf{p}) \equiv \frac{\mathbf{k}^2}{2\mu} t_\uparrow(\mathbf{k}; \mathbf{p} + \frac{m_\uparrow}{M+m_\uparrow} \mathbf{k}). \quad (\text{B5})$$

This function solves a simpler integral equation

$$s_\uparrow(\mathbf{p}) = -\mathcal{I}(\mathbf{p}) - \int \frac{d\mathbf{q}}{(2\pi)^3} \mathcal{J}_a(\mathbf{p}, \mathbf{q}) s_\uparrow(\mathbf{q}), \quad (\text{B6})$$

where the new inhomogeneous term $\mathcal{I}(\mathbf{p})$ and integral kernel $\mathcal{J}_a(\mathbf{p}, \mathbf{q})$ are defined by

$$\mathcal{I}(\mathbf{p}) \equiv \frac{\mathbf{k}^2}{\left(\mathbf{p} + \frac{m_\uparrow}{M+m_\uparrow} \mathbf{k}\right)^2} \quad (\text{B7})$$

and

$$\begin{aligned} \mathcal{J}_a(\mathbf{p}, \mathbf{q}) &\equiv \mathcal{K}_a(\mathbf{k}; \mathbf{p} + \frac{m_\uparrow}{M+m_\uparrow}\mathbf{k}, \mathbf{q} + \frac{m_\uparrow}{M+m_\uparrow}\mathbf{k}) \\ &= \frac{4\pi}{\sqrt{m_\downarrow \frac{M+m_\uparrow}{M^2}\mathbf{q}^2 - \frac{m_\downarrow}{M+m_\uparrow}\mathbf{k}^2 - i0^+ - \frac{1}{a}\mathbf{p}^2 + \mathbf{q}^2 + \frac{2m_\uparrow}{M}\mathbf{p} \cdot \mathbf{q} - \frac{m_\downarrow}{M+m_\uparrow}\mathbf{k}^2 - i0^+}}. \end{aligned} \quad (\text{B8})$$

Since $\mathcal{J}_a(\mathbf{p}, \mathbf{q})$ now depends on the angle only between \mathbf{p} and \mathbf{q} , each component of the partial-wave expansion

$$s_\uparrow(\mathbf{p}) = \sum_{\ell=0}^{\infty} s_\uparrow^{(\ell)}(p) P_\ell(\cos \theta) \quad (\cos \theta \equiv \hat{\mathbf{k}} \cdot \hat{\mathbf{p}}) \quad (\text{B9})$$

solves an independent one-dimensional integral equation

$$s_\uparrow^{(\ell)}(p) = -\mathcal{I}^{(\ell)}(p) - \int_0^\infty dq \mathcal{J}_a^{(\ell)}(p, q) s_\uparrow^{(\ell)}(q), \quad (\text{B10})$$

where the partial-wave projections of the inhomogeneous term and integral kernel are given by

$$\mathcal{I}^{(\ell)}(p) = \frac{2\ell+1}{2} \int_{-1}^1 d\cos \theta P_\ell(\cos \theta) \mathcal{I}(\mathbf{p}) = \frac{2\ell+1}{2} \int_{-1}^1 d\cos \theta \frac{P_\ell(\cos \theta)}{p^2 + \left(\frac{u}{2u+1}\right)^2 + \frac{2u}{2u+1}p \cos \theta} \quad (\text{B11})$$

and

$$\begin{aligned} \mathcal{J}_a^{(\ell)}(p, q) &= \frac{2\pi q^2}{(2\pi)^3} \int_{-1}^1 d\cos \theta P_\ell(\cos \theta) \mathcal{J}_a(\mathbf{p}, \mathbf{q}) \\ &= \frac{q^2}{\pi} \frac{1}{\sqrt{\frac{2u+1}{(u+1)^2}q^2 - \frac{1}{2u+1} - i0^+ - \frac{1}{ak}}} \int_{-1}^1 d\cos \theta \frac{P_\ell(\cos \theta)}{p^2 + q^2 + \frac{2u}{u+1}pq \cos \theta - \frac{1}{2u+1} - i0^+}. \end{aligned} \quad (\text{B12})$$

Here, $p = |\mathbf{p}|/|\mathbf{k}|$, $q = |\mathbf{q}|/|\mathbf{k}|$ are dimensionless momenta and the mass ratio is denoted by $u = m_\uparrow/m_\downarrow$. Note that the integrations over $\cos \theta$ can be done analytically by using Gauss's hypergeometric function:

$$\int_{-1}^1 d\cos \theta \frac{P_\ell(\cos \theta)}{x + y \cos \theta} = \frac{2\ell!}{x(2\ell+1)!!} \left(-\frac{y}{x}\right)^\ell {}_2F_1\left[\frac{\ell+1}{2}, \frac{\ell+2}{2}; \ell + \frac{3}{2}; \left(\frac{y}{x}\right)^2\right]. \quad (\text{B13})$$

In terms of $s_\uparrow^{(\ell)}(p)$, the last term in Eq. (B3) is written as

$$\begin{aligned} - \int \frac{d\mathbf{q}}{(2\pi)^3} \mathcal{K}_a(\mathbf{k}; \mathbf{k}, \mathbf{q}) \left[t_\uparrow(\mathbf{k}; \mathbf{q}) + \frac{2\mu}{q^2} \right] &= - \int \frac{d\mathbf{q}}{(2\pi)^3} \mathcal{J}_a\left(\frac{M}{M+m_\uparrow}\mathbf{k}, \mathbf{q}\right) [s_\uparrow(\mathbf{q}) + \mathcal{I}(\mathbf{q})] \frac{2\mu}{\mathbf{k}^2} \\ &= - \sum_{\ell=0}^{\infty} \int_0^\infty dq \mathcal{J}_a^{(\ell)}\left(\frac{u+1}{2u+1}, q\right) [s_\uparrow^{(\ell)}(q) + \mathcal{I}^{(\ell)}(q)] \frac{2\mu}{\mathbf{k}^2} \\ &= \sum_{\ell=0}^{\infty} \left[s_\uparrow^{(\ell)}\left(\frac{u+1}{2u+1}\right) + \mathcal{I}^{(\ell)}\left(\frac{u+1}{2u+1}\right) - \int_0^\infty dq \mathcal{J}_a^{(\ell)}\left(\frac{u+1}{2u+1}, q\right) \mathcal{I}^{(\ell)}(q) \right] \frac{2\mu}{\mathbf{k}^2}. \end{aligned} \quad (\text{B14})$$

In the last line, we used the integral equation for $s_\uparrow^{(\ell)}(p)$ in Eq. (B10). Because $s_\uparrow^{(\ell)}(p)$ is singular at $p = \left| \frac{u^2 - (2u+1)}{(u+1)(2u+1)} \right|$ and $\frac{u+1}{2u+1}$, it is better to work on the following function:

$$\delta s_\uparrow^{(\ell)}(p) \equiv s_\uparrow^{(\ell)}(p) + \mathcal{I}^{(\ell)}(p) - \int_0^\infty dq \mathcal{J}_a^{(\ell)}(p, q) \mathcal{I}^{(\ell)}(q), \quad (\text{B15})$$

in which the singularity at $p = \left| \frac{u^2 - (2u+1)}{(u+1)(2u+1)} \right|$ is eliminated and the singularity at $p = \frac{u+1}{2u+1}$ is weaker. This new function solves an integral equation

$$\delta s_\uparrow^{(\ell)}(p) = - \int_0^\infty dq \int_0^\infty dq' \mathcal{J}_a^{(\ell)}(p, q) \mathcal{J}_a^{(\ell)}(q, q') \mathcal{I}^{(\ell)}(q') - \int_0^\infty dq \mathcal{J}_a^{(\ell)}(p, q) \delta s_\uparrow^{(\ell)}(q), \quad (\text{B16})$$

and the last term in Eq. (B3) is given by its value at $p = \frac{u+1}{2u+1}$:

$$-\int \frac{d\mathbf{q}}{(2\pi)^3} \mathcal{K}_a(\mathbf{k}; \mathbf{k}, \mathbf{q}) \left[t_\uparrow(\mathbf{k}; \mathbf{q}) + \frac{2\mu}{q^2} \right] = \left[\sum_{\ell=0}^{\infty} \delta s_\uparrow^{(\ell)} \left(\frac{u+1}{2u+1} \right) \right] \frac{2\mu}{\mathbf{k}^2}. \quad (\text{B17})$$

In the case of equal masses $u = 1$, we numerically solved the integral equation (B16) at $(ak)^{-1} \simeq 0$ for $0 \leq \ell \leq \ell_{\max}$ up to $\ell_{\max} = 20$. By extrapolating the result to $\ell_{\max} \rightarrow \infty$, we obtain

$$\sum_{\ell=0}^{\infty} \delta s_\uparrow^{(\ell)} \left(\frac{2}{3} \right) \simeq 2.335 + \frac{7.047}{a|\mathbf{k}|} i + O(\mathbf{k}^{-2}). \quad (\text{B18})$$

Since we find that the imaginary part of $O(\mathbf{k}^0)$ term is as small as $\sim 2 \times 10^{-6}$ and the real part of $O(\mathbf{k}^{-1})$ term is as small as $\sim 4 \times 10^{-5}$, we assume that their actual values are zero. This result combined with Eqs. (B3) and (B4) is presented in Eq. (3.50).

2. Spinless Bose gas

In the case of spinless bosons, the quantity we would like to compute is Eq. (4.29):

$$t^{\text{reg}}(\mathbf{k}; \mathbf{k}) = \frac{m}{\mathbf{k}^2} + 2 \int \frac{d\mathbf{q}}{(2\pi)^3} \left[\mathcal{K}_a(\mathbf{k}; \mathbf{k}, \mathbf{q}) - \frac{4\pi}{-i\frac{|\mathbf{k}|}{2} - \frac{1}{a} q^2} \frac{1}{q^2} \right] \frac{m}{q^2} + 2 \int \frac{d\mathbf{q}}{(2\pi)^3} \mathcal{K}_a(\mathbf{k}; \mathbf{k}, \mathbf{q}) \left[t(\mathbf{k}; \mathbf{q}) - \frac{m}{q^2} \right], \quad (\text{B19})$$

in which $t(\mathbf{k}; \mathbf{p})$ solves the integral equation in Eq. (4.26):

$$t(\mathbf{k}; \mathbf{p}) = \frac{m}{\mathbf{p}^2} + 2 \int \frac{d\mathbf{q}}{(2\pi)^3} \mathcal{K}_a(\mathbf{k}; \mathbf{p}, \mathbf{q}) t(\mathbf{k}; \mathbf{q}). \quad (\text{B20})$$

Since the second term in Eq. (B19) is twice as large as that in Eq. (B3), its expansion in terms of $(a|\mathbf{k}|)^{-1}$ is obtained from Eq. (B4) with $u = 1$ by multiplying it by two. In analogy with the case of spin-1/2 fermions, we shift momentum variables as $\mathbf{p}(\mathbf{q}) \rightarrow \mathbf{p}(\mathbf{q}) + \mathbf{k}/3$ to move to the center-of-mass frame and introduce a dimensionless function

$$s(\mathbf{p}) \equiv \frac{\mathbf{k}^2}{m} t(\mathbf{k}; \mathbf{p} + \frac{\mathbf{k}}{3}). \quad (\text{B21})$$

Each component of its partial-wave expansion

$$s(\mathbf{p}) = \sum_{\ell=0}^{\infty} s^{(\ell)}(p) P_\ell(\cos \theta) \quad (\cos \theta \equiv \hat{\mathbf{k}} \cdot \hat{\mathbf{p}}) \quad (\text{B22})$$

solves an independent one-dimensional integral equation

$$s^{(\ell)}(p) = \mathcal{I}^{(\ell)}(p) + 2 \int_0^\infty dq \mathcal{J}_a^{(\ell)}(p, q) s^{(\ell)}(q). \quad (\text{B23})$$

Here the inhomogeneous term $\mathcal{I}^{(\ell)}(p)$ and integral kernel $\mathcal{J}_a^{(\ell)}(p, q)$ are obtained from Eqs. (B11) and (B12), respectively, by setting $u = 1$.

Then by defining the better behaving function

$$\delta s^{(\ell)}(p) \equiv s^{(\ell)}(p) - \mathcal{I}^{(\ell)}(p) - 2 \int_0^\infty dq \mathcal{J}_a^{(\ell)}(p, q) \mathcal{I}^{(\ell)}(q), \quad (\text{B24})$$

with its integral equation

$$\delta s^{(\ell)}(p) = 4 \int_0^\infty dq \int_0^\infty dq' \mathcal{J}_a^{(\ell)}(p, q) \mathcal{J}_a^{(\ell)}(q, q') \mathcal{I}^{(\ell)}(q') + 2 \int_0^\infty dq \mathcal{J}_a^{(\ell)}(p, q) \delta s^{(\ell)}(q), \quad (\text{B25})$$

the last term in Eq. (B19) is given by its value at $p = 2/3$:

$$2 \int \frac{d\mathbf{q}}{(2\pi)^3} \mathcal{K}_a(\mathbf{k}; \mathbf{k}, \mathbf{q}) \left[t(\mathbf{k}; \mathbf{q}) - \frac{m}{q^2} \right] = \left[\sum_{\ell=0}^{\infty} \delta s^{(\ell)} \left(\frac{2}{3} \right) \right] \frac{m}{\mathbf{k}^2}. \quad (\text{B26})$$

We numerically solved the integral equation (B25) at $(ak)^{-1} = 0$ for $1 \leq \ell \leq \ell_{\max}$ up to $\ell_{\max} = 20$. By extrapolating the result to $\ell_{\max} \rightarrow \infty$, we obtain

$$\sum_{\ell=1}^{\infty} \delta s^{(\ell)}\left(\frac{2}{3}\right) \simeq -2.044 + O(k^{-1}). \quad (\text{B27})$$

Since we find that the imaginary part of $O(k^0)$ term is as small as $\sim 4 \times 10^{-6}$, we assume that its actual value is zero. On the other hand, the $\ell = 0$ channel has to be treated specially due to the Efimov effect.

As is known [109, 110], the integral equation (B25) in the $\ell = 0$ channel is ill defined without introducing an ultraviolet momentum cutoff Λ :

$$\delta s^{(0)}(p) = 4 \int_0^{\infty} dq \int_0^{\infty} dq' \mathcal{J}_a^{(0)}(p, q) \mathcal{J}_a^{(0)}(q, q') \mathcal{I}^{(0)}(q') + 2 \int_0^{\Lambda/|\mathbf{k}|} dq \mathcal{J}_a^{(0)}(p, q) \delta s^{(0)}(q). \quad (\text{B28})$$

First we find that $\delta s^{(0)}(2/3)$ obtained by solving this integral equation is a log-periodic function of $|\mathbf{k}|/\Lambda$ in the limit $\Lambda/|\mathbf{k}| \rightarrow \infty$, which is approximated by

$$\delta s^{(0)}\left(\frac{2}{3}\right) \approx -3.9246 - i 12.20 + \frac{1.036 \cos(2s_0 \ln |\mathbf{k}|/\Lambda + 3.9604) - i 1.032 \sin(2s_0 \ln |\mathbf{k}|/\Lambda + 3.9604)}{1 - 0.08460 \sin(2s_0 \ln |\mathbf{k}|/\Lambda + 3.9604)}, \quad (\text{B29})$$

with $s_0 = 1.00624$ being the solution to the transcendental equation

$$\frac{8}{\sqrt{3} s_0} \frac{\sinh(\frac{\pi}{6} s_0)}{\cosh(\frac{\pi}{2} s_0)} = 1. \quad (\text{B30})$$

Then this artificial cutoff Λ has to be related to the physical Efimov parameter κ_* defined in Eq. (4.27). To this end, we observe that Eq. (B28) without the inhomogeneous term

$$\delta s^{(0)}(p) = \frac{2}{\pi} \int_0^{\Lambda} dq \frac{q^2}{\sqrt{\frac{3}{4}q^2 - \frac{k^2}{3} - i0^+ - \frac{1}{a}}} \int_{-1}^1 d \cos \theta \frac{\delta s^{(0)}(q)}{p^2 + q^2 + p q \cos \theta - \frac{k^2}{3} - i0^+} \quad (\text{B31})$$

is the Skorniakov–Ter-Martirosian equation to determine the binding energy of three identical bosons by identifying $k^2/3$ as the collision energy mE [110]. By solving this homogeneous integral equation at infinite scattering length $a \rightarrow \infty$, we find an infinite tower of binding energies given by

$$mE_n \rightarrow -e^{-2\pi n/s_0} \left(\frac{\Lambda}{5.67865} \right)^2 \quad (n \rightarrow \infty), \quad (\text{B32})$$

from which we can read off the relationship between Λ and κ_* as

$$\Lambda = 5.67865 \times \kappa_*. \quad (\text{B33})$$

This result combined with Eqs. (B4), (B19), (B27), and (B29) is presented in Eq. (4.31), which determines the universal log-periodic function $f(|\mathbf{k}|/\kappa_*)$ introduced in Eq. (4.30).

Appendix C: Derivation of optical theorem in Eq. (5.24)

Here we derive the optical theorem used in Eq. (5.24) by a direct calculation starting with the set of integral equations in Eq. (5.10). We only consider the case in which $a_{\uparrow}^{-1} = a_{\downarrow}^{-1} = a^{-1} = 0$ and thus $t_{\psi}(\mathbf{k}; \mathbf{p}) \equiv t_{\uparrow}(\mathbf{k}; \mathbf{p}) = t_{\downarrow}(\mathbf{k}; \mathbf{p})$ because this case is sufficient for the analysis presented in the text. By using the definitions of $t_{F,B}(\mathbf{k}; \mathbf{p})$ in Eqs. (5.11) and (5.12), the three coupled integral equations in Eq. (5.10) can be brought into the two independent integral equations in Eq. (5.13):

$$t_F(\mathbf{k}; \mathbf{p}) = -\frac{m}{\mathbf{p}^2} - \int \frac{d\mathbf{q}}{(2\pi)^3} t_F(\mathbf{k}; \mathbf{q}) A(\epsilon_{\mathbf{k}} - \epsilon_{\mathbf{q}}, \mathbf{k} - \mathbf{q}) \frac{1}{\epsilon_{\mathbf{p}} + \epsilon_{\mathbf{q}} + \epsilon_{\mathbf{k}-\mathbf{p}-\mathbf{q}} - \epsilon_{\mathbf{k}} - i0^+} \quad (\text{C1a})$$

and

$$t_B(\mathbf{k}; \mathbf{p}) = \frac{m}{\mathbf{p}^2} + 2 \int \frac{d\mathbf{q}}{(2\pi)^3} t_B(\mathbf{k}; \mathbf{q}) A(\epsilon_{\mathbf{k}} - \epsilon_{\mathbf{q}}, \mathbf{k} - \mathbf{q}) \frac{1}{\epsilon_{\mathbf{p}} + \epsilon_{\mathbf{q}} + \epsilon_{\mathbf{k}-\mathbf{p}-\mathbf{q}} - \epsilon_{\mathbf{k}} - i0^+}. \quad (\text{C1b})$$

Here we used the expression of $\mathcal{K}_a(\mathbf{k}; \mathbf{p}, \mathbf{q})$ in Eq. (3.46) and $A(k) = -D(k)$ is the two-body scattering amplitude in Eq. (3.5) at infinite scattering length. Their complex conjugates are

$$t_F^*(\mathbf{k}; \mathbf{p}) = -\frac{m}{\mathbf{p}^2} - \int \frac{d\mathbf{q}}{(2\pi)^3} t_F^*(\mathbf{k}; \mathbf{q}) A^*(\epsilon_{\mathbf{k}} - \epsilon_{\mathbf{q}}, \mathbf{k} - \mathbf{q}) \frac{1}{\epsilon_{\mathbf{p}} + \epsilon_{\mathbf{q}} + \epsilon_{\mathbf{k}-\mathbf{p}-\mathbf{q}} - \epsilon_{\mathbf{k}} + i0^+} \quad (\text{C2a})$$

and

$$t_B^*(\mathbf{k}; \mathbf{p}) = \frac{m}{\mathbf{p}^2} + 2 \int \frac{d\mathbf{q}}{(2\pi)^3} t_B^*(\mathbf{k}; \mathbf{q}) A^*(\epsilon_{\mathbf{k}} - \epsilon_{\mathbf{q}}, \mathbf{k} - \mathbf{q}) \frac{1}{\epsilon_{\mathbf{p}} + \epsilon_{\mathbf{q}} + \epsilon_{\mathbf{k}-\mathbf{p}-\mathbf{q}} - \epsilon_{\mathbf{k}} + i0^+}. \quad (\text{C2b})$$

By using these complex conjugates, $t_{F,B}(\mathbf{k}; \mathbf{p})$ at $\mathbf{p} = \mathbf{k}$ can be written as

$$\begin{aligned} t_F(\mathbf{k}; \mathbf{k}) &= -\frac{m}{\mathbf{p}^2} - \int \frac{d\mathbf{p}}{(2\pi)^3} t_F(\mathbf{k}; \mathbf{p}) A(\epsilon_{\mathbf{k}} - \epsilon_{\mathbf{p}}, \mathbf{k} - \mathbf{p}) \frac{m}{\mathbf{p}^2} \\ &= -\frac{m}{\mathbf{p}^2} + \int \frac{d\mathbf{p}}{(2\pi)^3} |t_F(\mathbf{k}; \mathbf{p})|^2 A(\epsilon_{\mathbf{k}} - \epsilon_{\mathbf{p}}, \mathbf{k} - \mathbf{p}) \\ &\quad + \int \frac{d\mathbf{p} d\mathbf{q}}{(2\pi)^6} t_F(\mathbf{k}; \mathbf{p}) A(\epsilon_{\mathbf{k}} - \epsilon_{\mathbf{p}}, \mathbf{k} - \mathbf{p}) t_F^*(\mathbf{k}; \mathbf{q}) A^*(\epsilon_{\mathbf{k}} - \epsilon_{\mathbf{q}}, \mathbf{k} - \mathbf{q}) \frac{1}{\epsilon_{\mathbf{p}} + \epsilon_{\mathbf{q}} + \epsilon_{\mathbf{k}-\mathbf{p}-\mathbf{q}} - \epsilon_{\mathbf{k}} + i0^+} \end{aligned} \quad (\text{C3a})$$

and

$$\begin{aligned} t_B(\mathbf{k}; \mathbf{k}) &= \frac{m}{\mathbf{p}^2} + 2 \int \frac{d\mathbf{p}}{(2\pi)^3} t_B(\mathbf{k}; \mathbf{p}) A(\epsilon_{\mathbf{k}} - \epsilon_{\mathbf{p}}, \mathbf{k} - \mathbf{p}) \frac{m}{\mathbf{p}^2} \\ &= \frac{m}{\mathbf{p}^2} + 2 \int \frac{d\mathbf{p}}{(2\pi)^3} |t_B(\mathbf{k}; \mathbf{p})|^2 A(\epsilon_{\mathbf{k}} - \epsilon_{\mathbf{p}}, \mathbf{k} - \mathbf{p}) \\ &\quad - 4 \int \frac{d\mathbf{p} d\mathbf{q}}{(2\pi)^6} t_B(\mathbf{k}; \mathbf{p}) A(\epsilon_{\mathbf{k}} - \epsilon_{\mathbf{p}}, \mathbf{k} - \mathbf{p}) t_B^*(\mathbf{k}; \mathbf{q}) A^*(\epsilon_{\mathbf{k}} - \epsilon_{\mathbf{q}}, \mathbf{k} - \mathbf{q}) \frac{1}{\epsilon_{\mathbf{p}} + \epsilon_{\mathbf{q}} + \epsilon_{\mathbf{k}-\mathbf{p}-\mathbf{q}} - \epsilon_{\mathbf{k}} + i0^+}. \end{aligned} \quad (\text{C3b})$$

Then by using the identity

$$2 \text{Im} A(\epsilon_{\mathbf{k}} - \epsilon_{\mathbf{p}}, \mathbf{k} - \mathbf{p}) = \int \frac{d\mathbf{q}_{\uparrow} d\mathbf{q}_{\downarrow}}{(2\pi)^6} |A(\epsilon_{\mathbf{k}} - \epsilon_{\mathbf{p}}, \mathbf{k} - \mathbf{p})|^2 (2\pi)^4 \delta(\mathbf{p} + \mathbf{q}_{\uparrow} + \mathbf{q}_{\downarrow} - \mathbf{k}) \delta(\epsilon_{\mathbf{p}} + \epsilon_{\mathbf{q}_{\uparrow}} + \epsilon_{\mathbf{q}_{\downarrow}} - \epsilon_{\mathbf{k}}), \quad (\text{C4})$$

the imaginary parts of $t_{F,B}(\mathbf{k}; \mathbf{k})$ become

$$\begin{aligned} 2 \text{Im} t_F(\mathbf{k}; \mathbf{k}) &= \frac{1}{2} \int \frac{d\mathbf{p} d\mathbf{q}_{\uparrow} d\mathbf{q}_{\downarrow}}{(2\pi)^9} |t_F(\mathbf{k}; \mathbf{p}) A(\epsilon_{\mathbf{k}} - \epsilon_{\mathbf{p}}, \mathbf{k} - \mathbf{p}) - t_F(\mathbf{k}; \mathbf{q}_{\uparrow}) A(\epsilon_{\mathbf{k}} - \epsilon_{\mathbf{q}_{\uparrow}}, \mathbf{k} - \mathbf{q}_{\uparrow})|^2 \\ &\quad \times (2\pi)^4 \delta(\mathbf{p} + \mathbf{q}_{\uparrow} + \mathbf{q}_{\downarrow} - \mathbf{k}) \delta(\epsilon_{\mathbf{p}} + \epsilon_{\mathbf{q}_{\uparrow}} + \epsilon_{\mathbf{q}_{\downarrow}} - \epsilon_{\mathbf{k}}) \end{aligned} \quad (\text{C5a})$$

and

$$\begin{aligned} 2 \text{Im} t_B(\mathbf{k}; \mathbf{k}) &= \frac{2}{3} \int \frac{d\mathbf{p} d\mathbf{q}_{\uparrow} d\mathbf{q}_{\downarrow}}{(2\pi)^9} |t_B(\mathbf{k}; \mathbf{p}) A(\epsilon_{\mathbf{k}} - \epsilon_{\mathbf{p}}, \mathbf{k} - \mathbf{p}) + t_B(\mathbf{k}; \mathbf{q}_{\uparrow}) A(\epsilon_{\mathbf{k}} - \epsilon_{\mathbf{q}_{\uparrow}}, \mathbf{k} - \mathbf{q}_{\uparrow}) \\ &\quad + t_B(\mathbf{k}; \mathbf{q}_{\downarrow}) A(\epsilon_{\mathbf{k}} - \epsilon_{\mathbf{q}_{\downarrow}}, \mathbf{k} - \mathbf{q}_{\downarrow})|^2 (2\pi)^4 \delta(\mathbf{p} + \mathbf{q}_{\uparrow} + \mathbf{q}_{\downarrow} - \mathbf{k}) \delta(\epsilon_{\mathbf{p}} + \epsilon_{\mathbf{q}_{\uparrow}} + \epsilon_{\mathbf{q}_{\downarrow}} - \epsilon_{\mathbf{k}}). \end{aligned} \quad (\text{C5b})$$

Finally, by using the definitions of $t_{F,B}(\mathbf{k}; \mathbf{p})$ in Eqs. (5.11) and (5.12) again, the imaginary part of the forward three-body scattering amplitude $t_{\chi}(\mathbf{k}; \mathbf{k})$ is found to be

$$\begin{aligned} 2 \text{Im} t_{\chi}(\mathbf{k}; \mathbf{k}) &= \frac{4}{3} \text{Im} [t_F(\mathbf{k}; \mathbf{k}) + t_B(\mathbf{k}; \mathbf{k})] \\ &= \int \frac{d\mathbf{p} d\mathbf{q}_{\uparrow} d\mathbf{q}_{\downarrow}}{(2\pi)^9} |t_{\chi}(\mathbf{k}; \mathbf{p}) A(\epsilon_{\mathbf{k}} - \epsilon_{\mathbf{p}}, \mathbf{k} - \mathbf{p}) + t_{\psi}(\mathbf{k}; \mathbf{q}_{\uparrow}) A(\epsilon_{\mathbf{k}} - \epsilon_{\mathbf{q}_{\uparrow}}, \mathbf{k} - \mathbf{q}_{\uparrow}) \\ &\quad + t_{\psi}(\mathbf{k}; \mathbf{q}_{\downarrow}) A(\epsilon_{\mathbf{k}} - \epsilon_{\mathbf{q}_{\downarrow}}, \mathbf{k} - \mathbf{q}_{\downarrow})|^2 (2\pi)^4 \delta(\mathbf{p} + \mathbf{q}_{\uparrow} + \mathbf{q}_{\downarrow} - \mathbf{k}) \delta(\epsilon_{\mathbf{p}} + \epsilon_{\mathbf{q}_{\uparrow}} + \epsilon_{\mathbf{q}_{\downarrow}} - \epsilon_{\mathbf{k}}), \end{aligned} \quad (\text{C6})$$

which is equivalent to Eq. (5.24) when $a_{\uparrow}^{-1} = a_{\downarrow}^{-1} = a^{-1} = 0$.

On the other hand, in the case of spinless bosons, the definitions of $t_{F,B}(\mathbf{k}; \mathbf{p})$ in Eqs. (5.39) and (5.40) lead to

$$\begin{aligned} 2 \operatorname{Im} t_{\chi}(\mathbf{k}; \mathbf{k}) &= \frac{2}{3} \operatorname{Im} [t_F(\mathbf{k}; \mathbf{k}) + t_B(\mathbf{k}; \mathbf{k})] \\ &= \int \frac{d\mathbf{p} d\mathbf{q}_{\uparrow} d\mathbf{q}_{\downarrow}}{(2\pi)^9} \frac{1}{2} |2t_{\chi}(\mathbf{k}; \mathbf{p})A(\epsilon_{\mathbf{k}} - \epsilon_{\mathbf{p}}, \mathbf{k} - \mathbf{p}) + t_{\psi}(\mathbf{k}; \mathbf{q}_{\uparrow})A(\epsilon_{\mathbf{k}} - \epsilon_{\mathbf{q}_{\uparrow}}, \mathbf{k} - \mathbf{q}_{\uparrow}) \\ &\quad + t_{\psi}(\mathbf{k}; \mathbf{q}_{\downarrow})A(\epsilon_{\mathbf{k}} - \epsilon_{\mathbf{q}_{\downarrow}}, \mathbf{k} - \mathbf{q}_{\downarrow})|^2 (2\pi)^4 \delta(\mathbf{p} + \mathbf{q}_{\uparrow} + \mathbf{q}_{\downarrow} - \mathbf{k}) \delta(\epsilon_{\mathbf{p}} + \epsilon_{\mathbf{q}_{\uparrow}} + \epsilon_{\mathbf{q}_{\downarrow}} - \epsilon_{\mathbf{k}}). \end{aligned} \quad (C7)$$

Since $t_{\chi}(\mathbf{k}; \mathbf{p})$ in Eq. (C7) is a half of that in Eq. (C6), the integrand in Eq. (C7) is also a half of that in Eq. (C6). This establishes that the contribution of the contact density to the differential scattering rate of the χ atom in a spinless Bose gas is a half of that in a spin-1/2 Fermi gas.

-
- [1] I. Bloch, J. Dalibard, and W. Zwerger, *Rev. Mod. Phys.* **80**, 885 (2008).
- [2] S. Giorgini, L. P. Pitaevskii, and S. Stringari, *Rev. Mod. Phys.* **80**, 1215 (2008).
- [3] W. Ketterle and M. W. Zwierlein, in *Ultracold Fermi Gases; Proceedings of the International School of Physics “Enrico Fermi,”* edited by M. Inguscio, W. Ketterle, and C. Salomon (IOS Press, Amsterdam, 2008).
- [4] K. M. O’Hara, S. L. Hemmer, M. E. Gehm, S. R. Granade, and J. E. Thomas, *Science* **298**, 2179 (2002).
- [5] B. Clancy, L. Luo, and J. E. Thomas, *Phys. Rev. Lett.* **99**, 140401 (2007).
- [6] C. Cao, E. Elliott, J. Joseph, H. Wu, J. Petricka, T. Schäfer, and J. E. Thomas, *Science* **331**, 58 (2010).
- [7] S. Riedl, E. R. Sánchez Guajardo, C. Kohstall, J. Hecker Denschlag, and R. Grimm, *New J. Phys.* **13** 035003 (2011).
- [8] A. Trenkwalder, C. Kohstall, M. Zaccanti, D. Naik, A. I. Sidorov, F. Schreck, and R. Grimm, *Phys. Rev. Lett.* **106**, 115304 (2011).
- [9] G. Veeravalli, E. Kuhnle, P. Dyke, and C. J. Vale, *Phys. Rev. Lett.* **101**, 250403 (2008).
- [10] E. D. Kuhnle, H. Hu, X.-J. Liu, P. Dyke, M. Mark, P. D. Drummond, P. Hannaford, and C. J. Vale, *Phys. Rev. Lett.* **105**, 070402 (2010).
- [11] E. D. Kuhnle, S. Hoinka, P. Dyke, H. Hu, P. Hannaford, and C. J. Vale, *Phys. Rev. Lett.* **106**, 170402 (2011).
- [12] S. Hoinka, M. Lingham, M. Delehay, and C. J. Vale, arXiv:1203.4657 [cond-mat.quant-gas].
- [13] A. Schirotzek, C.-H. Wu, A. Sommer, and M. W. Zwierlein, *Phys. Rev. Lett.* **102**, 230402 (2009).
- [14] P. Pieri, A. Perali, G. C. Strinati, S. Riedl, M. J. Wright, A. Altmeyer, C. Kohstall, E. R. Sánchez Guajardo, J. Hecker Denschlag, and R. Grimm, *Phys. Rev. A* **84**, 011608(R) (2011).
- [15] A. T. Sommer, L. W. Cheuk, M. J.-H. Ku, W. S. Bakr, and M. W. Zwierlein, *Phys. Rev. Lett.* **108**, 045302 (2012).
- [16] M. Horikoshi, S. Nakajima, M. Ueda, and T. Mukaiyama, *Science* **327**, 442 (2010).
- [17] S. Nascimbène, N. Navon, K. J. Jiang, F. Chevy, and C. Salomon, *Nature (London)* **463**, 1057 (2010).
- [18] N. Navon, S. Nascimbène, F. Chevy, and C. Salomon, *Science* **328**, 729 (2010).
- [19] S. Nascimbène, N. Navon, S. Pilati, F. Chevy, S. Giorgini, A. Georges, and C. Salomon, *Phys. Rev. Lett.* **106**, 215303 (2011).
- [20] N. Navon, S. Piątek, K. J. Günter, B. Rem, T. C. Nguyen, F. Chevy, W. Krauth, and C. Salomon, *Phys. Rev. Lett.* **107**, 135301 (2011).
- [21] M. J. H. Ku, A. T. Sommer, L. W. Cheuk, and M. W. Zwierlein, *Science* **335**, 563 (2012).
- [22] K. V. Houcke, F. Werner, E. Kozik, N. Prokof’ev, B. Svistunov, M. J. H. Ku, A. T. Sommer, L. W. Cheuk, A. Schirotzek, and M. W. Zwierlein, *Nature Phys.* **8**, 366 (2012).
- [23] J. A. Joseph, J. E. Thomas, M. Kulkarni, and A. G. Abanov, *Phys. Rev. Lett.* **106**, 150401 (2011).
- [24] A. Sommer, M. Ku, G. Roati, and M. W. Zwierlein, *Nature (London)* **472**, 201 (2011).
- [25] A. Sommer, M. Ku, and M. W. Zwierlein, *New J. Phys.* **13**, 055009 (2011).
- [26] J. T. Stewart, J. P. Gaebler, and D. S. Jin, *Nature (London)* **454**, 744 (2008).
- [27] J. P. Gaebler, J. T. Stewart, T. E. Drake, D. S. Jin, A. Perali, P. Pieri, and G. C. Strinati, *Nature Phys.* **6**, 569 (2010).
- [28] A. Damascelli, *Physica Scripta* **T109**, 61 (2004).
- [29] H. Witała, W. Glöckle, D. Hüber, J. Golak, and H. Kamada, *Phys. Rev. Lett.* **81**, 1183 (1998).
- [30] S. Nemoto, K. Chmielewski, S. Oryu, and P. U. Sauer, *Phys. Rev. C* **58**, 2599 (1998).
- [31] For a recent review, see N. Kalantar-Nayestanaki, E. Epelbaum, J. G. Messchendorp, and A. Nogga, *Rep. Prog. Phys.* **75**, 016301 (2012).
- [32] R. Subedi *et al.*, *Science* **320**, 1476 (2008); http://www.jlab.org/news/articles/2008/Nuclear_Pairs.html
- [33] For a recent review, see J. Arrington, D. W. Higinbotham, G. Rosner, and M. Sargsian, *Prog. Part. Nucl. Phys.* (2012) [arXiv:1104.1196 (nucl-ex)].
- [34] K. Adcox *et al.* (PHENIX Collaboration), *Phys. Rev. Lett.* **88**, 022301 (2001).
- [35] C. Adler *et al.* (STAR Collaboration), *Phys. Rev. Lett.* **90**, 082302 (2003).
- [36] G. Aad *et al.* (ATLAS Collaboration), *Phys. Rev. Lett.* **105**, 252303 (2010).
- [37] S. Chatrchyan *et al.* (CMS Collaboration), *Phys. Rev. C* **84**, 024906 (2011).
- [38] CERN Press Release, *LHC experiments bring new insight into primordial universe* (November 2010) [<http://press.web.cern.ch/press/PressReleases/Releases2010>]
- [39] See, for example, *Proceedings of the 4th International Conference on Hard and Electromagnetic Probes of*

- High-Energy Nuclear Collisions (Hard Probes 2010)*, Nucl. Phys. A **855**, 1-542 (2011).
- [40] A. Miller, D. Pines, and P. Nozières, Phys. Rev. **127**, 1452 (1962).
- [41] P. C. Hohenberg and P. M. Platzman, Phys. Rev. **152**, 198 (1966).
- [42] For a review, see A. D. B. Woods and R. A. Cowley, Rep. Prog. Phys. **36**, 1135 (1973).
- [43] A. Griffin, *Excitations in a Bose-Condensed Liquid* (Cambridge University Press, Cambridge, 1993).
- [44] W. M. Snow and P. E. Sokol, J. Low Temp. Phys. **101**, 881 (1995), and references therein.
- [45] D. S. Petrov, C. Salomon, and G. V. Shlyapnikov, Phys. Rev. Lett. **93**, 090404 (2004); Phys. Rev. A **71**, 012708 (2005); J. Phys. B **38**, S645 (2005).
- [46] T. Kraemer, M. Mark, P. Waldburger, J. G. Danzl, C. Chin, B. Engeser, A. D. Lange, K. Pilch, A. Jaakkol, H.-C. Nägerl, and R. Grimm, Nature (London) **440**, 315 (2006).
- [47] M. Zaccanti, B. Deissler, C. D'Errico, M. Fattori, M. Jona-Lasinio, S. Müller, G. Roati, M. Inguscio, and G. Modugno, Nature Phys. **5**, 586 (2009).
- [48] S. E. Pollack, D. Dries, and R. G. Hulet, Science **326**, 1683 (2009).
- [49] F. Ferlaino and R. Grimm, Physics **3**, 9 (2010).
- [50] F. Ferlaino, A. Zenesini, M. Berninger, B. Huang, H.-C. Nägerl, and R. Grimm, Few-Body Syst. **51**, 113 (2011), and references therein.
- [51] H. C. W. Beijerinck, Phys. Rev. A **62**, 063614 (2000).
- [52] J. Schuster, A. Marte, S. Amthage, B. Sang, G. Rempe, and H. C. W. Beijerinck, Phys. Rev. Lett. **87**, 170404 (2001).
- [53] O. Machtey, D. A. Kessler, and L. Khaykovich, Phys. Rev. Lett. **108**, 130403 (2012).
- [54] N. R. Thomas, N. Kjærgaard, P. S. Julienne, and A. C. Wilson, Phys. Rev. Lett. **93**, 173201 (2004).
- [55] Ch. Buggle, J. Léonard, W. von Klitzing, and J. T. M. Walraven, Phys. Rev. Lett. **93**, 173202 (2004).
- [56] N. Kjærgaard, A. S. Mellish, and A. C. Wilson, New J. Phys. **6**, 146 (2004).
- [57] A. S. Mellish, N. Kjærgaard, P. S. Julienne, and A. C. Wilson, Phys. Rev. A **75**, 020701(R) (2007).
- [58] A. Perrin, H. Chang, V. Krachmalnicoff, M. Schellekens, D. Boiron, A. Aspect, and C. I. Westbrook, Phys. Rev. Lett. **99**, 150405 (2007).
- [59] V. Krachmalnicoff, J.-C. Jaskula, M. Bonneau, V. Leung, G. B. Partridge, D. Boiron, C. I. Westbrook, P. Deuar, P. Ziń, M. Trippenbach, and K. V. Kheruntsyan, Phys. Rev. Lett. **104**, 150402 (2010).
- [60] R. A. Williams, L. J. LeBlanc, K. Jiménez-García, M. C. Beeler, A. R. Perry, W. D. Phillips, and I. B. Spielman, Science **335**, 314 (2012).
- [61] A. Rakonjac, A. B. Deb, S. Hoinka, D. Hudson, B. J. Sawyer, and N. Kjærgaard, Opt. Lett. **37**, 1085 (2012).
- [62] D. Wulin, H. Guo, C.-C. Chien, and K. Levin, Phys. Rev. A **83**, 061601(R) (2011).
- [63] E. Taylor, S. Zhang, W. Schneider, and M. Randeria, Phys. Rev. A **84**, 063622 (2011).
- [64] O. Goulko, F. Chevy, and C. Lobo, Phys. Rev. A **84**, 051605(R) (2011); arXiv:1201.6235 [cond-mat.quant-gas].
- [65] G. M. Bruun, A. Recati, C. J. Pethick, H. Smith, and S. Stringari, Phys. Rev. Lett. **100**, 240406 (2008); G. M. Bruun and C. J. Pethick, Phys. Rev. Lett. **107**, 255302 (2011).
- [66] See, for example, T. Schäfer, Physics **2**, 88 (2009); T. Schäfer and D. Teaney, Rep. Prog. Phys. **72**, 126001 (2009).
- [67] S. Tan, Ann. Phys. (NY) **323**, 2952 (2008); **323**, 2971 (2008); **323**, 2987 (2008).
- [68] E. Braaten and L. Platter, Phys. Rev. Lett. **100**, 205301 (2008).
- [69] For a review, see E. Braaten, in *The BCS-BEC Crossover and the Unitary Fermi Gas*, Lecture Notes in Physics, edited by W. Zwerger, Chap. 6 (Springer, Berlin, 2012).
- [70] E. Braaten, D. Kang, and L. Platter, Phys. Rev. Lett. **106**, 153005 (2011).
- [71] G. B. Partridge, K. E. Strecker, R. I. Kamar, M. W. Jack, and R. G. Hulet, Phys. Rev. Lett. **95**, 020404 (2005); F. Werner, L. Tarruell, and Y. Castin, Eur. Phys. J. B **68**, 401 (2009).
- [72] J. T. Stewart, J. P. Gaebler, T. E. Drake, and D. S. Jin, Phys. Rev. Lett. **104**, 235301 (2010).
- [73] P. Magierski, G. Wlazłowski, A. Bulgac, and J. E. Drut, Phys. Rev. Lett. **103**, 210403 (2009).
- [74] P. Magierski, G. Wlazłowski, and A. Bulgac, supplemental online material for Phys. Rev. Lett. **107**, 145304 (2011).
- [75] O. Goulko and M. Wingate, Proc. Sci. Lattice2010, 187 (2010).
- [76] S. Gandolfi, K. E. Schmidt, and J. Carlson, Phys. Rev. A **83**, 041601(R) (2011).
- [77] R. Combescot, S. Giorgini, and S. Stringari, Europhys. Lett. **75**, 695 (2006).
- [78] C. Lobo, I. Carusotto, S. Giorgini, A. Recati, and S. Stringari, Phys. Rev. Lett. **97**, 100405 (2006).
- [79] J. E. Drut, T. A. Lähde, and T. Ten, Phys. Rev. Lett. **106**, 205302 (2011); arXiv:1111.0951 [hep-lat].
- [80] E. Braaten, D. Kang, and L. Platter, Phys. Rev. A **78**, 053606 (2008).
- [81] E. Braaten, D. Kang, and L. Platter, Phys. Rev. Lett. **104**, 223004 (2010).
- [82] D. T. Son and E. G. Thompson, Phys. Rev. A **81**, 063634 (2010).
- [83] W. D. Goldberger and I. Z. Rothstein, Phys. Rev. A **85**, 013613 (2012).
- [84] M. Barth and W. Zwerger, Ann. Phys. (NY) **326**, 2544 (2011).
- [85] J. Hofmann, Phys. Rev. A **84**, 043603 (2011).
- [86] W. D. Goldberger and Z. U. Khandker, Phys. Rev. A **85**, 013624 (2012).
- [87] Y. Nishida and D. T. Son, Phys. Rev. D **76**, 086004 (2007).
- [88] Y. Nishida and D. T. Son, in *The BCS-BEC Crossover and the Unitary Fermi Gas*, Lecture Notes in Physics, edited by W. Zwerger, Chap. 7 (Springer, Berlin, 2012).
- [89] S. Tan, arXiv:cond-mat/0412764.
- [90] F. Werner and Y. Castin, Phys. Rev. Lett. **97**, 150401 (2006); Phys. Rev. A **74**, 053604 (2006).
- [91] S. Y. Chang and G. F. Bertsch, Phys. Rev. A **76**, 021603(R) (2007).
- [92] J. von Stecher, C. H. Greene, and D. Blume, Phys. Rev. A **76**, 053613 (2007).
- [93] D. Blume, J. von Stecher, and C. H. Greene, Phys. Rev. Lett. **99**, 233201 (2007).

- [94] J. von Stecher, C. H. Greene, and D. Blume, Phys. Rev. A **77**, 043619 (2008).
- [95] D. Blume, Phys. Rev. A **78**, 013635 (2008).
- [96] K. M. Daily and D. Blume, Phys. Rev. A **81**, 053615 (2010).
- [97] D. Blume and K. M. Daily, Comptes Rendus Physique, **12**, 86 (2011).
- [98] A. N. Nicholson, M. G. Endres, D. B. Kaplan, and J.-W. Lee, Proc. Sci. Lattice2010, 206 (2010).
- [99] M. G. Endres, D. B. Kaplan, J.-W. Lee, and A. N. Nicholson, Phys. Rev. A **84**, 043644 (2011).
- [100] D. Blume, Rep. Prog. Phys. **75** 046401, (2012), and references therein.
- [101] D. S. Petrov, Phys. Rev. A **67**, 010703(R) (2003).
- [102] Y. Castin, C. Mora, and L. Pricoupenko, Phys. Rev. Lett. **105**, 223201 (2010).
- [103] A. A. Abrikosov, L. P. Gorkov, and I. E. Dzyaloshinski, *Methods of Quantum Field Theory in Statistical Physics* (Dover, New York, 1963).
- [104] A. L. Fetter and J. D. Walecka, *Quantum Theory of Many-Particle Systems* (Dover, New York, 1971).
- [105] W. Schneider and M. Randeria, Phys. Rev. A **81**, 021601(R) (2010).
- [106] R. Hausmann, M. Punk, and W. Zwerger, Phys. Rev. A **80**, 063612 (2009).
- [107] H. Hu, X.-J. Liu, P. D. Drummond, and H. Dong, Phys. Rev. Lett. **104**, 240407 (2010).
- [108] V. Efimov, Phys. Lett. B **33**, 563 (1970); Nucl. Phys. A **210**, 157 (1973).
- [109] P. F. Bedaque, H.-W. Hammer, and U. van Kolck, Phys. Rev. Lett. **82**, 463 (1999); Nucl. Phys. A **646**, 444 (1999).
- [110] E. Braaten and H.-W. Hammer, Phys. Rept. **428**, 259 (2006); Ann. Phys. **322**, 120 (2007).
- [111] E. Nielsen, D. V. Fedorov, A. S. Jensen, and E. Garrido, Phys. Rept. **347**, 373 (2001).
- [112] L. Van Hove, Phys. Rev. **95**, 249 (1954).
- [113] M. Cohen and R. P. Feynman, Phys. Rev. **107**, 13 (1957).
- [114] H. Hu and X.-J. Liu, Phys. Rev. A **85**, 023612 (2012).
- [115] Up to a factor of 2/3, our result is also consistent with that reported in E. Taylor and M. Randeria, Phys. Rev. A **81**, 053610 (2010).